AB

USAAVLABS TECHNICAL REPORT 64-68A

HEAVY-LIFT TIP TURBOJET ROTOR SYSTEM
VOLUME I

SUMMARY REPORT

October 1965

U. S. ARMY AVIATION MATERIEL LABORATORIES
FORT EUSTIS, VIRGINIA

CONTRACT DA 44-177-AMC-25(T)
HILLER AIRCRAFT COMPANY, INC.

DISCLAIMER NOTICE

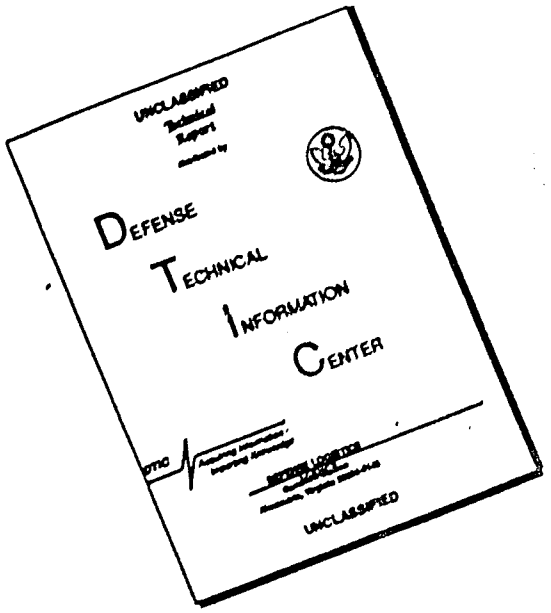

THIS DOCUMENT IS BEST QUALITY AVAILABLE. THE COPY FURNISHED TO DTIC CONTAINED A SIGNIFICANT NUMBER OF PAGES WHICH DO NOT REPRODUCE LEGIBLY.

DEPARTMENT OF THE ARMY
U. S. ARMY AVIATION MATERIEL LABORATORIES
FORT EUSTIS, VIRGINIA 23604

This report describes the results of a comprehensive analytical and preliminary design study of the tip turbojet rotor system concept as applied to a heavy-lift helicopter mission. As such, the report is offered for the stimulation and exchange of ideas.

NOTE

On 1 March 1965, *after this report had been prepared,* the name of this command was changed from U. S. Army Transportation Research Command to:

U.S. ARMY AVIATION MATERIEL LABORATORIES

Task 1M121401D14412
Contract DA 44-177-AMC-25(T)
USAAVLABS Technical Report 64-68A
October 1965

HEAVY-LIFT TIP TURBOJET ROTOR SYSTEM

VOLUME I

SUMMARY REPORT

Hiller Engineering Report No. 64-41

Prepared by

Hiller Aircraft Company, Inc.
Subsidiary of Fairchild Hiller Corporation
Palo Alto, California

For

U. S. ARMY AVIATION MATERIEL LABORATORIES
FORT EUSTIS, VIRGINIA

CONTENTS

CONTENTS (CONTINUED)

ILLUSTRATIONS

ILLUSTRATIONS (CONTINUED)

TABLES

1.0 SUMMARY

1.1 Task I

This report summarizes the Task I accomplishments as required by contract DA 44-177-AMC-25(T) and reported in Hiller Aircraft Company, Reports No. 64-42 through 64-50 (see Reference 1 - 9). Task I, as defined in the work statement of the subject contract, requires the completion of a rotor system parametric design study and a rotor system preliminary design (with appropriate design studies) for a heavy-lift tip turbojet system which will meet the following mission requirements and design objectives:

Mission Description

a) Payload (outbound) - 12 tons
b) Radius - 50 nautical miles
c) Cruising speed-(i) outbound, 60 knots; (ii) inbound (no payload) - 100 knots
d) Take-off and destination elevation - sea level
e) Cruising altitude - sea level
f) Atmospheric condition - sea level, standard atmosphere
g) Hovering time (out-of-ground effect) - (i) at take-off, 3 minutes; (ii) at destination, 2 minutes
h) Reserve fuel (percent initial fuel) - 10 percent
i) Hovering capability - (i) altitude, 6000 feet, (ii) temperature, 95°F.

Design Objectives

a) Design gross weight - 60,000 - 80,000 pounds
b) Design maximum speed - 125 miles per hour
c) Minimum flight load factor + 2.5 and - 0.5
d) Rotor tip environment - 235g

1.2 Task II

Task II of the subject contract requires an analysis and design of such modifications as may be required to permit satisfactory continuous operation of the Continental (CAE) Model 357-1 (Modified J69-T-29) engine in a helicopter rotor tip environment. A summary of the accomplishments under this task may be found in Continental Aviation and Engineering Corporation Reports 942, 943, and CAE Engine Specification No. 2253. (See References 17 - 19).

2.0 CONCLUSIONS

2.1 Parametric Design Study

2.1.1 Structural and Dynamic Limitations

Previous parametric design studies for helicopters with conventional rotors have consistently produced optimum configurations which consist of rotor blades with aspect ratios (radius/chord) of 18-22. Thus, it was considered appropriate, prior to conducting the parametric study, to examine aspect ratio limits which might be imposed by the unconventional high tip weight concentrated at the rotor tip. Both static deflection and fundamental in-plane frequency requirements were examined in this regard.

The requirements for rotor static droop, not to exceed 10 percent of rotor radius, and for the fundamental rotating in-plane frequency (uncoupled), not to be less than 1.3 times normal operating speed, both produce a maximum allowable aspect ratio range of 9-11; the range depends on rotor radius and tip weight-to-blade weight ratios. However, since the rotor blades optimized at aspect ratios less than 9, the static droop and in-plane frequency requirements did not, in fact, impose additional constraints on the study.

2.1.2 Optimum Configuration and Design Parameters

2.1.2.1 Optimum Helicopter with Generalized Engines

Within the scope of the parametric design study, the optimum helicopter was found to be one which utilized the minimum number of blades and engines.

Considering the two airframe configurations (i.e., crane and transport), both with identical rotor configurations and engine arrangements, the crane fuselage with external cargo was found to result in a lower gross weight than the transport fuselage with internal cargo.

Since an articulated rotor was found to be inappropriate for tip turbojet application due to engine-out unbalance condition (see Reference 6) and in consideration of the fact that the means (root spring restraint) of providing additional control power to a universally mounted rotor are not applicable to a two-blade rotor (see Reference 9), the optimum (gross weight = 63,200 pounds) helicopter configuration was thus determined to consist of:

a) A three-blade, 55.83-foot-radius, universally mounted rotor.
b) A single-engine installation at each blade tip.
c) A crane-type fuselage.

The values of the design parameters for this configuration are presented in Table 3 of Section 3.0 of this volume.

2.1.2.2 Optimum Parameters for Particular Configurations

The effect of configuration on minimum gross weight is shown in Table 2 of Section 3.0. It is concluded that the gross weight increased with the following ascending order of engine arrangements.

a) Single engine per blade (minimum number of blades) - lowest gross weight).
b) Side-by-side engine arrangement (minimum number of blades) two engines per blade.
c) Over-under engine arrangement, two engines per blade - highest gross weight.

2.1.2.3 Optimum Helicopter With CAE 357-1 Engine

With the present limit on the rotor tip centrifugal force environment of 235g, a rotor having three blades, a 55.8-foot radius, over-under engines (six), and crane-type fuselage is the optimum (minimum gross weight of 64,250 pounds) configuration which utilized the CAE 357-1 engine. This model is referred to as the 1119. However, the 357-1 engine must be available with a military, static-sea-level-thrust rating of 1,900 pounds which is an 11.8 percent growth of the 357-1 engine version considered by Continental Aviation and Engineering Corp. in Task II of this study.

A four-blade, eight-engine, rotor configuration with a gross weight of 72,104 pounds is required to meet the mission requirements and the hot day hover requirements (6,000 feet, 95° F.) with a 1,700-pound, static-sea-level rating for the 357-1 engine. This model is referred to as 1108.

A complete listing of the component weights and design parameters of the above three- and four-blade configurations is presented in Table 4 of Section 3.0 of this volume.

2.1.3 Nonoptimum and Nonlimited Configurations

2.1.3.1 Weight Penalties

Reference 1 indicated that for the generalized engine parametric study the optimum configuration is three blades and three engines with a crane-type fuselage. The following penalties result from using engine arrangements other than the optimum, depending on the number of blades and the condition being considered.

Single engine per blade	no weight penalty
Side-by-side engine arrangement . .	1,900 to 3,400 pounds
Over-under engine arrangement . . .	3,080 to 4,800 pounds

The greatest percentage of the penalty is fuel weight since the primary effect of using the nonoptimum configurations is to increase the

nacelle drag. It is also possible to observe the differences in the use of the nonoptimum number of blades (Reference 1) and to determine the range of these values from Table 2 as follows:

Two blades . . . . . 3,000- to 6,400-pound decrease
Three blades . . . . . no weight penalty
Four blades . . . . . 3,700- to 7,850-pound penalty

The weight penalties for more blades than optimum are compounded from fuel weight for the additional drag of the blade profile, the nacelles, and the weight of the additional blade.

Use of the transport fuselage with internal cargo results in a weight penalty as discussed in Reference 1 as follows:

Crane-type fuselage . . no weight penalty
Transport-type fuselage. 1,000- to 1,700-pound weight penalty

2.1.3.2 Effects of Engine-Rotor Tip "g" Field

Results of the parametric design study indicate that configuration gross weight varies inversely with rotor tip acceleration. This variation is shown in Reference 1 (Volume II), which indicates that configuration gross weight continues to decrease up to a limiting value of rotor tip "g", at which point the advancing blade compressibility limit occurs.

2.1.3.3 Changing Rotor Lift Coefficient and/or Tip Speed Ranges

It does not appear that changing the upper limit of the design rotor mean lift coefficient, $C_{L_{r_o}}$, range would be of any significant benefit, since only small reductions in gross weight may be obtained above a $C_{L_{r_o}}$ of 0.50, which is the maximum value considered acceptable. For the optimum three-blade configurations, the design rotor mean lift coefficients all occur between .375 and .50. Reducing the lower limit on the hover tip speed for 235g tip acceleration limit, to 598 feet per second would realize a reduction of 3,400 pounds for the optimum three-blade, three-engine configuration. A lower limit on the tip speed of 565 feet per second would be necessary to take maximum benefit of the weight reduction indicated for the four-blade configurations.

Increasing the upper limit on tip speed would not appear to be desirable since the rotor is presently limited to 743 feet per second tip speed by advancing blade compressibility at 125 miles per hour. However, increasing the hover tip speed and tip acceleration limit would allow the hover requirement at 6,000 feet, 95° F. to be met with a smaller engine for a given rotor radius; but the forward flight tip speed would have to be limited to 743 feet per second or less.

2.1.4 In-Flight Engine Shutdown for Reduced Fuel Consumption

While not included as an integral portion of the parametric design study, the effects of engine shutdown in cruise on fuel consumption were studied for the Model 1108. Effects of engine cold drag on power required were combined with the effects of increased operating power level (per engine) on specific fuel consumption. The resulting net effect was a better than three percent reduction in required fuel per nonoperating engine without provisions for fairing to minimize cold drag.

2.2 Design Layout Studies

2.2.1 State-of-the-Art Feasibility

Development of a heavy-lift tip turbojet helicopter of 60,000 to 80,000 pounds gross weight is concluded to be within the state-of-the-art of all technologies associated with the design and fabrication of a rotorcraft of this type.

Conventional flight controls which utilize hydraulic boost cylinders are employed on the Model 1108 helicopter; the rotor suspension is a standard universal mounting system; all design aspects of the electrical system, including rotor tip located components, are considered to be basically conventional and require minimum development programs; and the attachment of the turbojet engines and nacelles to the rotor tips requires only the application of current structural design techniques.

2.2.2 Design Features

While several different rotor suspension systems were studied, it was concluded that the most desirable (i.e., weight, cost, maintainability, etc.) configuration employed a simple full gimbal support system.

Design studies indicate (see Section 4.0) that a hollow rotor mast can be designed to accommodate the transfer of system fluids and electrical power from the stationary airframe to the rotating engines, this design being compatible with the dynamic and structural support requirements of the rotor. These design studies further indicated that it is practical and, in fact, preferable to store all fluids and to originate all electrical power in the fuselage, and to transfer these to the rotor mast and rotor blades by a system of rotating manifolds, swivels, and slip rings.

Studies of primary and secondary power sources for tail rotor, electrical, hydraulic, and accessory requirements indicate that the optimum design (minimum weight) is accomplished by employing an auxiliary power unit and providing a small mast-driven gearbox.

The optimum power plant configuration, from an installation point of view, is quite evidently a single-engine nacelle. For twin-engine tip installations, the over-under configuration is superior to the side-by-side configuration as regards structural design, electrical, and fuel line installation.

2.2.3 Power Management Studies

Studies of the power management requirements of a multiengine heavy-lift tip turbojet rotor system conclude that such a system should be optionally manual or automatic, should include fail-safe and back-up features for all its functions, and that the required design is well within available equipment state-of-the-art.

2.2.4 Materials

Design/Dynamics studies indicate that rotor blade structural requirements are established by in-plane and out-of-plane frequency criteria, and not by centrifugal restraint of the blade-engine combination of bending considerations. Thus, high stiffness-to-weight ratio materials are sought for optimum design. Structural design studies conclude that extensive use of titanium alloys in the rotor blades, hub, and mast will yield the required structure for minimum weight consistent with the dynamic criteria and the requirements for high endurance limits and corrosion resistance.

2.3 Static and Dynamic Loads

An investigation was conducted to determine the loading conditions that would produce the critical design loads for the tip turbojet rotor system. The investigation includes all of the possible design loading conditions and presents either analytically or graphically the magnitude of these loads. The following conclusions pertain to the relative importance of the different static and dynamic loading conditions.

2.3.1 Critical Static Design Loads

2.3.1.1 Centrifugal Load

The critical centrifugal limit loading for the rotor system is due to a rotor speed of 105 percent of the design maximum speed (650 feet per second). The critical centrifugal limit loading for the rotor system attachments is due to a rotor speed of 125 percent of the design maximum speed.

2.3.1.2 Rotor Blade Torque

Design torque for the rotor blade is a nose down torque. This is due primarily to the gyroscopic moment caused by the tip engines. For the

maximum limit design torque condition, three conditions are combined giving a conservative loading. These conditions include tip engine gyroscopic moment, rigid coning torque, and centrifugal centering torque.

2.3.1.3 Aerodynamic Loading

The rotor blade airloads were analyzed using Cornell Aeronautical Laboratory (CAL) airload program. This program produces the steady plus first through seventh harmonic alternating lift and drag airloads. An iterative procedure was necessary to obtain the proper steady airload, which corresponds with the proper thrust for different flight conditions. The inflow distribution and collective pitch were the two inputs changed for the iterative process.

2.3.1.4 Flapwise Bending Moments

The 2.5g pullup is the condition which yields the largest steady bending moment in combination with its complement of harmonic moments. The 1g forward flight conditions yield the harmonic bending moments of the longest duration (i.e., for fatigue considerations). The -0.5g hover condition produces the largest negative in-flight bending moment at the root of the blade while negative static droop moments are critical at blade sections outboard of the root retention.

2.3.1.5 Chordwise Bending Moments

The largest steady chordwise bending moment occurs with two engines inoperative. Only the flight conditions which produce the maximum harmonic chordwise coupled bending moments were presented in the design loads report. These steady and harmonic chordwise loads are combined to produce a conservative design condition.

2.3.2 Dynamic (Transient) Design Loads

2.3.2.1 Gust

Gust load factors were derived by two separate methods. First, considering the rotor blades to be rigid and treating the hovering rotor as having undergone an instantaneous change in inflow equal to the gust velocity. Second, considering the rotor blade to be flexible and using the direct analog computer simulation method (Reference 3). Considering the blade as rigid gives a load factor greater than the design maximum of 2.5g while consideration of the flexible blade reduces the load factor to 2.25g. The rigid rotor analysis is considered to be too conservative and therefore the analog computer simulation of the flexible blade will be used for design loading.

2.3.2.2 Cyclic Pitch Transient

The direct analog computer studies simulated a whirling of the cyclic

stick at a critical frequency which is considered to be within the pilot's capability. This condition results in the maximum positive and negative chordwise bending moments.

2.3.2.3 Collective Pitch Transient

An exponential collective pitch input of 0.01 radian was used to determine the blade response using the direct analog computer. The transient collective pitch in-plane bending moment is less than that resulting from the transient cyclic pitch condition. The pitching (torsional) deflection at the tip is similar in character to the flapwise deflection curve insofar as there is no transient overshoot from the initial tip angle to the final steady-state value. Therefore, the transient torsional moments on the blade will be noncritical for the collective pitch input condition.

2.3.2.4 Dynamic Tip Environment

The maximum g loadings at the tip occur during a forward flight condition, and a 40-foot-per-second gust during hover. This tip acceleration environment was determined by considering the second harmonic motion of the blade and the deflection at the tip, then differentiating the motion twice to produce acceleration.

2.4 Structural Analysis

A static and fatigue stress analysis was conducted for the Model 1108 rotor system utilizing the static and dynamic loads which were developed in Reference 3. The following conclusions pertain to the primary structural components of the rotor system and indicate which of the various loading conditions are design-critical.

2.4.1 Component Critical Static Design Conditions

2.4.1.1 Engine Mount System and Attachment

The critical engine mount system and attachment loading occurs during the rotor limit speed condition, and during the rotor overspeed operation, both-engines-operating condition. The critical engine mount areas are the attachment bolts and lugs and the heat expansion fitting.

2.4.1.2 Main Rotor Blade Tip and Attachments

The critical main rotor blade tip and attachments loading occurs during the rotor limit speed condition, and during the rotor overspeed operation, two engines condition. The critical areas are the attachment lugs.

2.4.1.3 Main Rotor Blade Typical Section

The critical main rotor blade typical section is at rotor station 170.00 during the static droop condition due to compressive buckling stress.

2.4.1.4 Main Rotor Blade Root Retention Structure

The critical main rotor blade root retention structure loading occurs during the rotor limit speed condition. The critical areas are the tension-torsion strap and its retention bolt.

2.4.1.5 Stub Blade and Retention

The critical stub blade loading occurs during the transient cyclic stick whirl condition. The adjustable link attachment lug is critical.

2.4.1.6 Main Rotor Hub Assembly

The critical main rotor hub assembly loading occurs during forward flight, 41 miles per hour; 2.5g's, 562 feet per second tip velocity condition. The critical hub areas are the blade retention lugs and pins.

2.4.1.7 Gimbal and Attachments

The critical gimbal and attachments loading occurs during the 2.5g's loading condition. The critical areas are the bearings and Section 17-17 as defined on page 87 of Reference 4.

2.4.1.8 Restraint Spring Assembly

The outside spring fiber stress is critical.

2.4.1.9 Static Margins of Safety

A summary of the critical static margins of safety is presented in tabular form on page 5 of Reference 4.

2.4.2 Component Critical Fatigue Design Conditions

The "stop-start" cycle produces the critical main rotor system fatigue design conditions. The rotor components which experience service life limiting stresses during this cycle are the engine-to-mount attachment bolts, pins, and lugs, and the tension-torsion strap assembly.

The alternating stresses developed during a steady-state, in-trim, normal flight condition are below the rotor system component material endurance limit and nondamaging.

2.5 Dynamic, and Aeroelastic Studies

The dynamic and aeroelastic behavior of the four-bladed, universally mounted teetering rotor system proposed for the heavy-lift tip turbojet helicopter is discussed and evaluated in Reference 4. Conclusions concerning the dynamic adequacy of the rotor system are outlined in the following paragraphs for all phases of the dynamic investigations.

2.5.1 Uncoupled and Coupled Rotor Blade Frequencies

A comparison of uncoupled and coupled rotor blade frequencies, calculated using independent methods, indicates that flapwise frequencies can be satisfactorily approximated using an uncoupled model of the rotor blade whereas coupling has a more pronounced effect on in-plane frequencies. The frequency of primary interest from both a loading and dynamic point of view is the first cyclic in-plane frequency. The flapwise/in-plane coupling increases with collective pitch to reduce this first in-plane frequency by 16 percent from minimum to maximum collective pitch settings.

The natural frequency study presented in Reference 1 shows that the first six coupled cyclic and collective modes avoid resonance with their respective airload excitation harmonics throughout the collective pitch range.

2.5.2 Periodic Engine Thrust

The thrust of the tip engines will vary periodically with rotor azimuth position for all helicopter flight conditions except hover and vertical flight. The magnitude and phasing of this thrust variation will depend largely upon the engine-governor dynamics, which have not been thoroughly investigated at this time. The quantitative effect of engine inlet velocity changes on the engine alone is to change the engine thrust by a much smaller amount than the periodic variation of engine nacelle drag, and so the thrust variation should not be of primary concern.

2.5.3 Vibrations Resulting From One Engine Inoperative

The loss of one engine in flight would cause an in-plane circular motion of the rotor system and an out-of-track condition. The in-plane motion at one cycle per rotor revolution would result from a rotor system center of gravity movement away from the centerline of rotation due to unsymmetrical in-plane bending of the four blades. The rotating load due to this center of gravity displacement is in phase with the rotating unbalanced engine thrust vector. Analytical studies performed in References 4 and 6 indicate that the net load for a hover condition at design gross weight will be between 1,000 and 2,300 pounds for one or two engines out. This is a small load when compared with the gross weight of the aircraft. With an adequate rotor isolation system, this rotating force should be virtually unfelt in the fuselage.

An out-of-track condition would result from a pitch angle change on only the one blade supporting the inoperative engine. Analytical studies performed in Reference 4 indicate that the helicopter roughness which would result, however, is not expected to be more severe than that caused by occasional out-of-track conditions for smaller helicopters.

2.5.4 Mechanical Instability

Ground resonance, which is caused by a first cyclic in-plane natural frequency which is less than one cycle per rotor revolution, will be avoided with the proposed helicopter by designing the rotor blades to have a first cyclic in-plane frequency well above one cycle per revolution. Increasing collective pitch tends to lower this frequency due to flapwise/in-plane coupling and so design steps have been taken to assure a frequency margin throughout the collective pitch range. The influence of the engine rotating parts is shown to have negligible effect upon this frequency.

2.5.5 Torsional Divergence

The prospective location of the rotor blade shear center ahead of the rotor section center of pressure produces a design in which the pure torsional divergence problem is nonexistent. The torsional stiffnesses of the proposed rotor blade and root control spring, however, are large enough that the divergence tip speed would be far above normal rotor speed even if the shear center were located 15 percent of the chord aft of the center of pressure.

2.5.6 Special Dynamic Considerations

Due to the low first cyclic in-plane natural frequency of the rotor blades, it is well within pilot capability to perform a cyclic stick whirl which will excite this mode. This condition cannot be avoided and so is considered a design condition.

The possibility of carrying cargo which is slung beneath the helicopter has been investigated from the standpoint of dynamic coupling with rotor blade frequencies. The frequency of oscillation of such a sling load would be so far below any frequencies of the rotor system that no effects on rotor dynamics are to be expected.

2.5.7 Rotor Blade Flutter

The Model 1108 rotor system, as presently designed, possesses positive damping for all modes of vibration investigated in Reference 4. A variation of parameters study on blade flutter points out the following damping changes as functions of parameter changes.

a) The second cyclic mode (first in-plane mode) would be the first mode to become unstable with decreasing root control spring stiffness. This spring would have to be about 0.1 of its design stiffness to approach the stability boundary.

b) A chordwise movement of the blade tip mass from the nominal design location (0.22 chord) affects the damping of various modes in different ways. In no case does the blade flutter for center of gravity locations between the 16 percent and 28 percent chord points.

c) An increase in pitch-flap coupling (δ_3 angle) decreases the aerodynamic damping of the second cyclic mode. For a structural damping factor of .03, however, this mode should be stable for δ_3 angles up to 45 degrees.

d) The aerodynamic damping is relatively unchanged with small chordwise variations in blade shear center.

e) The rotational speed and direction of rotation of the engine rotating parts have a negligible effect upon flutter boundaries.

f) Increased blade chord provides an increase in aerodynamic damping for a majority of the modes of vibration but has a slight destabilizing effect on the second cyclic, sixth cyclic, and the sixth collective modes.

g) A flapwise blade stiffness increase at the root of the blade has negligible effect on damping.

2.6 Weight and Balance Studies

Weight and balance studies of the Model 1108 were conducted in Reference 6. These studies resulted in the following conclusions.

2.6.1 Empty Weight

The empty weight of the Model 1108 helicopter was determined to be 34,700 pounds. A summary of group weights is presented in Section 8.0 of this volume, and it is observed that rotor system weight is 16,398 pounds, or 47.3 percent of empty weight. Rotor system weight is 100 percent calculated from preliminary design drawings while the remainder of the Model 1108 empty weight is 11.3 percent calculated, 29.2 percent estimated, and 12.2 percent actual weight.

2.6.2 Aircraft Balance

Accomplishing a proper aircraft balance, both longitudinal and lateral, will present no unusual conditions or restrictions due to the type of load-carrying procedure that is anticipated. The disposable items of

useful load (i.e., fuel and cargo) may be centered on or about the main rotor centerline of rotation resulting in a minimum requirement for allowable center-of-gravity control.

2.6.3 Rotor Balance

Rotor out-of-balance studies indicate that articulated rotor systems containing lag hinges are unsuited for tip turbojet propulsion due to the large rotor in-plane forces which occur as a result of inoperative engines. Conclusions regarding rotor unbalance for the Model 1108 with inoperative engines are presented in paragraph 2.5.3 of this volume.

2.7 Wind-Tunnel Studies

The nacelle installation on the tip turbojet rotor is provided to reduce the engine external drag to a minimum while maintaining smooth, even flow to the engine compressor inlet, regardless of the external environment. The environment of the tip turbojet nacelle consists of cyclic angle of attack changes to twelve degrees, cyclic sideslip angle changes to eighteen degrees, and cyclic Mach number variations between .35 and .75.

2.7.1 Engine-Stacking Configuration

Three engine-stacking configurations were evaluated by means of wind-tunnel tests described in Section 9.0 of this volume. The configurations tested were a single engine, a vertical placement of two engines (over-under), and a horizontal placement of two engines (side by side).

2.7.2 Nacelle Inlet Configurations

Four inlet configurations (based on NACA 1 - series inlets) were tested. One configuration employed a 30-degree conical spike, or an NACA 1-30-40 (Parabolic) centerbody. The centerbody effectively prevents internal lip separation to angles of sideslip (or attack) of 20 degrees. Either centerbody improved the inlet flow conditions such that acceptable velocity profiles and low inlet losses were maintained.

With dual engines the downstream engine of any pair experiences the highest inlet total pressure loss and the greatest nonuniformity of velocity.

The side-by-side engine configuration experiences the lowest losses in pitch and the highest losses in yaw, while the over-under configuration experiences the lowest losses in yaw and the highest losses in pitch. Since the anticipated maximum pitch angle is 12 degrees and the anticipated maximum yaw angle is 18 degrees, the over-under configuration produces minimum inlet losses for the dual engine configuration.

2.7.3 Nacelle Drag

The tip turbojet engine (or engines) and engine mounts determine the nacelle diameter. The length and fairing between blade and nacelle are then

the only free variable. If the nacelle length is increased beyond the optimum length, the drag increases due to skin friction; but if the length is decreased below the optimum, large increases in drag result from flow separation. The addition of the rotor blade on the side of the nacelle produces additional expansion on the airfoil, and this double expansion on the nacelle and blade cause separation and large increases in drag as though the nacelle length to diameter ratio were too small.

The tip turbojet wind-tunnel nacelle had a length to diameter ratio of three and was tested at a Reynolds Number of 1.8×10^6. The drag coefficient (based on frontal area) under these conditions should be C_D = .05 whereas the measured values were between .13 and .2 which indicates excessive separation did occur. The drag comparisons between configurations are valid regardless of the overall drag level. For equivalent installed power, the single engine configuration produces the minimum drag and net integrated side force of all three configurations, but the side-by-side configuration is a very close second. The over-under configuration has higher drag and a substantially higher net integrated side force than the other configurations.

2.7.4 Nacelle Drag Reduction

Increasing nacelle length would reduce separation and decrease drag as shown by NACA tests of a nacelle on a wing with $\ell/D = 5$ and $C_D = .054$. Large increases in nacelle length are undesirable and believed to be unnecessary. The separation is known to be locally induced since the nacelle alone would have low drag. The local separation can be reduced by various proven methods.

a) Vortex generators which would remove energy from the freestream and add this energy to the boundary layer.

b) Addition of a speed pod which provides volume in the local area and decreases the rate of expansion. This has the same effect on the local area as increasing length has on the overall nacelle.

c) Changing the position of the blade maximum thickness/chord ratio relative to the nacelle maximum diameter/length ratio, so as to decrease the rate of expansion.

d) Boundary layer control which removes or re-energizes the boundary layer so that greater expansion can take place without separation. See Reference (11) Figures 2.10, 2.11, and 2.12.

Any of the above items are capable of reducing the drag, but items a) and b) are considered the most deisrable. The speed pod should result in a nacelle drag between that of the isolated nacelle and the NACA nacelle-wing data. The use of boundary layer control is particularly attractive due to the proximity of the energy source. This could result in a drag coefficient below that for the isolated nacelle.

2.8 Performance Analysis

Model 1108 performance is calculated in Reference 8 and summarized in Section 10.0 of this volume. Performance calculations employed conventional prediction methods with exception of the additional treatment required to account for the tip-mounted nacelle.

Prediction of the additional power required by the nacelle was accomplished by defining the relative pitch and yaw angle environment of the nacelle, as functions of rotor aximuth and tip speed ratio, and combining this environment with predicted force coefficients. It is concluded that the presence of a tip-mounted nacelle simply adds 1) an additional term to rotor profile power due to the tangential nacelle forces and 2) an additional power term due to a net radial (fore and aft) in-plane force. Using wind-tunnel drag data in the performance calculations would result in approximately 15- to 20-percent increase in the rotor horsepower required.

2.9 Stability and Control Studies

2.9.1 MIL-H-8501A Feasibility

The heavy-lift, tip-mounted turbojet, universally mounted rotor configuration is feasible as regards flight stability and controllability. Basis for stability and controllability evaluation was MIL-H-8501A, as well as additional, more stringent criteria when it was deemed applicable.

It is concluded that the control power criteria of MIL-H-8501A is not adequate for helicopters of the Model 1108 weight class. A more appropriate criteria is one based on flight test studies of helicopter angular acceleration due to control input. These studies (reported in NASA TN D-58) indicate desirable levels of control power to be two to three times that required by MIL-H-8501A.

3.0 PARAMETRIC DESIGN STUDY

3.1 Objectives

3.1.1 Introduction

The objectives of this study are to determine the optimum design parameters of a heavy-lift helicopter powered by turbojet engines installed at the rotor blade tips. The design parameters that yield a minimum gross weight configuration, capable of meeting performance requirements within the design limitations, are considered optimum.

These optimum design parameters were found for each configuration considered by determining the minimum gross weight required to meet the fuel requirements of the mission set forth in Section 3.1.2, for each combination of the design parameters in Section 3.2. Meeting the hover requirement in the performance specification was ensured by selecting required power using a generalized method of engine size determination. A side study was made to ensure that each solution would meet the maximum forward speed requirement, and have a design mean lift coefficient not exceeding .5.

3.1.2 Mission Requirements

a) Payload (outbound only)	12 tons
b) Radius	50 nautical miles
c) Cruising speed:	
1. Outboard	60 knots
2. Inbound	100 knots
d) Atmospheric condition	Sea level standard
e) Hovering time (out-of-ground effect):	
1. At take-off	3 minutes
2. At destination (with payload) . .	2 minutes
f) Fuel reserve	10% percent of initial fuel

3.1.3 Performance Specifications

a) Hover capability (OGE):	
1. Altitude	6,000 feet
2. Temperature	+95° Fahrenheit
b) Design maximum speed	125 miles per hour

3.1.4 Design Objectives and Limitations

a) Maximum tip acceleration at outboard engine centerline	235g
b) Tip speed	650 to 750 feet per second
c) Gross weight	60,000 to 80,000 pounds

d) Design mean lift coefficient at sea level ($C_{L_{r_o}}$) ..... .30 to .60

e) Engine thrust, weight, and fuel consumption based on ..... CAE 357-1 turbojet

3.2 Design Parameters

The variable design parameters used with each configuration (see Section 3.3) are as follows:

a) Chord, c = 6.0, 6.5, 7.0, 7.5 feet

b) Hover tip speed, V_{T_H} = 550, 600, 650, 700, 743, 750 feet per second

c) Centrifugal force gravity field at centerline of outboard engine in gravity units, g.

3.3 Configurations

Table 1 lists the eight configurations considered in the parametric design study.

TABLE 1
CONFIGURATIONS

Number of Blades	Engine Arrangement	Fuselage			Equivalent Drag Area (square feet)
		Type	Loading	Landing Gear	
2	S	Crane	External	Fixed	Outbound: 200 Inbound: 100
3	S	Crane	External	Fixed	Outbound: 200 Inbound: 100
"	S-S	"	"	"	" " "
"	O-U	"	"	"	" " "
4	S	Crane	External	Fixed	Outbound: 200 Inbound: 100
"	S-S	"	"	"	" " "
"	O-U	"	"	"	" " "
4	O-U	Transport	Internal	Retractable	Outbound: Inbound: 50

S = one engine per blade.
S-S = side-by-side mounting of two engines per blade.
O-U = Over-under mounting of two engines per blade.

3.4 Optimum Configurations and Design Parameters

3.4.1 Generalized Engines

The generalized or "rubber" engines are based on the CAE 357-1 version of the J69-T-29 engine. The results of the parametric study with the generalized engines indicate that the lowest gross weight machine is obtained with the minimum permissible number of blades and the minimum number of engines per blade. The study also indicates that a configuration with a transport fuselage had a higher gross weight than a like configuration which utilized a crane-type fuselage.

The two blade rotor configuration is not considered appropriate because of control power considerations. The results of the Parametric Analysis indicate that the optimum configuration for the prescribed mission (see Section 3.1.2) is a helicopter with the following characteristics:

a) Three blades
b) A single engine per blade
c) A crane-type fuselage

The optimum design parameters for all eight configurations considered are presented in Table 2.

Table 2 is composed of three parts:

2a) This table lists the optimum design parameters which fall within the limitations of Section 3.1.4.

2b) The tip speed is optimized in this table without the limitations of Section 3.1.4 imposed.

2c) This table lists the optimum design parameters corresponding to a hover tip speed of 743 feet per second. (The advancing blade compressibility limit occurs with this hover tip speed at a helicopter forward speed of 125 miles per hour.) The g limitations of Section 3.1.4 are allowed to be exceeded in this table.

Detailed characteristics for the optimum three-bladed configurations of Tables 2a and 2b are provided in Table 3.

TABLE 2a
OPTIMUM DESIGN PARAMETERS

Condition	Configuration	W_G Pounds	n	V_{T_H} fps	C Feet	$C_{L_{r_o}}$	V_{T_V} fps	R Feet	F_R Pounds	F_R/n Pounds
n = 235, hover tip speed = 650 f.p.s. min. (min. allowed by Sect. 3.1.4) Chord is optimum for min. gross weight.	2 blades, S, crane	56,800	235	652	7.50	.500	V_{T_H}	55.83	9415	4708
	3 blades, S, "	63,200	235	650	6.91	.376	642	55.83	10868	3623
	3 blades, S-S, "	65,300	235	650	7.01	.382	641	55.83	12000	2000
	3 blades, O-U "	66,280	235	650	7.01	.388	622	55.83	12088	2016
	4 blades, S, "	70,340	235	650	6.91	.302	613	55.83	12746	3186
	4 blades, S-S, "	73,150	235	650	6.94	.314	615	55.83	14175	1772
	4 blades, O-U, "	73,800	235	650	7.21	.305	564	55.83	14268	1782
	4 blades, O-U, transport	74,800	235	650	6.99	.318	557	55.83	14450	1807

Legend: S = One engine per blade.

S-S = Side-by-side mounting of two engines per blade.

O-U = Over-under mounting of two engines per blade.

Table 2b
OPTIMUM DESIGN PARAMETERS

Condition	Configuration	W_G	n	V_{T_H}	C	$C_{L_{r_o}}$	V_{T_V}	R	F_R	F_R/n_e
n = 235 Chord and hover tip speed are optimum for min. gross wt.	2 blades, S, crane	56,800	235	632	7.50	.50	$=V_{T_H}$	56.3	9415	4708
	3 blades, S, "	59,800	235	598	6.82	.50	V_{T_H}	47.3	12148	4049
	3 blades, S-S, "	62,100	235	600	7.01	.50	V_{T_H}	47.5	13425	2235
	3 blades, O-U, "	63,200	235	600	7.14	.50	V_{T_H}	47.5	13462	2244
	4 blades, S, "	63,800	235	565	7.04	.475	V_{T_H}	42.2	15256	3814
	4 blades, S-S, "	67,100	235	570	7.01	.490	V_{T_H}	43.0	16920	2116
	4 blades, O-U, "	68,600	235	565	7.18	.50	V_{T_H}	42.2	17391	2155
	4 blades, O-U, transport	70,000	235	565	7.34	.50	V_{T_H}	42.2	17882	2234

Legend: S = One engine per blade.
S-S = Side by side mounting of two engines per blade.
O-U = Over-under mounting of two engines per blade.

Table 2c
OPTIMUM DESIGN PARAMETERS

Condition	Configuration	W_G	n	V_{T_H}	C	$C_{L_{T_O}}$	V_{T_V}	R	F_R	F_R/n_e
n = Opt. Hover tip speed = 743 f.p.s. Chord = optimum. No n limitation	2 blades, S, crane	52,300	401	743	7.0	.50	$=V_{T_H}$	43.0	9498	4750
	3 blades, S, "	56,100	453	743	6.5	.40	V_{T_H}	38.1	11383	3796
	3 blades, S-S, "	58,000	453	743	7.0	.375	V_{T_H}	38.1	12736	2121
	3 blades, O-U, "	59,400	427	743	6.75	.385	740	40.4	12373	2060
	4 blades, S, "	59,800	490	743	6.55	.335	743	35.2	13346	3338
	4 blades, S-S, "	63,200	457	743	6.55	.325	743	37.5	14563	1819
	4 blades, O-U, "	64,100	463	743	6.75	.325	706	37.3	14814	1852
	4 blades, O-U, transport	65,800	436	743	6.75	.315	679	39.7	14676	1836

Legend: S = One engine per blade.
S-S = Side by side mounting of two engines per blade.
O-U = Over-under mounting of two engines per blade.

TABLE 3
OPTIMUM CONFIGURATION DETAILS
GENERALIZED ENGINES

	Configuration (a)	Configuration (b)
Design gross weight, W_G, pounds	63,200	59,800
Hover tip speed at centerline of engine, V_{T_H}, fps	650	598
Chord length, c, feet	6.91	6.82
Main rotor radius, R (from centerline of rotor to centerline of engine shaft), feet	55.83	47.3
"a" field at engine centerline, g	235	235
Design mean lift coefficient, $C_{L_{r_o}}$	376	0.50
Cruise tip speed, V_{T_V}, fps	642	598
Number of main rotor blades, b	3	3
Number of engines, n	3	3
Engine arrangement	One engine at tip of each blade	
Solidity, σ	.1162	.138
Total engine rated thrust, pounds	10,868	12,148
Rated thrust per engine, pounds	3,623	4,049
Weight per engine, pounds	735	815
Net thrust, F_n, available per engine at S.L. standard atmosphere and 598 fps, pounds	3,304	3,670
Net thrust, F_n, available per engine at 6000 ft., 95° F. std. hot day, pounds	2,270	2,510
MRT sfc at 598 fps and S.L. standard atmosphere, lb/hr/lb.thrust	1.260	1.260
75 percent NRP sfc at 598 fps and S.L. std. atmosphere, lb/hr/lb.thrust	1.416	1.416
Maximum engine diameter, inches	31.9	33.16
Maximum nacelle diameter, inches	37.9	39.4
Engine length, inches	60.6	63.0
Nacelle length, inches	86.2	89.6
Empty weight, pounds	27,826	24,007
Fuel weight, pounds	10,774	11,193
Payload, pounds	24,000	24,000
Crew and oil, pounds	600	600

Configuration (a): Optimum configuration within limitations of Section 3.1.4.
Configuration (b): Optimum Configuration for tip speed not limited by Section 3.1.4.
(An empty weight breakdown for the above two configurations is given in Table 5.)

3.4.2 CAE 357-1 Version of the J69-T-29 Engine

As the Continental CAE 357-1 engine is one of the generalized engines used in the parametric study, a maximum thrust (1700-pound rating) limit line provided the necessary restrictions to allow the rotor design parameters to be determined for use with this engine. The description, performance, and installation of the CAE 357-1 engine is presented in the tip turbojet design layout study, Volume III. This version of the heavy-lift helicopter is designated as Model 1108.

An over-under engine installation arrangement was used for Model 1108 rather than side-by-side engine arrangement because of the anticipated difficulties associated with unequal inlet air distribution between engines at high advance ratios. At that time it was realized that the nacelle drag effect would be increased by using the over-under arrangement.

The parametric study indicated that, within the allowable design variables specified in Section 3.1.4, an optimum solution could be found which had excess thrust available. This configuration was identical to Model 1108 except that the rotor blade chord was 5.5 feet.

Rotor design studies showed the minimum chord which would provide clearance for engine service lines is 6.5 feet. The design studies also showed blade weight decreases with increasing chord but the new blade weight was 1,800 pounds greater than assumed in the parametric study.

The increase in blade chord and rotor weight required more power for hover so that the 1,700 pound rated thrust of the CAE 357-1 engine was marginal to provide HOGE capability at 6,000 feet, 95° F. To reduce gross weight, some consideration has been given to cruise on six of the engines with the cruise tip speed reduced to the optimum of 540 feet per second. This realized an 800-pound fuel weight reduction. However, performance for the Model 1108 as listed in Reference (8) is computed on the basis of all eight engines running, as ability to shutdown and relight engines in flight has not been provided. A total of 600 pounds was removed from other components where savings could be achieved over the statistical estimates (see Table 5 for final weight breakdown of this configuration compared to estimates used in the generalized engine study). The major differences between the final weight conditions and the parametric study weight are that the generalized helicopters were considered to be fitted with two auxiliary power units while the hardware engine versions were considered to have one. Also, three crew members were included in the generalized engine study and only two crew members in the CAE engine study.

The configuration details of the Model 1108 are summarized in Table 4.

By increasing the 235g tip environment to 282g for 6,000 feet, 95° F. HOGE, the Model 1108 could be made to meet all requirements with eight of the 1,700-pound rated thrust versions of the 357-1 engines without reducing tip speed below cruise tip speed or shutting down engines during cruise. The tip acceleration during cruise and sea level hover would be below the 235g limit presently imposed.

A three-blade, six engine, over-under crane configuration could be built to meet the hover and mission requirements with an 11.8 percent increase in the CAE 357-1 engine thrust rating. This solution is designated as Model 1119, and is listed with Model 1108 in Table 4.

TABLE 4
OPTIMUM CONFIGURATION DETAILS
CAE 357-1 ENGINE

	Model 1108	Model 1119
Gross Weight, W_G, pounds	72,104	64,250
Hover tip speed at centerline of engine, V_{T_H}, f.p.s.	650	650
Chord length, c, feet	6.5	6.5
Main rotor radius, R (from centerline of rotor to centerline of engine shaft), feet.	55.83	55.83
"n" field at engine centerline, g	235	235
Design mean lift coefficient, C_{Lr_o}	329	405
Cruise tip speed, f.p.s	592	639
Optimum tip speed, f.p.s	540	590
Number of main rotor blades, b	4	3
Number of engines, n	8	6
Engine arrangement	One over the other at each blade tip	Over-under at each tip
Solidity, σ	.148	.111
Total engine rated thrust, pounds	13,600	11,400
Rated thrust per engine, pounds	1,700	1,900
Weight per engine, pounds	365	428
Net thrust, F_n, available per engine at S.L. std. atmosphere and 650 f.p.s. pounds	1,550	1,730
Net thrust, F_n, available per engine at 6,000 ft, 95° F. std. hot day and 650 f.p.s. pounds	1,057	1,195
MRT sfc at 592 f.p.s. and S.L. std. atmosphere, lb/hr/lb. thrust	1.256	1.256
75 percent NRT sfc at 592 f.p.s. and S.L. std. atmosphere, lb/hr/lb. thrust	1.414	1.414
Maximum engine diameter, inches	25.25	25.25
Maximum nacelle height, inches	57.00	57.00
Maximum nacelle width	30.00	30.00
Engine length, inches	47.97	47.97
Nacelle length, inches	68.3	68.3
Empty weight, pounds	34,700	28,114
Fuel weight, pounds	12,924	11,676
Payload, pounds	24,000	24,000
Crew and oil	480	460

Model 1108: CAE 357-1 rated thrust.
Model 1119: CAE 357-1 engine with 11.8 percent growth in thrust.
(The weight breakdowns for the above configurations are given in Table 5.)

TABLE 5
WEIGHT BREAKDOWNS

Component	Configurations			
	Generalized Engines		CAE 357-1 Engines	
	Config. (a) of Table 3	Config. (b) of Table 3	Model 1108	Model 1119
Rotor group	11,892	8,432	16,673 ‡	12,620 ‡
Pylon	1,120	703	1,731	1,207
Gearbox	200	200	200	200
Tail Rotor and drive	328	306	383	332
Stabilizer	230	230	257	230
Body group	2,972	2,876	3,203	3,020
Landing gear	2,527	2,380	2,897	2,570
Flight controls	1,286	1,226	1,434	1,310
Engines	2,205	2,444	2,920	2,190
Engine components	1,434	1,548	1,679	1,260
APU	730	730	365	365
Fuel systems	1,077	1,119	1,292	1,168**
Instruments	296	296	296	296
Electrical	937	937	750	750
Electronics	275	275	275	275
Furnishings	317	305	345	321
Crew and oil	600	600	480	460
Cargo	24,000	24,000	24,000	24,000
Fuel	10,774	11,193	12,924*	11,676**
Total	63,200	59,800	72,104	64,250
Closure error	0	0	408	0

* Cruise with six of eight engines at optimum V_T.

** Cruise at optimum V_T.

‡ Based on latest design information 5-28-64.

3.5 Overload and/or Growth Versions

3.5.1 Overload Configurations

3.5.1.1 Model 1108

The requirement to HOGE at 6,000 feet, 95° F. at the mission gross weight necessitates the installation of power that is greatly in excess of the power required to HOGE at sea level standard. This excess power can be used to advantage, however, for overload missions under standard conditions. Table 6 illustrates the payload and range possibilities of the four-bladed Model 1108 under overload conditions.

TABLE 6
PAYLOAD AND RANGE CAPABILITIES

Payload (tons)	W_G (lb.)	HOGE	Radius (naut. mile)	Allowable Flt. Load Factor
12	72,104	6,000 ft/95° F.	50	+2.5
20	90,100	6,000 ft (std. temp.)	50	+2.0
26	103,200	1,000 ft (std. temp.)	50	+1.75
30	104,900	Sea level (std. temp.)	35	+1.72

3.5.1.2 Model 1119

The payload and range capabilities of the Model 1119 are shown in the following table. The sea level heavy-lift capability, because of the large amount of installed power, is evident as it was for the Model 1108.

TABLE 7
PAYLOAD AND RANGE CAPABILITIES

Payload (tons)	(lb.)	HOGE	Radius (naut. mile)	Allowable Flt. Load Factor
12	64,250	6,000 ft/95° F.	50	+2.5
20	82,850	5,500 ft (std. temp.)	50	+1.93
25	94,650	500 ft (std. temp.)	50	+1.68
28	95,650	Sea level (std. temp.)	35	+1.67

4.0 DESIGN LAYOUT STUDIES

4.1 Introduction

Optimizing the design of a tip turbojet rotor system entailed the careful blending of its aerodynamic, propulsion, dynamic, structural, mechanical, and subsystem characteristics. With this in mind, the initial design layouts were developed concurrently with the analytical studies. As areas of concern were resolved, the layouts established the configurations as described in the following paragraphs. All designs were reviewed to assure that the basic design criteria were met. In addition, minimum weight, low cost, reliability, and ease of maintenance were given thorough consideration.

4.2 Rotor System

A main rotor system that met all the requirements was designed considering rotor basic geometry, structural arrangement, retention, hub, mast, control and turbojet engine attachment at the tip. The rotor assembly is shown in Figures 1 and 2.

4.2.1 Hub Assembly

Four types of hubs for mounting the rotor were evaluated and the gimbal-type hub was chosen. This choice was principally in the interest of economy associated with reduced development risk plus the simplicity associated with designing the hub in a large size. Paragraphs 4.2.1.1 through 4.2.1.4 summarize the justifications for this decision.

4.2.1.1 Rigid Rotor Retention

The rigid rotor hub was eliminated because its structural integrity had not been proven and though mechanically simple as a hub it became complex when the rotor support and aircraft isolation system were included.

4.2.1.2 Articulated Rotor Retention

The articulated rotor hub suspension was eliminated because 1) it required heavy droop stops in connection with flapwise articulation, 2) adverse vibration from in-plane blade lag (in the event of an engine failure) with chordwise articulation and 3) ground resonance problems accompany this system, and relatively complex hinge retention at hub.

4.2.1.3 Teetering (See-Saw) Rotor Suspension

The teetering rotor hub suspension was eliminated because it is only applicable to a two-blade rotor system and the dynamics plus controllability analyses indicated that at least three blades would be required.

4.2.1.4 Universal Rotor Suspension

The gimbal (or universal) rotor hub incorporated details which tend to diminish the number of unknowns and is backed by a substantial amount of supporting data. The addition of an elastic restraint in combination with the gimbal mounting of the hub produces an arrangement that combines the features desired for satisfactory control and low vibration and stress levels at an acceptable weight. A constant velocity universal joint was also studied for this application but, because of its inherent complexity, greater weight, and negligible vibration improvement, it was discarded in favor of the simple, conventional gimbal ring suspension.

4.2.2 Rotor Blade Assembly

By process of iteration the many design requirements were evaluated on their merit and compared on the basis of low weight in order to define the root and tip retention, basic section, and materials requirement. Configurations evolved met the requirements for in-plane and flapwise stiffness, attachments, end fixity, centrifugal force, chordwise and flapwise weight distribution, manufacturability, etc.

4.2.2.1 Rotor Blade Retention

Rotor blade retention is very closely integrated with hub design. Six types of rotor retention arrangements were evaluated and the stub blade type was chosen as having the most features in its favor. Paragraphs 4.2.2.1.1 through 4.2.2.1.6 summarize the justification for the choice.

4.2.2.1.1 Internal Strap

The internal tension-torsion strap hollow cylinder type retention configuration with roller bearings for pitch was eliminated because the rather long slender tube would not provide the in-plane stiffness needed without increasing the flapwise stiffness considerably above the flapwise requirement. This is because the cylindrical shape is symmetrical about its axis. When attempting to shape or machine the cylinder to provide different stiffnesses in different planes, the cost and weight become excessive.

4.2.2.1.2 Modified Internal Strap

The modified internal tension-torsion strap retention arrangement was similar to that of 4.2.2.1.1 above except the hollow cylinder was changed to a hollow and shorter transition between the blade and the hub. However, this configuration was eliminated because the weight was high and because it was questionable whether the associated large hub forging could be manufactured with existing equipment.

4.2.2.1.3 External Strap In-Plane

The in-plane external tension-torsion strap retention was arranged much like the internal strap configuration except that two tension-torsion straps were located externally in the chord plane, one on each side of the rotor centerline. This configuration was eliminated because of high weight plus nonlinearity and complexity difficulties encountered from the feathering restraint not being on the feathering axis.

4.2.2.1.4 Laminated Rubber

The rubber laminated bearing retention scheme, which featured thin laminations of metal and rubber located in a hollow cylinder (or transition) that carried all loads except centrifugal, provided in-plane and flapping stiffness, and allowed motion for pitch change. This configuration was eliminated because of the high weight associated with the large laminated bearings, high pitch control loads, and the unproven reliability of the laminated bearing.

4.2.2.1.5 Flexure Hinge

The flexural hinge retention system is composed of four diagonally opposed straps which extend from the hub to the rotor carrying all loads and deflections except centrifugal. In order to accommodate the loads, the rotor hub must be large enough to provide attachment of the widely displaced straps. This configuration was eliminated because of high weight of hub, difficulty of exact matching of the four straps, plus the complexity, nonlinear, and interaction of in-plane, flapping, and pitch characteristics.

4.2.2.1.6 Stub Blade

The stub blade retention system features one tension-torsion strap and two bearings displaced spanwise on the feathering axis. Axial centrifugal force is taken by the strap and the bearings define feathering motion as well as carry nonaxial loads from the blade to the hub. The significant difference between this system and the internal strap (in a tube) is that one portion of the bearing support is part of the hub and the other portion is part of the blade and they complement each other on a hinge basis (rather than concentric tubes) so that in-plane and flapping stiffness can be appropriately distributed at low weight. For aerodynamic improvement the inboard portion is an airfoil shape and is thus called the "stub blade". Stiffness, or spring rate, of the bearings and bearing supports must be experimentally substantiated before optimization of the retention system geometry. In summary, the stub blade retention method was selected in preference to other configurations since it is superior from the standpoint of low weight, manufacturing feasibility, cost, versatility of design, growth potential, and aerodynamic cleanliness.

4.2.2.2 Blade Section

Design of the basic blade required individual optimization of each design criteria since the arbitrary use of a scaled-up version of an existing blade showed a prohibitive weight penalty. Through the use of structural optimization data and data for the first approximation of the weights of spar caps, webs, and skins, it was possible to determine from the parametric design study, stiffness parameters which define the blade section properties. Because of the structural, and thus weight advantages at the root and tip of the blade, plus the manufacturability benefits, the constant chord blade was adopted. The comparatively small increase in aerodynamic efficiency of a tapered blade chord was not considered sufficient to offset the nontapered advantages. Since the stiffness required is a function of the mass distribution, the net cross-sectional areas required to resist the centrifugal loads was computed for several blade stations. Stiffness, mass distribution, and natural frequency were found and checked against that required. This process was repeated until further changes did not show significant weight saving. Skin thicknesses were based on conservative torsional stiffness data that assures flutter-free operation throughout the complete feathering range spectrum.

A basic NACA 0015 airfoil represents the blade section contour. The actual blade section evolved to be a three-cell structure. The front cell from 0 to 5 percent forms the leading edge, is nonstructural, and is a (full-span) removable panel for fuel, oil, and electrical systems access. The middle cell from 5 percent to approximately 50 percent chord is a box structure composed of front and rear spar attached by skin panels. The aft cell from 50 percent to 100 percent chord, consists of skin panels supported by aluminum honeycomb and a load-carrying trailing edge. The primary means of attachment of the main and aft cells to each other will employ fatigue resistant bending plus mechanical fasteners only if required to provide redundancy. The fewest number of parts consistent with the manufacturing technique were planned. All parts can be manufactured with existing equipment through the use of special tools and jigs. A detailed comparison of many materials showed that for minimum weight structure the material that shows the best stiffness and fatigue properties for the rotor system is titanium. The wide acceptance of titanium for major components of high-speed aircraft and the routine type procedures for present-day fabrication, leave no question that titanium will be satisfactory in this application.

4.2.3 Rotor Mast

The rotor mast, in addition to its conventional function of carrying, lifting, bending, torque and spring restraint loads, was required to act as a transfer device from static to rotating for electrical and engine fluid systems, and to drive an accessory gearbox. Primarily in the interests of low weight, the main rotor mast driven gearbox will only

drive minimum accessories and tail rotor in the event of an auxiliary power unit (APU) failure. Primary tail rotor and accessory drive is by the auxiliary power unit. For whirl stand installation the mast will be mounted rigidly by two sets of bearings. For a flight installation elastomeric isolation components will be added.

4.2.4 Flight Controls

The flight controls are of a conventional hydraulically operated type with three dual boost cylinders and dual system throughout the safety. A spring restraint system can be incorporated, if required, between the rotor shaft and mast to provide satisfactory stability and control.

4.2.5 Hydraulic System

The two separate hydraulic systems, mentioned above for controls, are 3,000 p.s.i. systems; one powered by the main rotor-driven gearbox and the other by the APU. Additional capacity was designed into the hydraulic system to accommodate landing gear, wheel braking, and steering and cargo hoist requirements.

4.3 Power Plant Installation

The design layouts determined the installation of the turbojet engines (normal requirements) at the rotor tip while meeting other special environmental conditions such as gyroscopic moments, centrifugal loads, orientation relative to rotor blade, airflow paths, fluid and electrical system service, and close control of weight and center of gravity.

4.3.1 Engine Installation

The engine considered for the Model 1108 is the Continetal Model 357-1, a modified J69-T-29, rated at 1,700 pounds maximum military rated thrust. Design studies were made for three types of engine installation: 1) single engine on a blade tip, 2) two engines on a blade tip located one above the other vertically (over-under) and 3) two engines on a blade tip located one beside the other horizontally (side-by-side). As far as installation design was concerned, the single engine per blade proved to be the most advantageous. When two engines are needed, the over-under configuration is preferred to the side-by-side from the overall installation point of view (with the possible exception of aerodynamic effects).

The engine mount design required close coordination with Continental Aviation and Engineering Corp. to produce a mutually satisfactory interface. Primary loads are transferred from the engine to the blade by the main mount that attaches to two points on the inboard side of each of the two engines on one blade. These points were chosen because they are on a relatively rigid part of the engine structure and approximately on the

transverse plane of the engine center of gravity. A single point (per engine) mount attaches to the aft portion of each engine for stabilization and allows for engine growth due to temperature. This mount configuration was designed to meet all loads and combination of loads plus proper location relative to blade, supporting systems, and cowling.

4.3.2 Nacelle Design

Design of the nacelle for the engines was based on external lines, structural integrity, position relative to blade, inlet, exhaust, compatibility with firewall, accessories serviceability, cooling air flow paths, and materials. The cowl was attached to the rotor blade and is hinged to open for easy service. A study layout defined an inlet, body, and exhaust configuration that gave the best compromise between external aerodynamics and design for best overall air inlet distribution throughout the operating range. Firewalls, within the cowl, were placed so that engines were isolated from each other and engine accessory compartments were separated from the engine hot compartments. Fiberglass was used where compound shapes were involved, aluminum for skin panels, and titanium where high temperatures would not permit fiberglass or aluminum.

4.3.3 Engine Cooling

Engine compartments have air passing through to maintain compartment temperature limits. The air is supplied through the use of ram inlet bleed in the forward part and an ejector in the aft part of the nacelle. Cooling air passages and radiation shields were designed so that the rotor blade and its attachments, as well as the engine and its components, would be maintained within the specified limits. Engine oil is cooled by an oil-to-air radiator submerged in the rotor blade, which takes air from the higher pressure area under the blade and discharges the air in a lower pressure area on top of the blade. Engine compartment and engine oil cooling may be furnished, for static operation on the ground, by the ejector and a portable electric blower as applicable.

4.3.4 Engine Control and Power Management

The philosophy of the control of the helicopter rotor and the tip turbojet engines is to govern the speed of the rotor and let engine thrust correct off-speed conditions by a signal from the rotor governor. After studying many engine control schemes it was decided to give the pilot the control of rotor pitch in the collective stick and let the governor maintain the main rotor speed as desired from the rotor speed selector control. However, it was found that a "coarse" bias control relationship between collective stick position and engine thrust (engine r.p.m.), and between collective stick position and governor (governor droop compensation), did improve overall response time. Also the pilot has been provided with engine thrust trim controls and a twist grip control with "off,"

"idle-start", and "run" positions. The resultant "power management system" enables the pilot to control and coordinate all operating engines with a minimum of manual inputs to the system. It contains fail-safe features and back-up systems consistent with the high degree of safety and controllability demanded of primary flight/engine controls. The systems, both basic and back-up, are combined electronic and electro-mechanical. There are three modes of operation; manual, automatic, and mixed. Manual is used for engine start and shutdown, static ground running, and as a back-up for the automatic system. The automatic system is used in normal operation. The mixed, a combination of automatic and manual, is used to permit manual operation of a portion of the automatic system in case of partial automatic malfunction. These modes of operation are available to the pilot on a selection basis.

Inasmuch as all modes require electrical power, this system will be fed from the essential electrical bus. The primary AC generator supplies power to this bus, with the secondary generator as a back-up power source. In case of APU failure, the standby generator driven by the main rotor gearbox will be switched to the essential bus. All components in the manual system are separate from the automatic system, including the separate actuators, so a single failure cannot disable the power management system.

Oscillatory engine thrust and rotor drag may be encountered within a revolution of the rotor. Many factors, such as inertia of rotating components, control response, inlet velocity, engine attitude, etc., could contribute to such oscillations. These effects will be studied individually and concurrently in future programs; therefore, if warranted, the existing power management system incorporates provisions for cycling power control for any mode required.

4.3.5 Fuel and Lubrication Systems

Fuel and oil will be supplied to the engines from their own tank and tank pump at the foot of the rotor mast (nonrotating). Flow paths will continue across a rotating joint, up through the inside of the mast, distributed to the blades, and out the blades to the engines. The airframe pumps will feed fuel and oil to the rotor hub and centrifugal force, due to rotation, will supply the pressure required at the engines. Adequate pressure will be supplied from the pumps to sustain static engine operation on the ground. Plumbing for carrying fuel and oil through the rotor blade will be in the leading edge cell (0 to 5 percent chord) and be attached to the front spar. The leading edge nose section is removable for access to these and other engine systems. Materials, location relative to blade neutral axis, and attachments have been designed to satisfy the centrifugal force, blade flapping, and blade static droop requirements.

Since fuel is consumed at the rotor tip, this system was designed for continuous flow during operation. However, since the lubricating oil has storage at the tip, the oil system was designed to replenish only on demand so that the engine integral oil tank will always be full and there will not be any unbalance of oil weight from one engine to another and/or one blade to another. Being a demand system, both engines at the tip of one rotor blade needed only one oil replenishment line from the hub.

The fuel supply was designed to furnish two complete feed systems from the tank(s) to the rotor hub. One engine at the rotor tip of each blade will normally receive fuel from one of the systems through the mast, while the other engine will normally receive fuel from the other system through the mast. (Note that this provides each engine with a separate line from the hub.) Since the two systems that go through the mast have an emergency crossfeed valve at the rotor hub (after going through the mast), either system can supply all engines with fuel in case of malfunction of the other.

Fuel and oil systems were designed for complete control with back-up and fail-safe features throughout.

4.3.6 Starting System

Turbojet engine starting received extensive study by the contractor and Continental Aviation and Engineering Corp. to assure that the starting system which evolved would be practical, efficient, and optimum for the purpose. The methods of engine starting considered were electrical cranking, hydraulic cranking, cartridge cranking, windmill starting by cranking the main rotor, and air impingement cranking. On a comparison basis, five out of the six modes of starting were eliminated because of one or more undesirable characteristics such as high weight at rotor tip, high overall weight, high pressure plumbing in the rotor, and complexity. The air impingement cranking system design showed the greatest advantage in all characteristics. A single impingement air duct was routed from a nonrotating APU to one tip engine on each blade much in the same manner as the fuel and oil except that only one engine in each blade received impingement air to minimize weight at the tip and to simplify air starting controls. Other engines would be started by windmilling after the air impingement supplied engines had the rotor up to "lite-off" speed. For static ground starting, a ground supply attach connection was furnished on the one engine at each blade which did not have a blade-supplied impingement air system.

4.3.7 Auxiliary Power Unit

Reference has been made to an APU. The total drive system was designed to include a source of auxiliary power other than the main propulsion engines; and though the industry-accepted nomenclature for this device is

"Auxiliary Power Unit", it functions as a primary power unit in normal operation and only for emergency operation (APU failure) will the essential components be driven from the main rotor shaft. Under normal operation the APU provides power for tail rotor, two AC generators, and the hydraulic pump(s).

4.4 Electrical System

4.4.1 Power Distribution (Including Slip Rings)

The power distribution system is supplied by two separate sources. The auxiliary power unit (APU) is the primary source, and the main rotor accessory gearcase is the secondary, or emergency, source. The APU drives two 30-kilovolt-ampere, 400-cycle generators as primary electric power generation sources. One generator (primary) supplies AC power to the essential bus and the other generator (secondary) supplies AC power to the main bus. These two buses are separated by a power relay which allows the secondary generator to be switched to the essential bus in case of primary generator failure. This system was chosen over the more complicated parallel bus system. The APU also provides DC power from its starter generator and emergency DC power from its battery.

An emergency, or standby, electrical source consists of a 15KVA, 400-cycle generator driven from the main rotor accessory gearbox. If a failure occurs in the APU, this generator will provide AC power to the essential bus which feeds the primary flight electrical equipment. In this system consideration will be given either to a two-speed gearbox or a constant speed drive unit between the main rotor gearbox and the generator, to provide for constant generator speed if different rotor speeds are used for cruise and hover. Final selection will be evaluated in detail design, which is not within the scope of this study.

4.4.1.1 Slip Rings

The slip ring assembly is a primary item in the electrical distribution system. It distributes control and instrumentation power to the engine nacelles and is located at the base of the main rotor drive shaft. Approximately 320 rings are required. Thorough investigation has indicated that a modular "platter" type assembly will give highest reliability, low noise level, and long service life. It is most efficient from a space standpoint which allows wide rings and block-type brushes. This type has the rings arranged concentrically on the tops and on the bottoms of a series of discs, with two or more silver-graphite block brushes per ring.

4.4.3 Main and Auxiliary Power Unit Instrumentation

4.4.3.1 Power Plant Instrumentation System

The engine monitoring system has two basic systems: a) the primary, which is concerned with engine shaft speeds and turbine inlet temperature and b) the secondary, which monitors oil temperature, oil pressure, and fuel pressure. The components of these systems which operate in the high g environment have been extensively discussed with several prominent manufacturers. This has led to the conclusion that existing standard units, namely, the rotary tachometer generators, pressure synchros, and resistance-type temperature bulbs can be used without modification. Early centrifuge testing in the next program phase will determine the validity of this conclusion.

Each tip turbojet is provided with a group of sensors or transmitters with the exception of fuel pressure units. The fuel pressure is measured at each fuel system manifold located at the top of the rotor mast. It is considered unnecessary to indicate pressures at the engines because of the very large pressure increment provided by centrifugal force.

4.4.3.2 Auxiliary Power Unit Instrumentation

The instrumentation systems of the APU consists of a tachometer, oil temperature, oil pressure, and turbine inlet temperature. These instruments are of standard design and the same as those used for the main engines with the exception of the turbine inlet temperatures system where a direct reading thermocouple is used in place of a servo-type system.

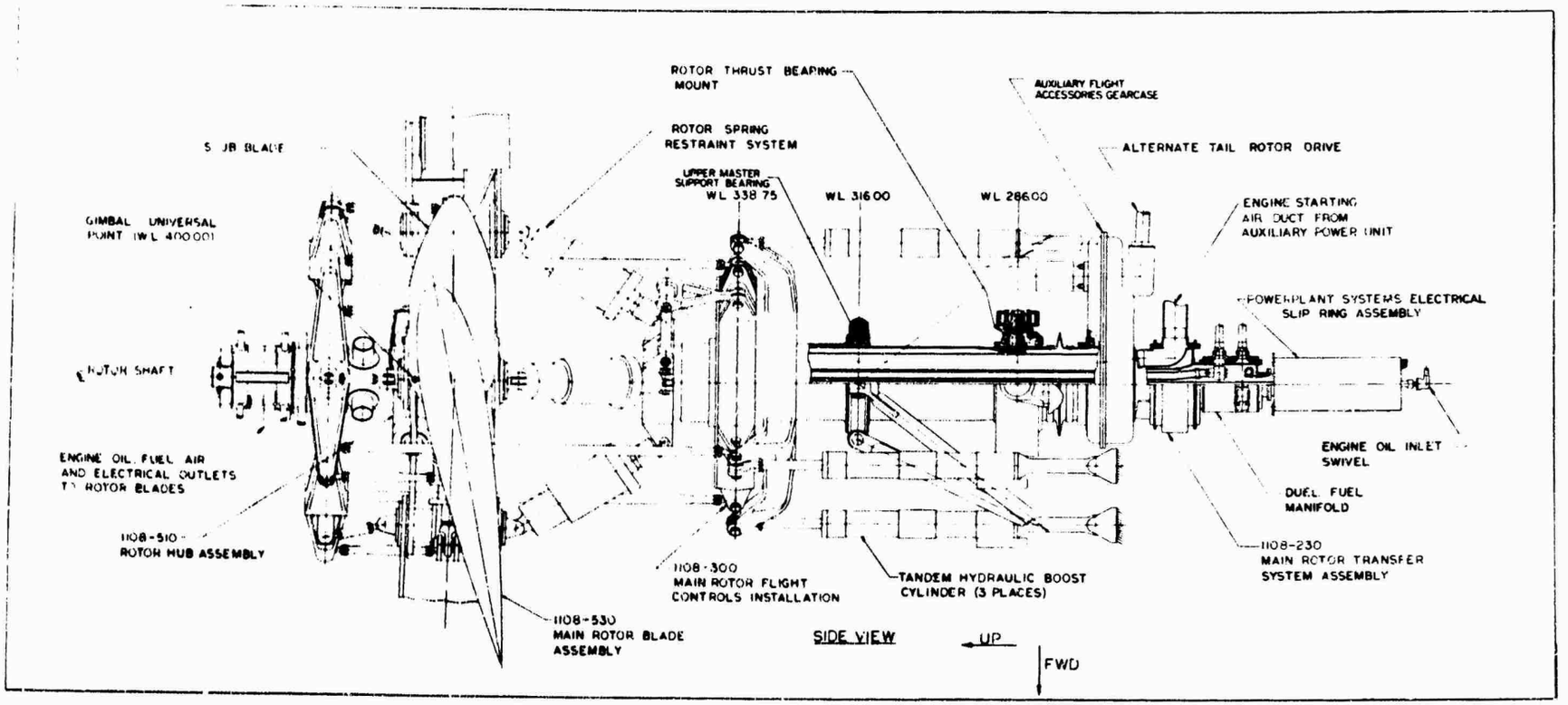

Figure 1. Rotor System Assembly - Tip Turbojet

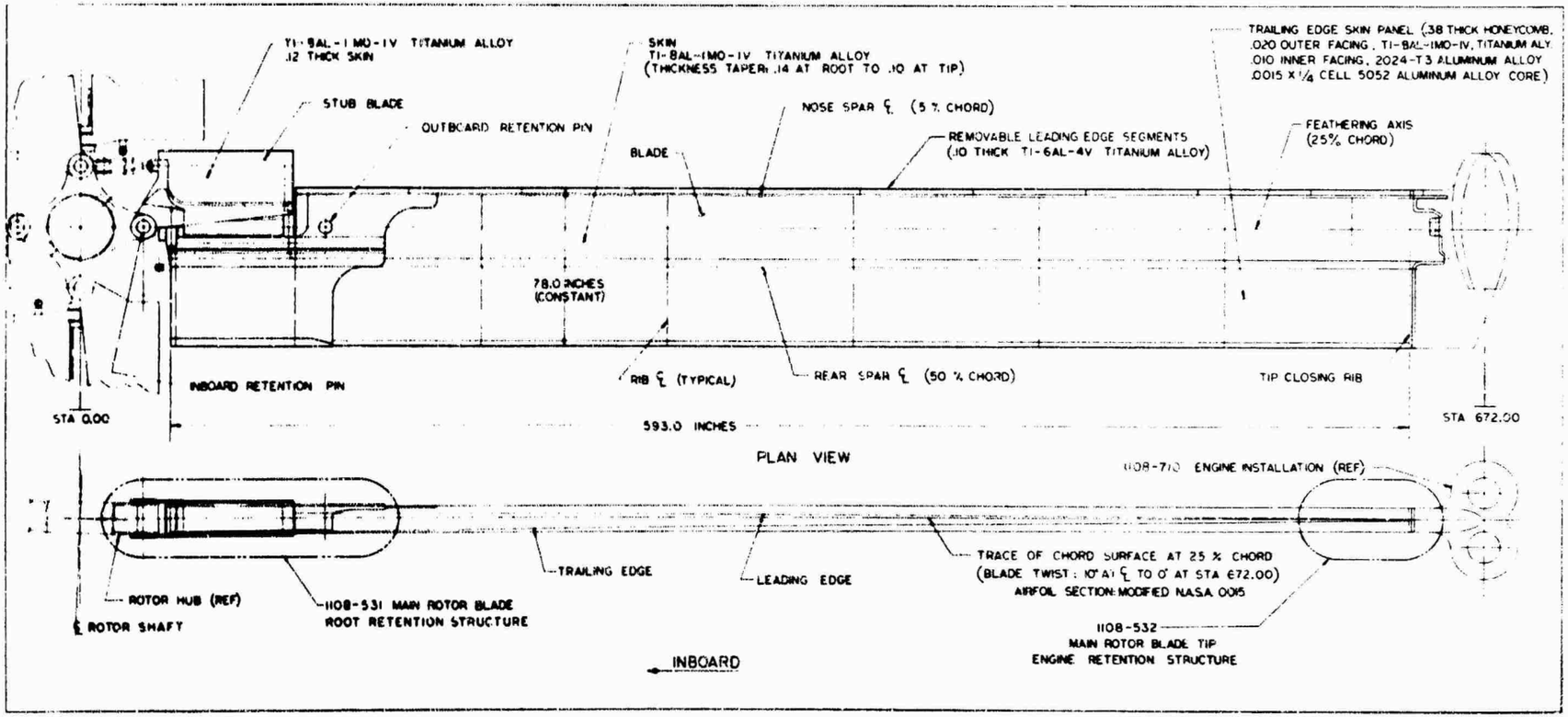

Figure 2. Main Rotor Blade Assembly.

5.0 STATIC AND DYNAMIC LOADS

Structural design criteria pertinent to a heavy-lift tip turbojet rotor system are outlined in Reference 3. These criteria describe a four-bladed rotor employing two turbojet engines at each blade tip. The static and dynamic in-plane, flapwise, and torsional blade loads have been developed for all regimes of steady-state and transient flight conditions considered critical for rotor design.

5.1 Structural Design Criteria

5.1.1 General Contents

The structural design criteria presented in Reference 3 are for a heavy-lift tip turbojet rotor system which is intended for use on a cargo helicopter having a payload of 24,000 pounds and a design gross weight of 72,000 pounds. The centerline of the tip-mounted engines, which are arranged in an over-under configuration, is located at a radius of 56 feet from the centerline of rotor rotation, and the design hovering tip speed is 650 feet per second. The rotor blades are connected to a universally teetering hub through a retention system which allows the blades to feather while supporting centrifugal load.

The design criteria further describe the proposed control system, fuel and oil systems, electrical system, and mechanical drive system as they affect rotor design. Dimensional data are presented which are necessary for blade design. The steady and transient flight conditions to be used for rotor blade design are summarized with load factor limitations being applicable to a cargo-type helicopter.

5.1.2 Criteria Peculiar to Tip Turbojet Configuration

The design criteria which pertain to the mounting and loading environment of the tip-mounted turbojet engines have been developed specifically for the J69-T-29 engine designed by the Continental Aviation and Engineering Corp. and designated Model 357-1 by that company. These criteria establish a maximum steady centrifugal load factor of 235g normal to the tip path plane axis with a rotor overspeed condition which produces a 259g load for no more than one minute with a cumulative operating time of thirty minutes per 1,000 hours of operation. A load factor of 367g normal to the tip path plane axis is to be used for nonrotating parts of the engine and blade attachment hardware. Dynamic and transient loadings on the engine are to be rationally determined.

5.2 Steady-State Design Loads

The rotor system steady-state design loads are defined as those loads which might be expected to occur for extended periods of time. These

loads have been developed using analytical procedures, digital computers; and direct analog computers using the same blade mass and stiffness properties which were used for the blade flutter analysis.

5.2.1 Centrifugal Loads

The mass of the rotor blade and its two tip-mounted engines creates a centrifugal force of 586,000 pounds at the centerline of rotation for the design hovering tip speed of 650 feet per second. This centrifugal force diminishes to 281,000 pounds at the engine centerline for a total tip weight of 1,200 lbs including engines and nacelle. Centrifugal force loadings at any other tip speeds can be calculated as these loads times the ratio of the squares of the tip speeds.

5.2.2 Rotor Blade Torques (Control Loads)

Engine gyroscopics, blade aerodynamics, and engine/blade mass properties combine to produce torque loadings on the rotor blades and pitch control mechanism. For the rotor design as presently proposed, the blade torque is always negative (nose down) so long as the rotor is at either cruise or hover tip speed. The only possibility for positive torque results with only the lower engine operating at zero tip speed (no gyroscopics), and this positive torque is small compared with the design negative torque. Since each flight condition entails a different engine turbine speed and collective pitch setting, a fictitious condition has been assumed which neglects all positive torque inputs and assumes all rotor parameters which contribute negative torque to be at their design limits. This analysis produces a conservative design torque of -183,000 inch-pounds at the centerline of rotation and -122,000 inch-pounds at the centerline of the engines.

5.2.3 Aerodynamic Loads

Airloads were generated for ten flight conditions using a Control Data 1604A digital computer and an airload program developed at Cornell Aeronautical Laboratory for the U. S. Army under Contract DA 44-177-TC-698, dated November 1962. This program uses assumed inflow distributions and considers the influence of bound and shed vortices from all of the blades to adjust these inflow distributions to final values from which the airloads are calculated. The most important aspect of this program is not the calculation of the steady airloads, since these can be determined with reasonable accuracy, using blade element theory, but the generation of the first seven harmonic sine and cosine airloads in both the lift and drag directions. Figures 3 through 12 present the lift and drag airloads for 1g forward flight at 144 miles per hour. The remaining conditions investigated have been examined, and the airloads for other critical flight conditions are similarly presented in Reference 3.

5.2.4 Rotor Blade Bending Moments

The direct analog computer simulation of the tip turbojet rotor blade, which is reported in Reference 5, offered a unique method for obtaining harmonic bending moments from the airloads described in Section 5.2.3. Since the direct analog computer simulation represented a completely coupled model of the rotor blade, the influence of flapwise airloads on in-plane bending moments, and vice versa, could be obtained with ease. The computer model was used to compile a complete set of dynamic influence coefficients by applying unit harmonic loads independently at several radial positions along the blade and tabulating the resulting flapwise and in-plane bending moments for each load at several other blade stations. Having applied these unit loads in both the flapwise and in-plane directions for airloads up to and including the eighth harmonic, the influence coefficients could now be applied to the actual harmonic airloads to obtain design bending moments. The critical bending moments which result from this study are plotted in Reference 3 in much the same manner as are the airloads in Figures 3 through 12. It is evident from these studies that in-plane bending moments resulting from airload harmonics above three cycles per revolution are negligible in comparison with the first three harmonics. It is also evident that the seventh harmonic flapwise bending moments are more severe than several lower harmonics. This phenomenon results from the proximity of the third flapwise cyclic natural frequency to seven cycles per revolution of the rotor.

While the 2.5g pullup condition creates the largest positive steady bending moments in the flapwise direction, the static droop condition produces the largest negative flapwise bending outboard of $r/R = 0.2$. The -0.5g flight condition causes critical negative bending inboard of $r/R = 0.2$.

5.3 Dynamic (Transient) Loads

The rotor system dynamic loads are defined as those loads which are transient in application and experience peak magnitudes for only a limited period of time. The gust and control motion conditions which cause these loads were simulated on the direct analog computer and blade response was measured.

5.3.1 Gust Loads

The transient response to a sharp edged (step) 40 foot per second gust was recorded for three values of suspended (fuselage) weight varying from infinity to minimum flying weight. For each fuselage mass, the flapwise and in-plane bending moments were measured at four blade stations. Additional measurements provided vertical force at the hub (for the determination of gust-load factor) and vertical and in-plane accelerations of the tip mass. The gust condition does not result in critical blade bending moments although the flapwise moments approach those of the 2.5g pullup

condition in magnitude. The transient accelerations of the tip mass were maximum for minimum flying weight and were measured to be 8.35g vertically and 1.99g horizontally. For the design gross weight condition, the load factor caused by the gust is calculated to be 2.25g.

5.3.2 Rotor Response Due to Cyclic and Collective Control Inputs

Steady-state inputs of cyclic and collective pitch were simulated on the direct analog computer and resulted in noncritical transient bending moments in both the flapwise and in-plane directions. An investigation of cyclic stick whirl, however, revealed transient in-plane bending moments far in excess of those created by any other flight condition. The very low rotor angular velocity and correspondingly low first in-plane rotating natural frequency make it possible for the pilot to inadvertently whirl the cyclic stick at a frequency which would excite this first in-plane mode and produce large bending moments. The peak bending moment was measured at the critical whirling frequency to be $\pm 3,500,000$ inch-pounds at $r/R = .025$. Since the bending moments were not measured at any other blade station, a quarter cosine mode shape was assumed for this response and the resulting in-plane bending moment variation with radius taken to be $\pm 3,500,000 \cos (\pi r/2R)$ inch-pounds.

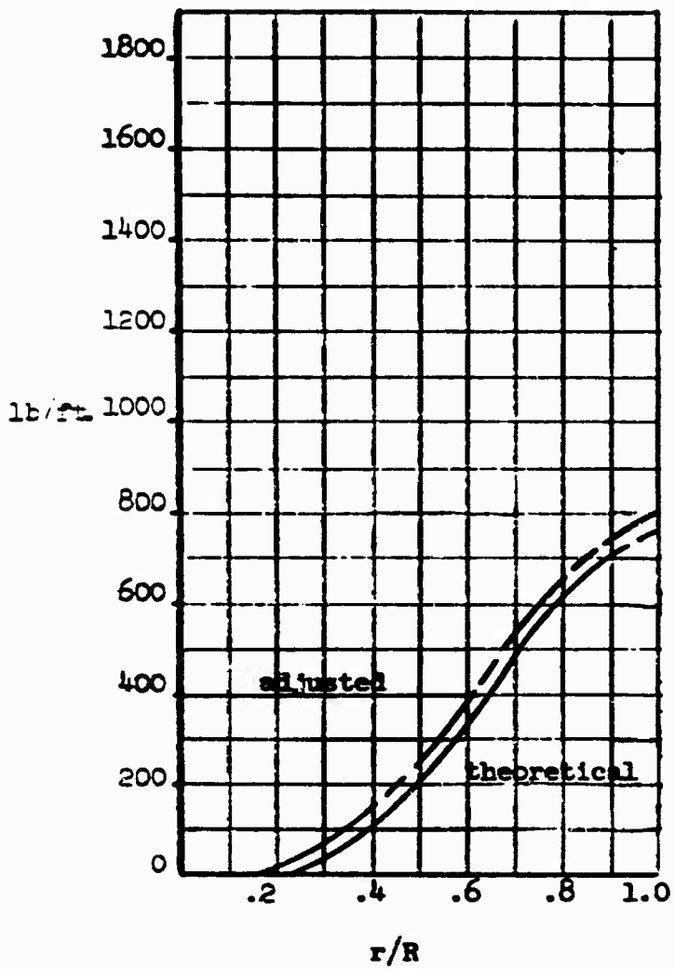

Figure 3. Lift - Zero Harmonic (Steady)
Forward Flight
(lg, 144 m.p.h.)
Condition 8

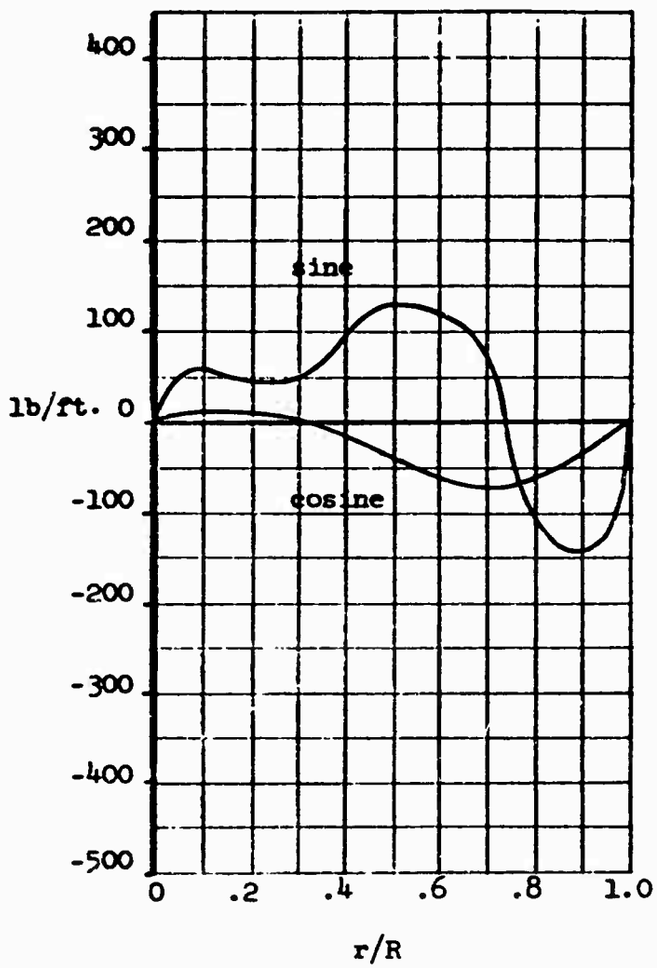

Figure 4. Lift - First Harmonic
Forward Flight
(lg, 144 m.p.h.)
Condition 8

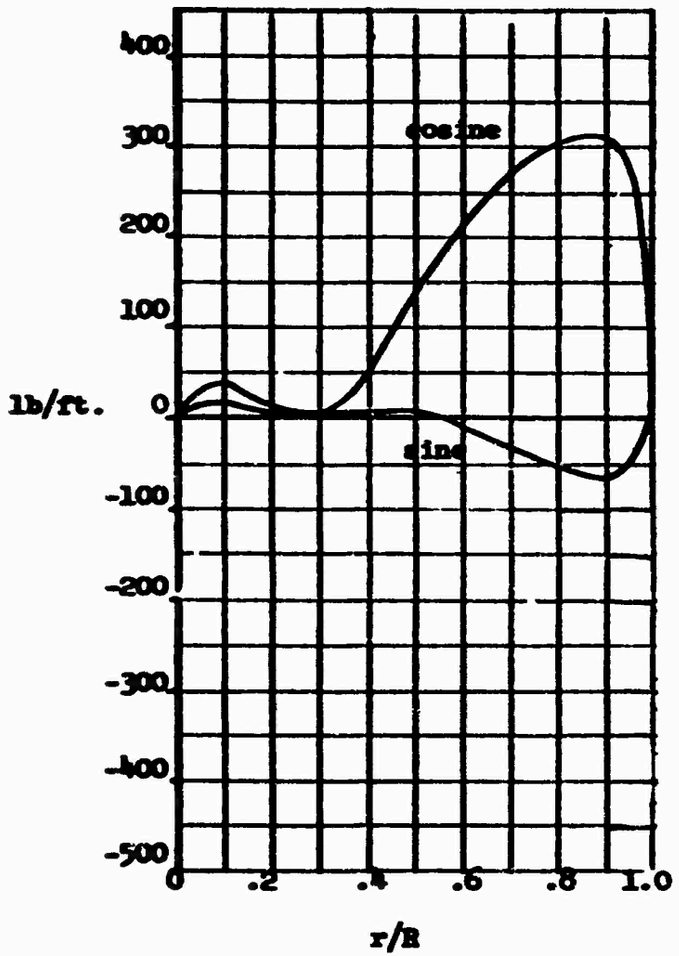

Figure 5. Lift - Second Harmonic
Forward Flight
(1g, 144 m.p.h.)
Condition 8

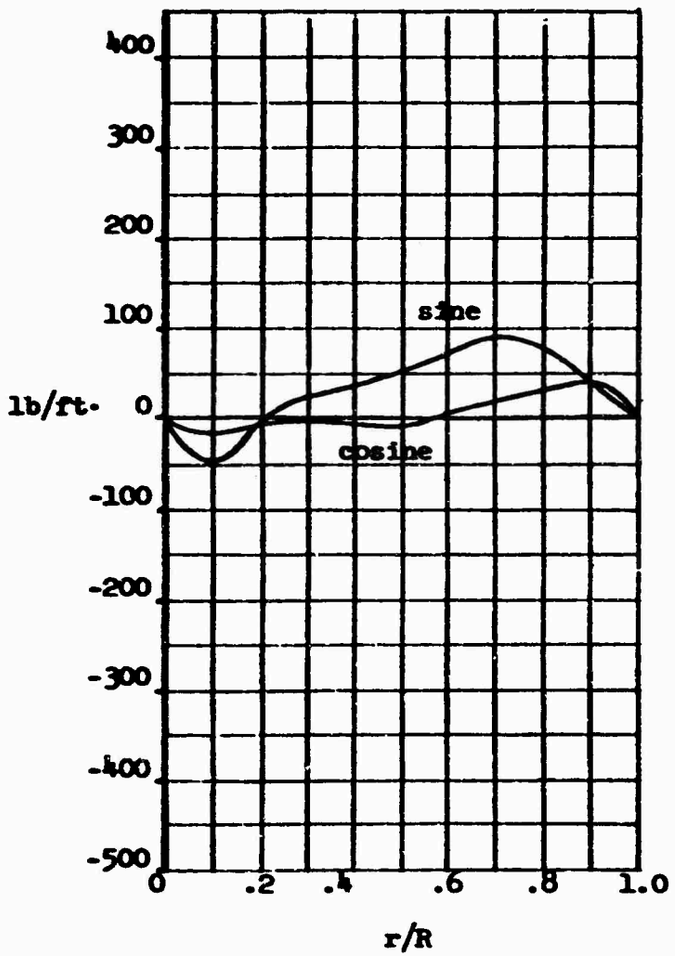

Figure 6. Lift - Third Harmonic
Forward Flight
(1g, 144 m.p.h.)
Condition 8

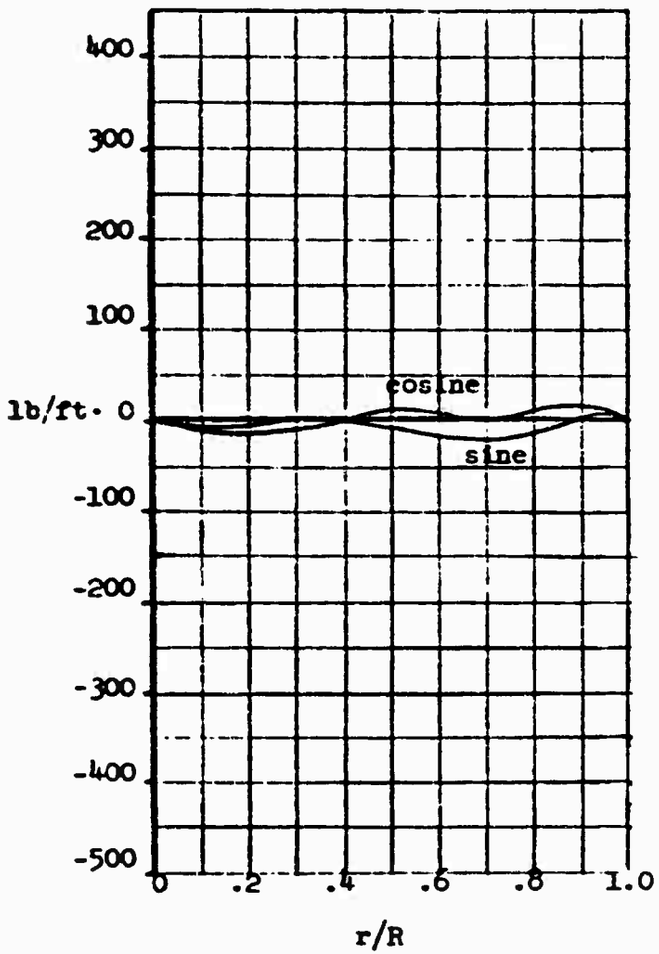

Figure 7. Lift - Fourth Harmonic
Forward Flight
(lg, 144 m.p.h.)
Condition 8

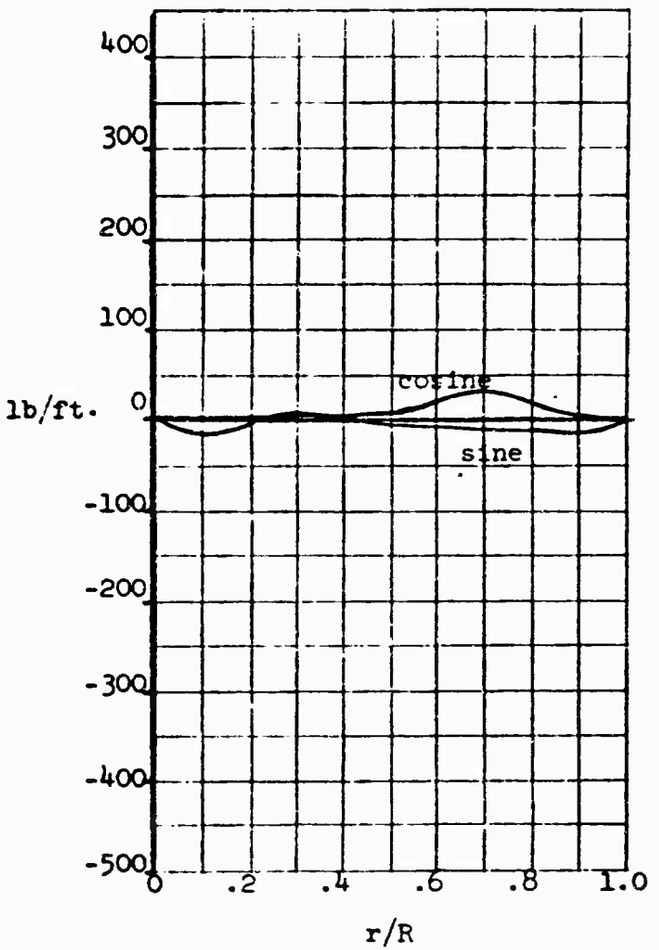

Figure 8. Lift - Fifth Harmonic
Forward Flight
(lg, 144 m.p.h.)
Condition 8

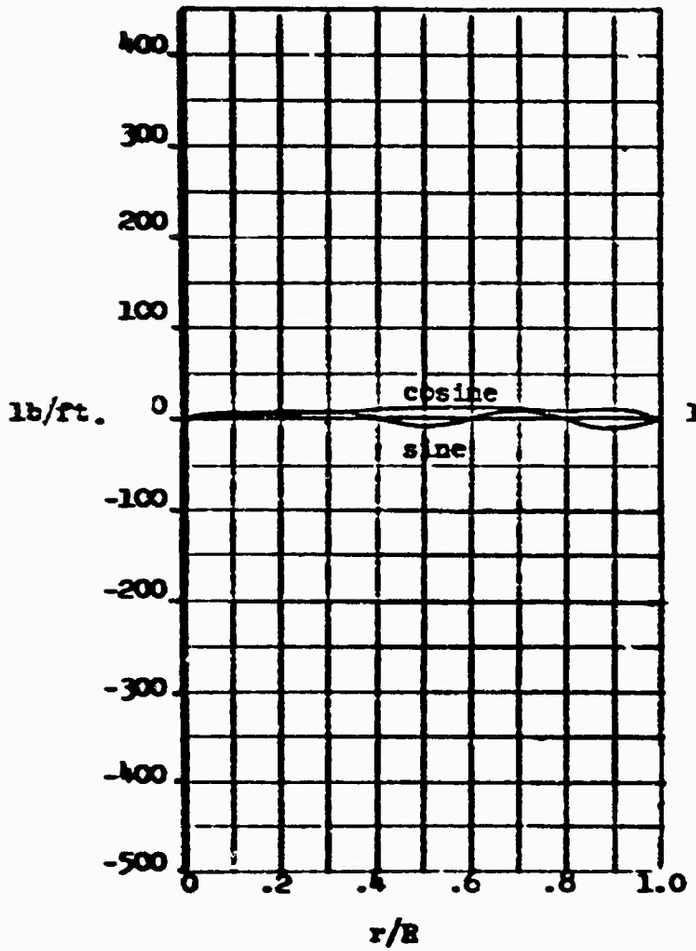

Figure 9. Lift - Sixth Harmonic
Forward Flight
(lg, 144 m.p.h.)
Condition 8

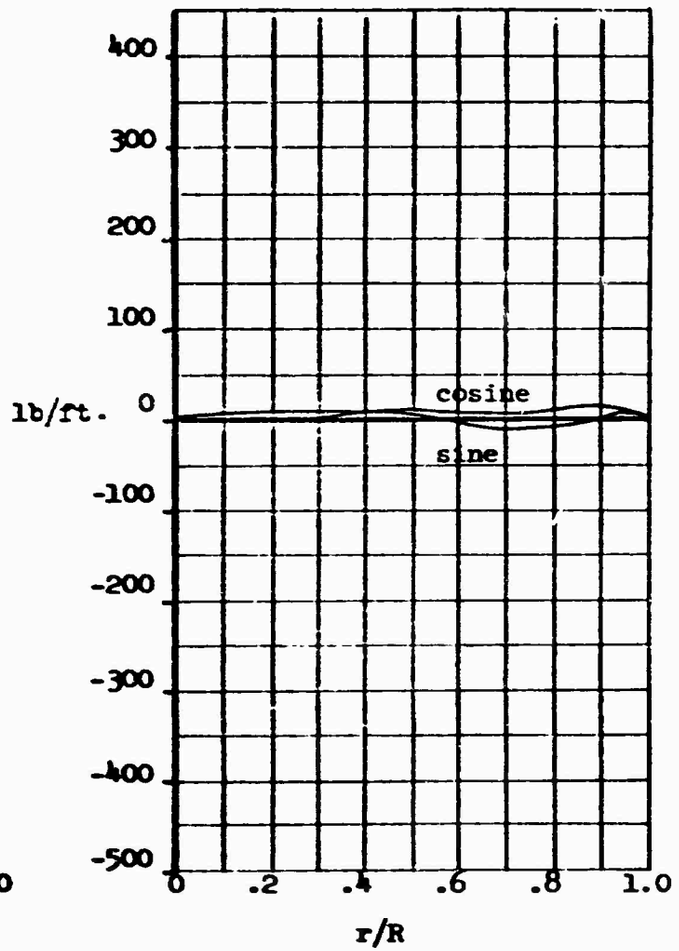

Figure 10. Lift - Seventh Harmonic
Forward Flight
(lg, 144 m.p.h.)
Condition 8

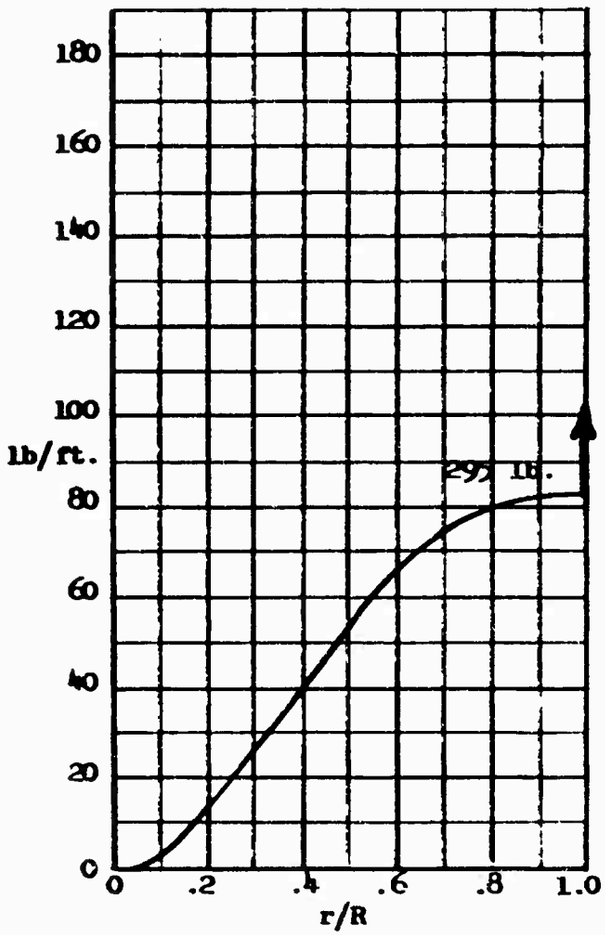

Figure 11. Drag - Zero Harmonic
Hover
Condition 2

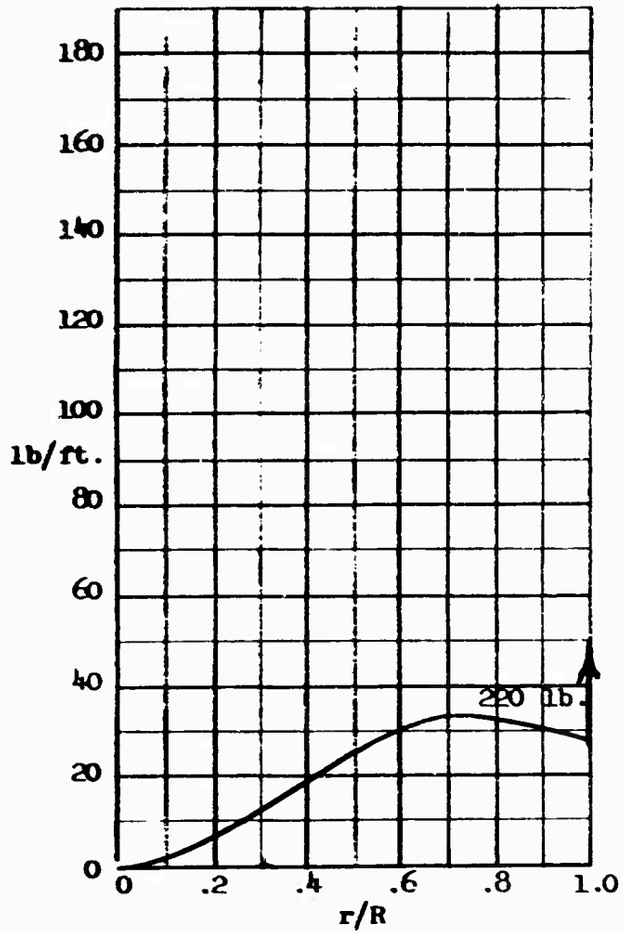

Figure 12. Drag - Zero Harmonic
Pushover (-0.5g, 0 m.p.h.)
Condition 5

6.0 STRUCTURAL ANALYSIS

6.1 Structural Philosophy

The philosophy adopted for the structural analysis phase of the preliminary design program is one of insuring that optimum load paths are developed, that service-proven structural design practiles are employed, and that structural materials and methods conform to the state of the art. Sufficient stress analysis has been performed to substantiate the basic design concept and is presented in Reference 4 in detail.

In general, static loads (for the purpose of analysis) consist of loads arising from dead weight considerations, transient loadings whose occurrence is so seldom as to preclude them from fa[illegible]e consideration, and loads resulting from possible operation far beyond the operating limits.

The static analysis of Reference 4 provides a measure of the basic strength of the principal components and attachments of the rotor system design. It will also serve as a guide in the future development of the rotor system by defining areas of overstrength as well as areas where additional detail design effort must be expended.

Fatigue loads are defined as loads which are periodic by nature and of sufficient amplitude and frequency as to induce failure of a material at stress levels less than its static capabilities.

The fatigue analysis of Reference 4 considers only the fundamental fatigue conditions required to provide assurance that proper consideration is given to this aspect of the structural design. An accurate prediction of component life depends upon measured flight strain data, component fatigue test data, and a detailed knowledge of the flight spectrum.

6.2 Critical Static Design Conditions

The conditions found to be critical during Phase I of this program are listed below.

1) Design maximum rotor speed - one engine out. Tip speed of 650 feet per second.

2) Rotor limit speed: A tip speed of 125 percent of the design maximum rotor speed; only the centrifugal force component is considered here.

3) Rotor overspeed - both engines on. A rotor tip speed of 105 percent of the design maximum rotor speed.

4) Pullup: The rotor tip speed is 562 feet per second, forward velocity is 41 miles per hour, and the vertical load factor is 2.5g.

5) Cyclic stick whirl: An arbitrary condition which arises when, in hover, the pilot moves the cyclic stick in a circular path at a particular frequency.

6) Static droop: The blade is considered a cantilever beam loaded by its own weight (1g).

6.2.1 Engine Mount System and Attachments

The critical engine mount system and attachment loading occurs during the rotor limit speed condition, and during the rotor overspeed operation - both-engines-operating condition. The critical engine mount areas are the attachment bolts and lugs and the heat expansion fitting.

6.2.2 Main Rotor Blade Tip and Attachments

The critical main rotor blade tip, and attachments, loading occurs during the rotor limit speed condition and during the rotor overspeed operation - two engines condition. The critical areas are the attachment lugs.

6.2.3 Main Rotor Blade Typical Section

The critical main rotor blade typical section is at rotor station 170.00 and occurs during the static droop condition due to compressive buckling stress.

6.2.4 Main Rotor Blade Root Retention Structure

The critical main rotor blade root retention structure loading occurs during the rotor limit speed condition. The critical areas are the tension-torsion strap and its retention bolt.

6.2.5 Stub Blade and Retention

The critical stub blade loading occurs during the transient cyclic stick whirl condition. The adjustable link attachment lug is the critical component.

6.2.6 Main Rotor Hub Assembly

The critical main rotor hub assembly loading occurs during the pullup condition. The critical hub areas are the blade retention lugs and pins.

6.2.7 Rotor Head Gimbal and Attachments

The critical gimbal and attachments loading results from the pullup condition. The critical areas are the bearings and the rotor shaft bearing lugs.

6.3 Critical Fatigue Conditions

The alternating stresses developed during a steady-state, in-trim, normal 1g flight condition are below the rotor system component material endurance limit and therefore nondamaging.

The start-stop condition is the critical main rotor system fatigue design condition considered in the Phase I analysis. The critical rotor system components during the start-stop condition are the engine-to-mount attachment heat-expansion fitting, the rotor system component attachment bolts, pins, and lugs, and the tension-torsion strap assembly.

7.0 DYNAMIC, AEROELASTIC, AND FLUTTER STUDIES

Studies have been conducted concerning the dynamic behavior of the rotor system for a heavy-lift tip turbojet helicopter. A description of the rotor parameters used in these studies can be found in Reference 5. A majority of the work was performed on a direct analog computer on which a completely coupled simulation of the rotor blade was analyzed for natural frequencies, flutter boundaries and transient loading phenomena. Complementary analyses pertaining to the effects of tip-mounted turbojet engines were performed to supplement the data compiled from the analog computer studies.

7.1 Rotor Blade Frequency Placement

7.1.1 Design Criteria

The flapwise, in-plane, and torsional natural frequencies of the rotor blades have been placed so as not to coincide with blade airload harmonics which create a resonant condition. This criteria is applied to frequencies as high as about eight cycles per revolution of the main rotor assuming that airload excitations above this value are negligible. The criteria governing the first in-plane rotating natural frequency not only considers avoidance of one-cycle-per-revolution airload excitation but also the phenomenon called ground resonance. To avoid airload resonance, the first in-plane uncoupled rotating natural frequency shall not be less than 1.3 cycles per revolution and any coupling effects throughout the collective pitch range shall not reduce this frequency below 1.1 cycles per revolution. If airload resonance is avoided in the above manner, freedom from ground resonance is assured.

7.1.2 Uncoupled and Coupled Frequencies

Rotor blade frequencies have been estimated by two independent methods; an uncoupled approach which neglects aerodynamic effects and a coupled approach which includes aerodynamic and gyroscopic effects. The completely coupled study, of course, yields frequencies which best approximate those which will result on the actual helicopter but a comparison of the two methods was considered appropriate to show the effect of coupling flapwise, in-plane, and torsional motions. In general, it is indicated that the first flapwise and in-plane natural frequencies can be accurately calculated as uncoupled modes if the blades are at a low-pitch setting. Higher uncoupled modes show less correlation as do all frequencies for the blades at high-pitch settings.

The results of these studies indicate that all natural frequencies are free from resonance with their airload harmonic excitations. It is also evident that the frequency margins of some modes vary with

collective pitch and care must be taken to avoid resonance throughout the pitch range. Figure 13, on page 57, shows the effects of collective pitch on four coupled frequencies. The first cyclic in-plane mode, which is of concern for the avoidance of ground resonance, deteriorates from a frequency of 1.34 cycles per revolution at minimum pitch to 1.15 cycles per revolution at maximum pitch.

7.2 Periodic Engine-Nacelle Thrust

During all forward flight conditions the aerodynamic environment of the tip-mounted turbojet engines and their nacelles will vary periodically resulting in both an engine thrust variation with blade azimuth position and a nacelle drag variation. It is difficult to treat the engine thrust oscillation accurately since the engines are to be governed, but preliminary estimates indicate that the change in engine thrust with azimuth will be less than the change of nacelle drag. Since the nacelle drag variation has been accounted for in the first harmonic in-plane airloads, and these loads create no design problem, any variation of engine thrust is assumed to be noncritical.

7.3 Rotor Dynamics with One Engine Inoperative

The symmetry which exists for the four rotor blades when all eight tip engines are properly operating is obviously destroyed if any one engine fails and the remaining seven continue to operate. Using a hover condition to illustrate this effect, it is not difficult to visualize a plan view of the rotor in which one blade has an in-plane deflected shape different from the other three. The center of gravity of the entire rotor system, then, would be offset from the centerline of rotation and a rotating force vector would result due both to centrifugal force and the unbalanced engine thrust vector. Analyses of this condition for one and two engines inoperative indicate that this total rotating force is small compared with helicopter gross weight, and adequate rotor isolation would insure that this excitation would be virtually unfelt in the fuselage.

Another effect of a one- or two-engine-out condition would be for one rotor blade to change pitch due to the loss of gyroscopic torque at the tip; thus, this blade would have effectively a twist angle different than the other three blades. The result would be an out-of-track condition which would induce some degree of roughness to the helicopter. Analyses conducted in Reference 5 indicate that this out-of-track condition is not expected to be more severe than out-of-track conditions which occasionally result with smaller helicopters.

7.4 Mechanical Instability

Ground resonance, which can occur when the first in-plane rotating natural frequency is less than one cycle per revolution of the main rotor, will be

avoided by designing the rotor blades to have a first in-plane frequency well above one cycle per revolution. Section 7.1.2 shows that a frequency margin is maintained throughout the collective pitch range but is smaller at maximum pitch than a minimum pitch.

7.5 Torsional Divergence

Torsional divergence of a lifting aerodynamic surface occurs when the rate of change of torque from external sources exceeds the rate of change of torque due to structural stiffness. In its simplest form, this problem is analyzed as a pure torsional problem; and divergence can occur only if the blade section center of pressure is located forward of the blade shear center. Such is not the case with the proposed tip turbojet blade and so torsional divergence will not occur. The torsional stability of the rotor blade, including effects of flapwise and in-plane deflections, is further assured as a result of the direct analog computer study reported in Reference 5. If static instability were present in the rotor, it would have become evident during these studies.

7.6 Dynamic Phenomena Peculiar to Large Tip Turbojet Rotors

A rotor system of the size proposed for Model 1108 can be expected to have dynamic considerations which are not necessary to investigate for smaller rotor systems. These considerations arise primarily from the very low rotor angular velocities which are required to obtain a desirable tip speed.

7.6.1 Low Rotor Natural Frequencies

Having established a first in-plane natural frequency which is adequate for avoidance of ground resonance, it is found that inadvertant whirling of the cyclic control at a frequency well within pilot capability will excite this first in-plane mode and cause large chordwise loads in the blades. This condition cannot be avoided without providing cyclic stick whirl limitations and so the rotor blades will be designed for this condition.

7.6.2 Effects of Sling Loads on Rotor Dynamics

It is presently envisioned that the cargo or useful load can be carried either as a rigidly attached load or a sling suspended load. All dynamic calculations have been made assuming that the design gross weight included a 12-ton cargo rigidly connected to the fuselage and, hence, an integral part of the fuselage. An investigation of the dynamic behavior of a sling suspended cargo verifies that the cargo and sling behave much like a simple pendulum. The sling length was varied from 16 feet to 200 feet with a cargo weight of 24,000 pounds and the frequency of the slung cargo was found to vary between 1.3 radians per second and 0.4 radians per second. Since the design minimum rotor speed is greater than 10 radians

per second and all rotor-blade frequencies exceed one cycle per revolution of the rotor, it is concluded that the sling length would never be short enough to produce frequencies which would affect the dynamics of the rotor blades.

7.7 Rotor Blade Flutter

A variation of parameters study of rotor blade flutter boundaries has been conducted on a direct analog computer for a completely coupled simulation of the proposed rotor blades. The stability of the rotor blades was determined by measuring the aerodynamic damping present for each mode of vibration. No attempt has been made to include structural damping in the rotor blade simulation, and so it is possible to have a small amount of negative aerodynamic damping present for any mode and still be flutter-free due to an offsetting amount of structural damping. Significant rotor parameters have been varied independently, and in some cases varied in combination, to determine the values at which flutter would be likely to occur.

7.7.1 Effects of Tip Rotating Mass

The rotating parts of the tip-mounted turbojet engines produce coupling between pitching and lead-lag motions of the blade. The effects of this coupling were investigated by varying the angular speed of these rotating parts from three times the maximum design value in the proposed direction (counterclockwise viewed from the rear) to three times the design value in the opposite direction. The effect of tip engine speed on aerodynamic damping for all modes of vibration is small when compared with the case when the engine speed is zero.

7.7.2 Effects of Tip Mass Location

The chordwise location of the center of gravity of the tip mass was varied between the 16-percent chordpoint and the 28-percent chordpoint, or ±6 percent at the chord from the proposed design location. Figure 14 on page 58 indicated that the tip mass location affects the aerodynamic damping of different modes in different ways. The two modes which are most affected are found to be the second collective mode and the second cyclic mode, with both modes becoming more sensitive to tip mass location as the root control spring stiffness becomes smaller. The present design location at the 22-percent chordpoint effects a compromise between the extremes investigated and will insure stability for control spring stiffnesses as low as 0.1 of the design value if a structural damping factor of G = .03 is assumed to be present.

7.7.3 Effects of Elastic Axis Location

The only mode of vibration which is critical for elastic axis location is the second cyclic mode as shown in Figure 15 on page 59. The other

modes are not of immediate interest since they all possess positive aerodynamic damping when using nominal blade parameters. The tendency toward a more stable second cyclic mode is indicated for a more forward elastic axis location. Even though the assumed structural damping is sufficient to guarantee stability of this mode, the elastic axis for the proposed blade design is estimated to be forward of the quarter chord (at approximately 19 percent) and, hence, in the proper direction to reduce aerodynamic instability of this mode.

7.7.4 Effects of δ_3 (Pitch-Flap Coupling)

A variation of δ_3 angle (pitch-flap coupling) affects only the second cyclic mode adversely and results in the largest negative aerodynamic damping at maximum collective pitch setting. Figure 15, page 59, shows this effect for δ_3 angles up to 45 degrees. Even though a structural damping factor of G = .03 would guarantee avoidance of flutter throughout this δ_3 range, no advantage to large δ_3 angles is foreseen and design values in excess of 10 degrees are not anticpated.

7.7.5 Effects of Control System Stiffness

The influence of root control spring stiffness on blade flutter is best shown in Figure 14, page 58 for the second cyclic and second collective modes, the only modes for which aerodynamic damping becomes more negative (destabilizing) with increasing control spring flexibility. If the structural damping factor is again assumed to be G = .03, a control spring stiffness at least equal to the blade torsional stiffness is required to avoid flutter in the second cyclic mode. This requirement is easily met since the design goal at present is for a stiffness ratio of 10:1 (flexibility ratio of 1:10).

7.7.6 Model 1108 Flutter Status

The rotor blade flutter analysis of Reference 5 shows that no single instance of flutter was found to exist for any operating condition or any moderate variation of rotor design parameters. The principal deterrents to flutter are the very high blade and control spring torsional stiffnesses in combination with a blade which is mass balanced near the quarter chord.

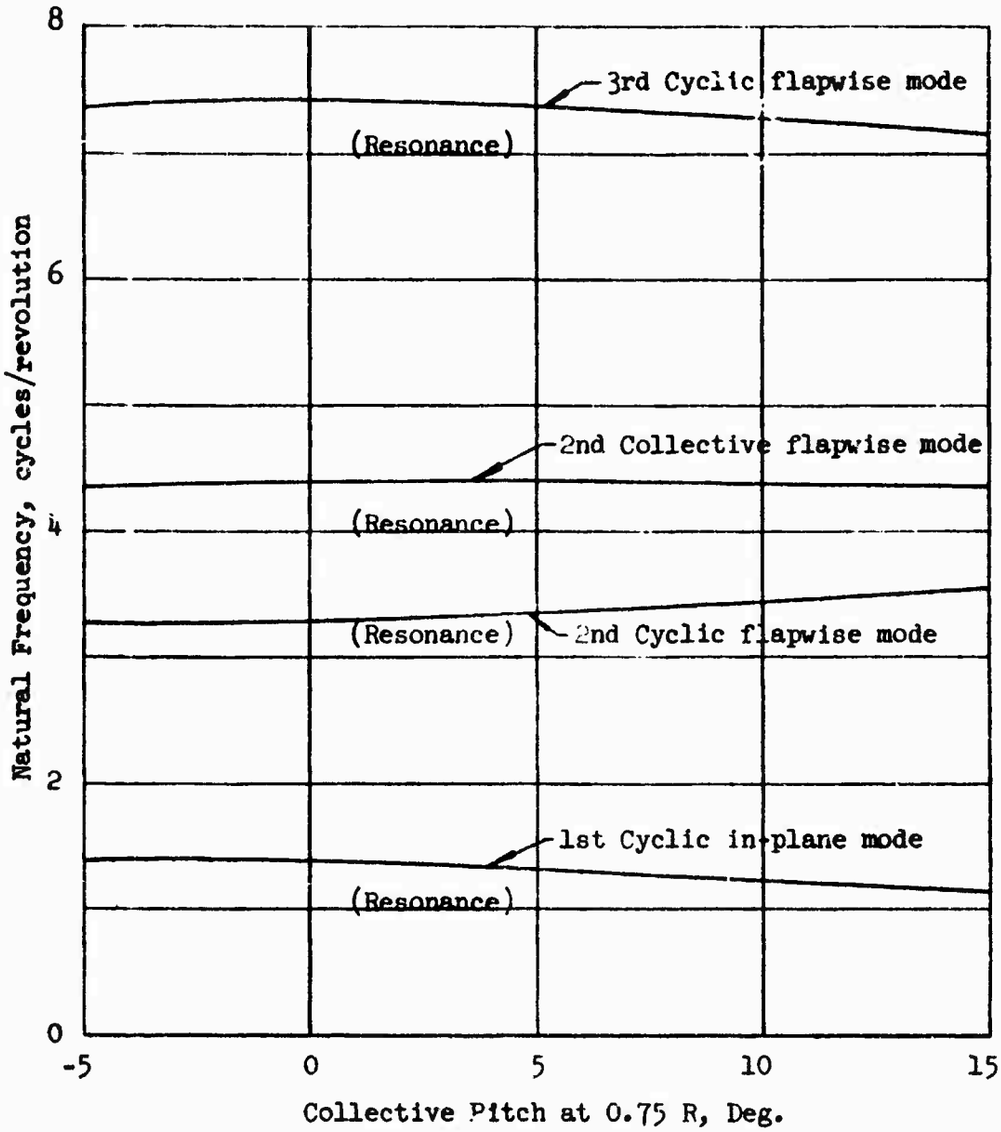

Figure 13. Coupled Natural Frequency Versus Collective Pitch.

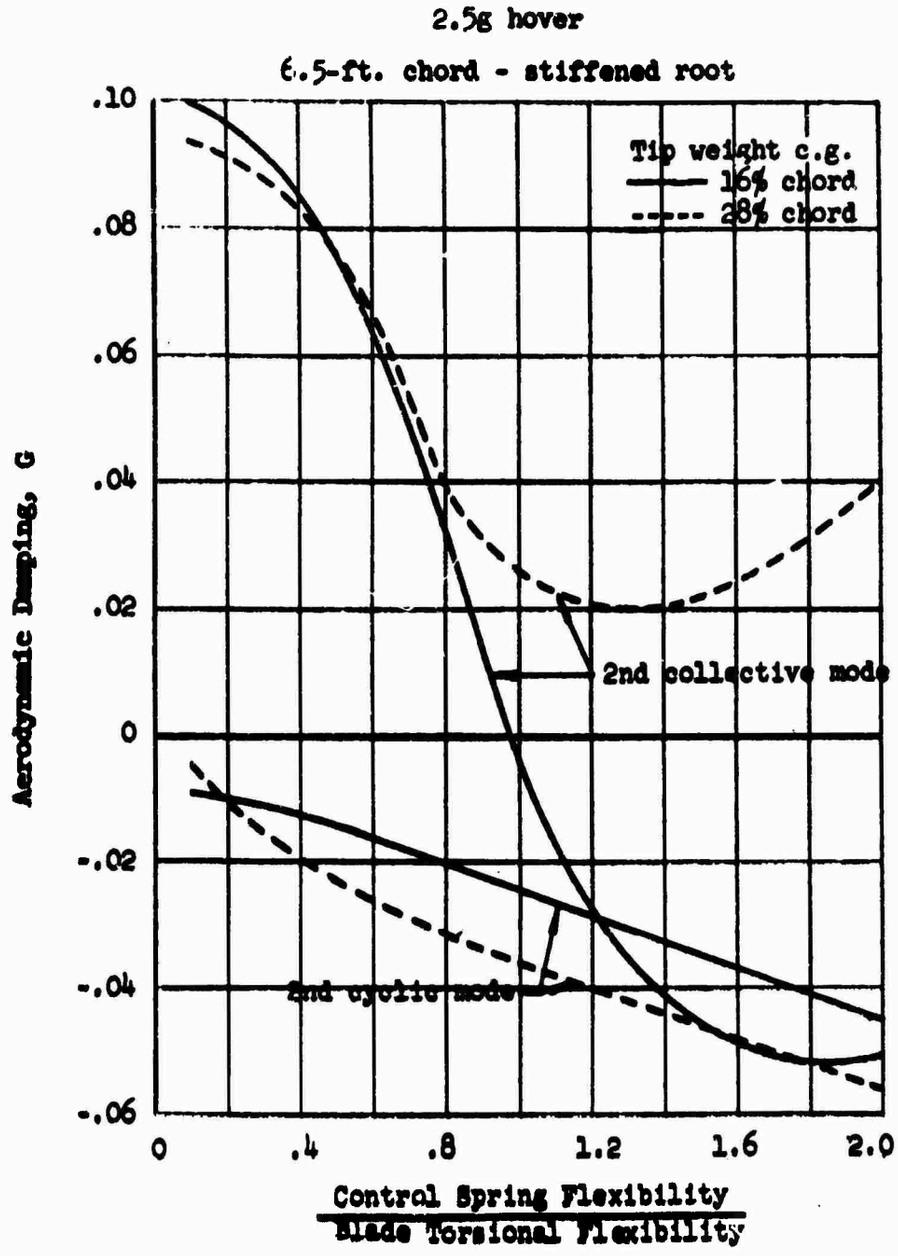

Figure 14. Aerodynamic Damping Versus Control Spring Flexibility.

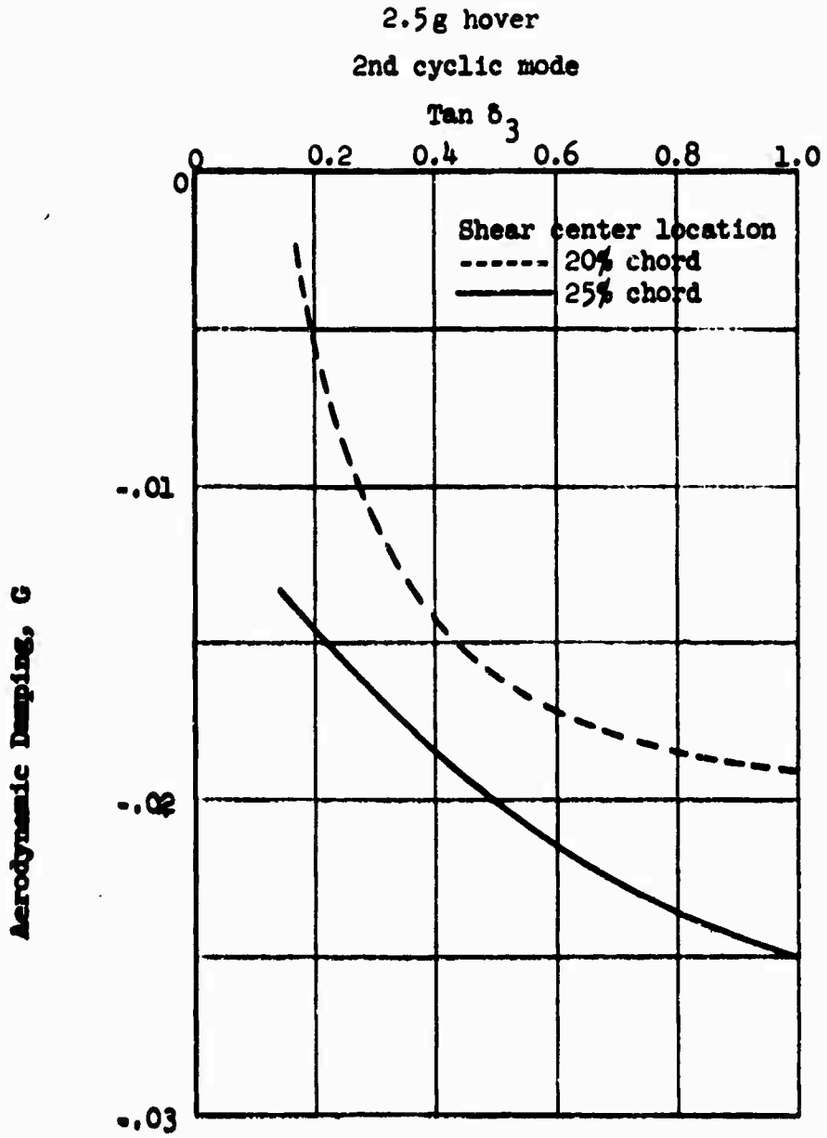

Figure 15. Aerodynamic Damping Versus Pitch-Flap Coupling (δ_3)

8.0 WEIGHT AND BALANCE STUDIES

8.1 Weight Studies

The final weight breakdown for the Model 1108 is the result of the parametric study, with the limiting factors involved by the use of actual hardware engines, plus such components on which design layouts have been completed.

The actual weight status of the components comprising the "final" empty weight configuration is as follows:

Rotor Group	(Blades, retention, hub). Weights calculated from design layouts and semi-detailed drawings.
Tail Group	(Tail rotor and stabilizer). Weights computed by means of statistical equations.
Body Group	(Primary and secondary structure, and provisions for equipment). Weights computed by means of statistical equations.
Landing Gear Group	(Wheels, struts, mechanism). Weights computed by means of statistical equations.
Flight Controls Group	(Cockpit controls, linkage rotating and nonrotating items, boost systems, and tail rotor controls). Weights computed by means of statistical equations.
Pylon Group	(Rotor support structure and isolation provisions). Weights computed by means of statistical equations.
Engine Section Group	(Nacelle fairing, engine mounts, starting system, provisions for oil and fuel lines, oil coolers, inlet and exhaust provisions, engine controls, electrical provisions). Weight calculated from layouts and semi-detailed drawings.
Engines	Weight of Continental 357-1 was used for this study.
Fuel System	Weight of fuel system was computed as a fixed percentage of fuel required for the mission.
Auxiliary Power Units	Actual weights of selected units were used. (AiResearch GTCP 100-54).
Gearboxes and Drives	(Equipment drives and gearboxes). Weights calculated from layouts.

Engine Controls	Weight calculated from layouts.
Starting System	(Lines, valves, and ducts). Weight calculated from design layouts.
Instrument Group	(Instrument, installation, and wiring and piping). Weights evaluated by design requirements.
Electrical Group	(Wiring, relays, inverters, batteries, etc.). Weights evaluated by design requirements.
Electronics Group	(Radios, antennas, intercom). Weights evaluated by design requirements.
Furnishings Group	(Crew seats, belts, reels, pyrotechnics, air conditioning, emergency equipment). Weights computed by means of statistical equations.

In view of the fact that the primary purpose of the subject study was to investigate the feasibility of the tip turbine rotor system concept, much design time was utilized in "sizing" the rotor group. The final decision to employ a four-blade, eight-engine rotor configuration was dictated by the requirement that the Continental 357-1 engine (1700 pounds thrust) be utilized. Therefore, the major weight study effort was directed toward the satisfactory preliminary design of a four-blade rotor system utilizing the most efficient design techniques and the optimum combination of structural materials available.

After numerous design studies which considered combinations of steel, titanium and aluminum, and after investigations dealing with the most efficient chordwise mass distribution for providing required chordwise EI values, the following blade and hub construction was decided on:

Engine Nacelles

Titanium	Engine nacelle skins Engine nacelle firewall Engine-mount installation
Aluminum	Center body and supports Splice plates Frames and doors Honeycomb structures Channels and ducts

Hub Assembly

Titanium	Bearings - pins and retainers Rotor mast and gimbal ring Hub plates Center shaft Retention pins Drag link assembly

Steel	-	Gimbal bearings

Blades

Titanium	Ribs - retention i/b and o/b bearing supports - retention Blade retention webs and supports - retention Leading and trailing edge buildup - retention Leading edge nose cap and extrusion - retention Skins and nose plates - retention Trailing edge skins - blade Trailing edge caps - blade Trailing edge extrusion - blade Blade ribs - blade Leading edge skins - blade Root and tip fittings - blade
Steel	Leading edge cover - blade Bushings and bearings - retention
Aluminum	Trailing edge core - retention Leading edge filler - blade Inner sandwich skin - trailing edge - blade Core - blade

8.2 Balance Studies

8.2.1 Rotor Balance Considerations

In selecting a type of rotor system to fulfill the requirements of a heavy-lift helicopter, it is necessary to consider the size of rotor and type of propulsion employed. In the case of the subject design, turbojet engines are mounted on the blade tips thereby changing the blade mass characteristics from those considered to be a conventional system.

In a rotor system of the size proposed, complexity of hub and flight controls, and hence weight, is dictated by the number of blades in the system. In this regard then, the rotor with the minimum number of blades will be the optimum. Further to this selection, a study had to be conducted regarding the merits of both articulated and universally mounted systems.

In steady flight with constant angular velocity, thrust and centrifugal moments are equal to drag moments and the blades are in equilibrium in the rotor plane. Theoretically, at this stage there should be no tendency for dissimilarity of blade geometry within the system. Each blade has identical thrust, drag, and centrifugal forces acting upon it; and the entire system is balanced. However, if one or two engines lost power or failed completely, the effect on the system would be to upset the balance of the rotor, and the blades would seek new equilibrium positions.

It is apparent that a rotor system with articulation, free to hinge about a lag axis, would rotate about that axis until a new equilibrium point was reached, which in this case would be the drag moments being balanced by blade centrifugal moments only. In order to determine the magnitude of such a lag angle change, a generalized equation was derived from inputs that were taken from the rotor geometry in a one-blade power loss condition. The inputs are as follows:

The equilibrium equation with engines out may be rated as

$$D(3/4R - eR) - CF_{WB}(Z_1) - CF_{WT}(Z_2) = 0$$

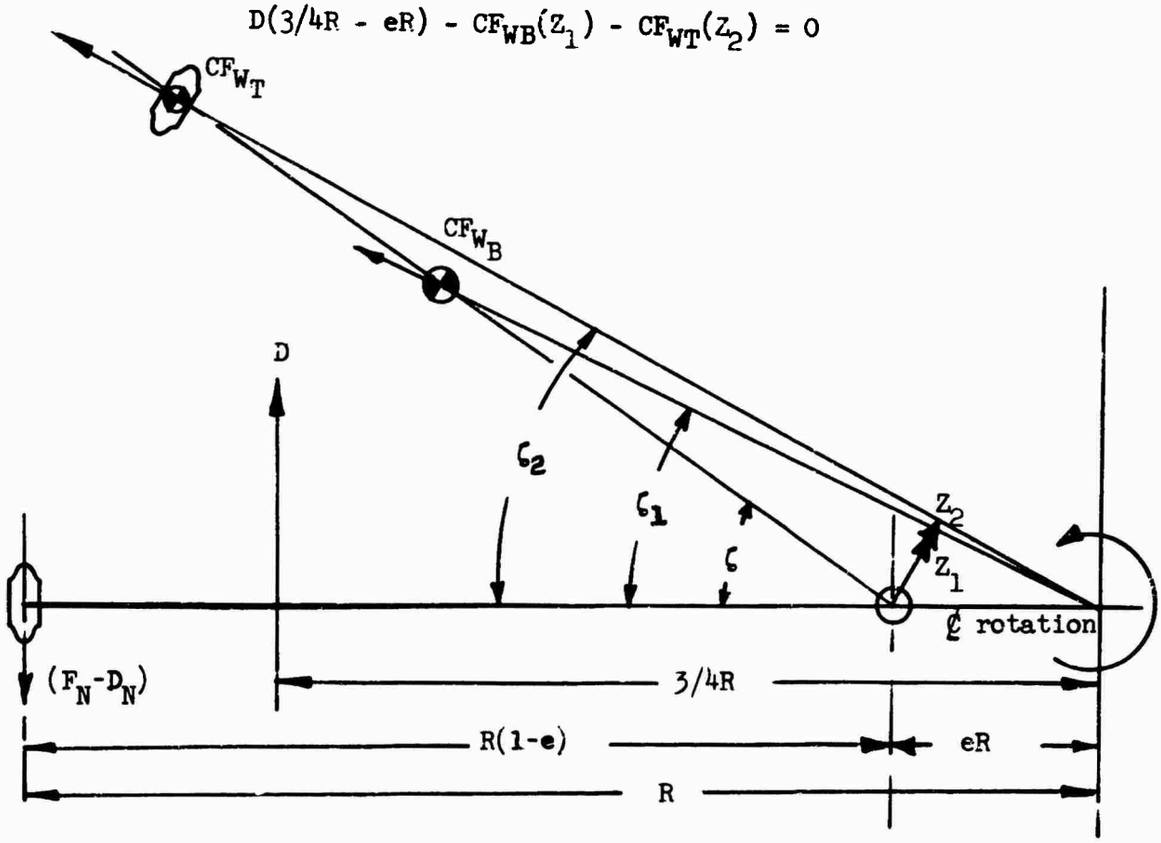

Figure 16. Blade Lag Relationship

Using the equation to investigate the effects of a power loss indicates that the articulated system will have a blade angular displacement which produced an in-plane unbalance of approximately twelve times greater than the rigid system. The elastic deflection due to one- and two-engine-out conditions on the universally mounted rotor produces in-plane of the balance forces of 1,011 pounds and 2,310 pounds, respectively, while the same conditions of the articulated rotor produce dorces of 13,715 pounds and 27,431 pounds. By virtue of this, the decision was made to eliminate the articulated system from further study and adopt a universally mounted rotor system.

8.2.2 Aircraft Balance

Experience at Hiller Aircraft Company has indicated that a helicopter employing a universally mounted rotor is generally at a disadvantage when the center of gravity travel is compared to that of a helicopter with an articulated system. However, when a helicopter of the size of the Model 1108 is considered, the linear center-of-gravity travel of universally mounted rotor system becomes sufficiently extensive to encompass all loading variations.

Due to the configuration of Model 1108, it is readily apparent that the load-carrying capabilities are restricted to a pod-type cargo slung between the fore and aft landing gears, and by virtue of this arrangement, the cargo center of gravity may always be confined to a location below the centerline of rotation.

For purposes of balance control, it is considered feasible to design the fuel system center of gravity to coincide with the centerline of rotation, thereby minimizing adverse balance effects due to the fuel consumption. The new weight, being only 1.1 percent of the empty weight, will have a negligible effect on the longitudinal balance and need not be considered further.

In order to eliminate undesirable balance characteristics, the empty weight balance was computed so that the center-of-gravity in the empty condition was as close to the centerline of rotation as possible.

The total available center-of-gravity range as computed in Reference 6 indicates that 12.7 inches is available for loading variations. It is expected that this range will be expanded with the incorporation of the rotor spring restraint system.

A weight and balance breakdown showing horizontal and vertical centers of gravity has been compiled and indicates the feasibility of the mission loading within the confines of the computed center-of-gravity range.

9.0 WIND-TUNNEL STUDIES

Wind-tunnel tests were conducted to provide design information which would assist in the design of a turbojet installation at the tip of a rotor blade The results of these tests are presented in Reference 7 and are summarized in the paragraphs below.

9.1 Engine Stacking Configurations

The tip turbojet wind-tunnel studies were conducted at the United States Naval Postgraduate School, Monterey, California, using a 1/4 scale partial span model (Figure 17) which was tested at $R_N = 1.8 \times 10^6$. The nacelle test configurations were mounted on a short blade of 0015 airfoil section which was attached to a supporting structure outside of the test section. This supporting structure allowed freedom of movement in both the pitch and yaw planes (Figure 18). The reference pitch axis was the blade quarter chord; and, for yaw the reference axis was a vertical axis just outside of the tunnel wall.

The loads were transmitted from the nacelle and blade through strain-gage balances to the supporting structure. One balance was mounted in the nacelle, parallel to the nacelle axis, and measured nacelle forces only. The second balance was mounted in the wing parallel to the quarter chord axis and measured the combined forces of the nacelle and wing. Static pressure taps were located on the wing and on the forebody and afterbody of all nacelle configurations to aid in the evaluation of the wing and nacelle lift distribution.

Three-engine stacking configurations were tested through a range of pitch and yaw angles to determine which configuration would be most suitable for a tip turbojet nacelle. The nacelle configurations tested were a single engine, a vertical placement of two engines, and a side-by-side placement of two engines. The single engine nacelle was sized in model scale to represent the geometric proportions of the Continental J-69 engine. The vertical and horizontal multiple engine configurations were also patterned to enclose the J-69 engine.

For an equivalent installed power, the single-engine configuration produced the minimum drag and net integrated side force of all three configurations.

Of the two multiple-engine configurations, the over-under engine configuration had a higher drag coefficient than that of the side-by-side configuration. It had in addition a higher side force coefficient. This side force coefficient, when integrated around the rotor disk, produces a downstream drag force which adds to the overall power required. The vertical configuration, while exhibiting higher drag, was nevertheless selected for the design layout studies due to considerations of structural mounting, weight, and improved inlet flow conditions.

9.2 Nacelle Inlet Configuration

Four single nacelle configurations were tested. They are identified as 1-40-100, 1-40-115, 1-40-130, and 1-50-100. Figure 19 shows cross sections of these nacelles, illustrating their relative size and common dimensions. The above code numbers identify the forebody contour which, along with the ordinates of the nose shape, are based on data taken from NACA Report No. 920. The afterbody contours (aft of the maximum diameter) are identical for all nacelles and are based on data for a modified NACA 111 body taken from NACA TR 1038.

Two centerbody inlet shapes were tested with nacelle 1-50-100 only. This nacelle shape was selected to give the same inlet area with the centerbody installed as the -40 series. One centerbody was a conical shape and the other an NACA 1-30-40 series spinner. Each engine inlet had a total pressure survey rake for measuring compressor inlet velocity profile and net inlet pressure recovery.

At nominal pitch angles (less than 6°) and zero yaw angle, the inlet flow conditions for all configurations are acceptable. As the nacelle is yawed, the distribution becomes more distorted and the inlet losses rapidly increase. As would be expected, the side-by-side engine configuration as compared to the over/under configuration shows the lowest losses in pitch ($\alpha_{max} = 12^{\circ}$) and the highest losses in yaw ($\beta_{max} = 20^{\circ}$). In positive pitch attitudes, the bottom engine has the best flow distribution and in right and left yaw attitudes, the upstream engine of the side-by-side configuration always exhibits the best flow conditions. Since the inlet losses increase rapidly with both pitch and yaw angle, it is desirable to favor the configuration whose critical distortion plane has the least inlet flow angle change. The maximum inlet flow angle in pitch is $\alpha = 12^{\circ}$ and in yaw, for an assumed value of $\mu = .364$, $\beta = 20^{\circ}$. Therefore, the over/under configuration shows a lower integrated inlet loss and a more favorable velocity distribution. The addition of either centerbody improved the inlet flow conditions such that acceptable velocity profiles and low inlet losses were maintained throughout the full pitch and yaw range.

9.3 Nacelle Drag - Measured Versus Predicted

Since the results of the wind-tunnel program were not available early enough to be used in the parametric study, it was necessary to use data which was available from NACA tests and reference texts. A conservative drag polar was selected and this drag polar was applied to the pitch and side-slip angles independently as a simplifying conservative assumption.

A comparison of the nacelle drag coefficients from wind-tunnel data to those used in the parametric study are shown in Figures 20 through 22 for two single nacelle configurations, a twin over/under nacelle and a twin side-by-side nacelle, respectively. In order that the effect of

both yaw and pitch on drag can be seen, separate graphs are presented where alternate angles are held constant and the other varied.

The results of this comparison show that the drag of the wind-tunnel models is approximately double that used in the parametric study for the entire α range and the positive β range. The fact that the drag coefficient curve for varying yaw angle is not symmetrical about $\beta = 0$, as assumed in the parametric study, is due to the presence of the rotor blade on the inboard side of the nacelle.

As a result of engine mount studies and the desire to maintain minimum nacelle volume and weight, the maximum thickness of the blade and nacelle fell at approximately the same blade chordwise station. The combined diffusion along the aft end of the nacelle and blade caused local separation and excessive drag. This had the same effect as though the ℓ/D of the nacelle were too small and large increases in drag resulted (Figure 23).

The results of the tunnel tests define the character of the nacelle drag and the problem areas, and should not be considered to be the final configuration or the lowest achievable drag coefficient. The drag coefficients as used in the parametric study are achievable as shown from the data presented in Figure 23 This source data is taken from the text Fluid Dynamic Drag by Hoerner and is based on tests of similar shapes, fineness ratio, and Reynolds Number. Based on a comparison against Reynolds Number (Figure 24) a similar reduction in drag coefficient is evident.

The necessary area of nacelle redesign as noted from the tuft flow photographs is the juncture between the nacelle and wing. The flow in this area is largely separated due to the three-dimensional diverging flow angle, caused by the simultaneous curvature of the nacelle and blade. It is felt that further tests using a "speed pod"-type fairing, boundary layer control utilizing the engine exhaust for pumping power, or vortex generators will reduce the separated area to a minimum and bring the drag coefficient below the predicted values.

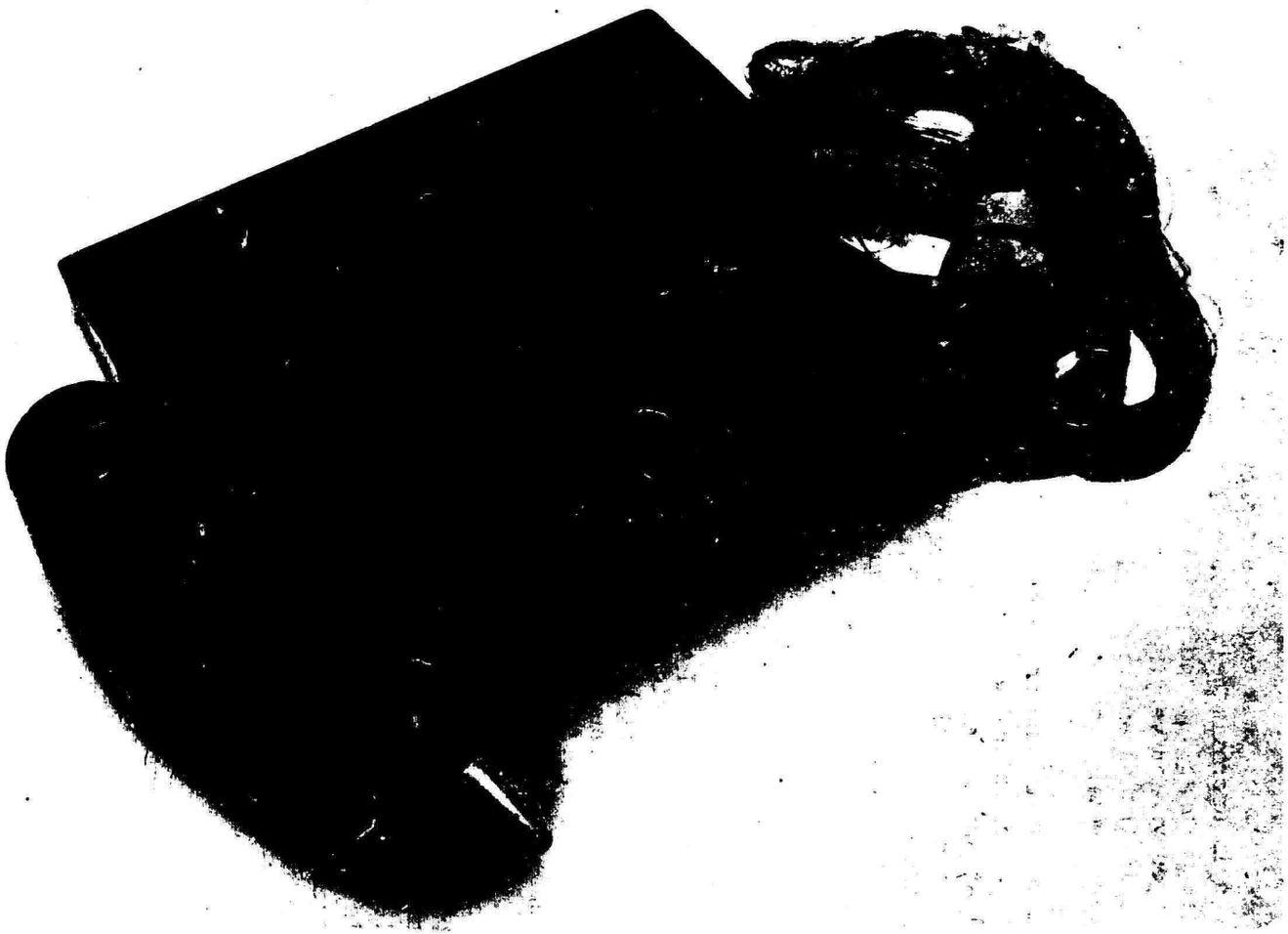

Figure 17. Single 1-50-100 Nacelle With Conical Centerbody and Blade. Runs 118 Through 132.

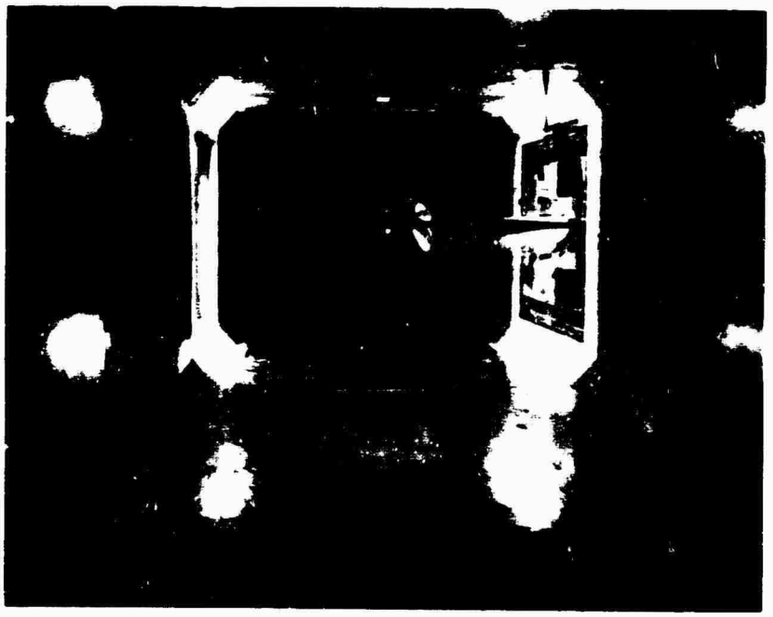

Figure 18a. Model Positioned in Test Section.

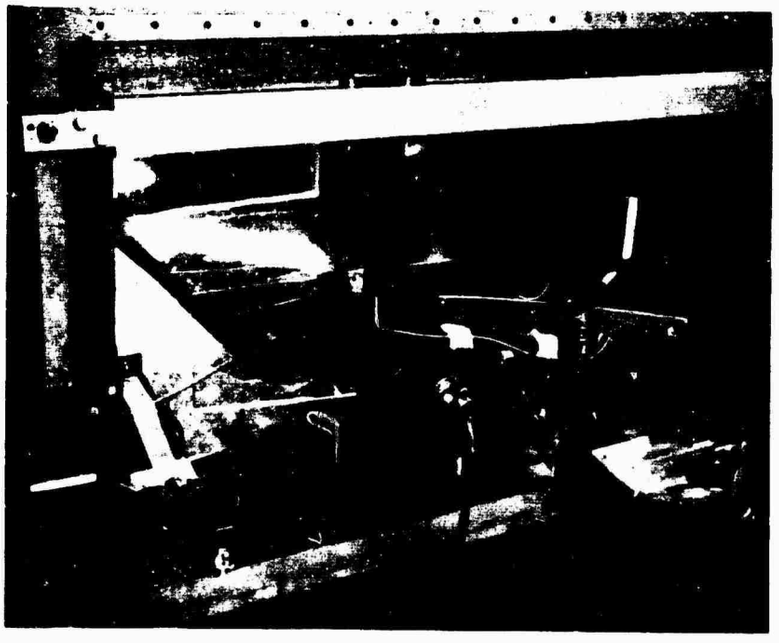

Figure 18b. Model Support Structure.

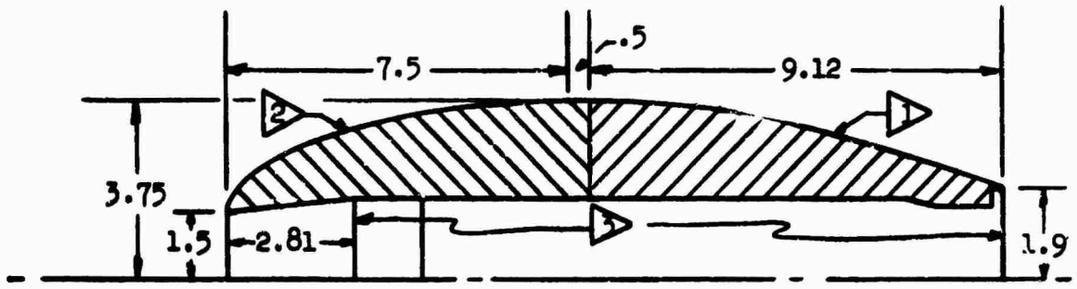

1-40-100 Nacelle

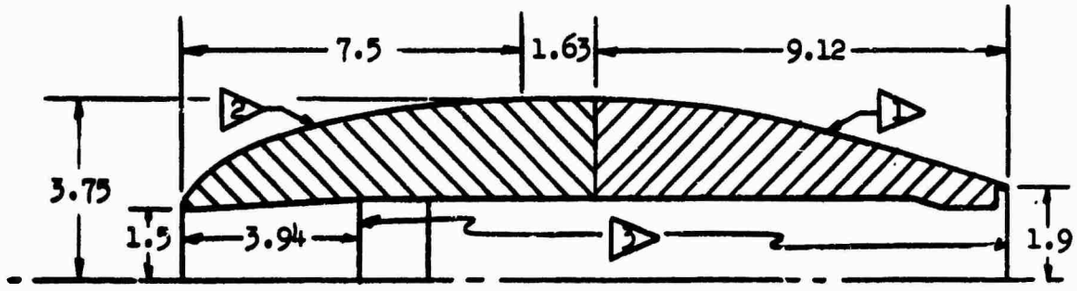

1-40-115 Nacelle

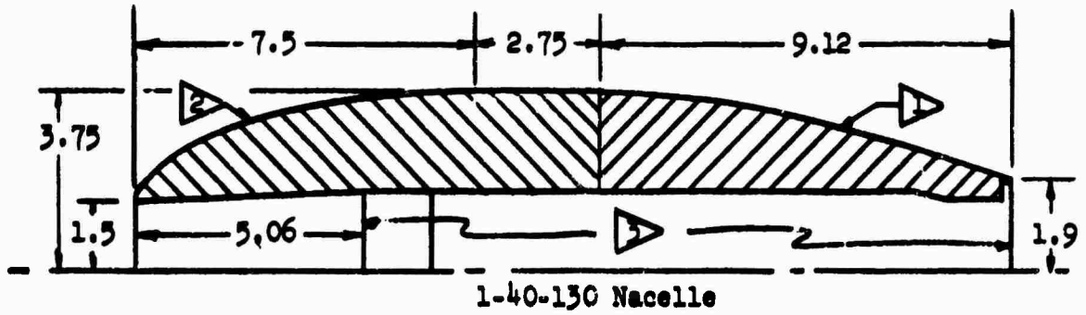

1-40-130 Nacelle

Notes:

1. Afterbody contour identical all nacelles. See Fig. 11.
2. 1-40 forebody contour. See Figure 9.
3. Internal dimensions identical all nacelles. See Fig. 6.

Figure 19a. Single Nacelle Comparisons.

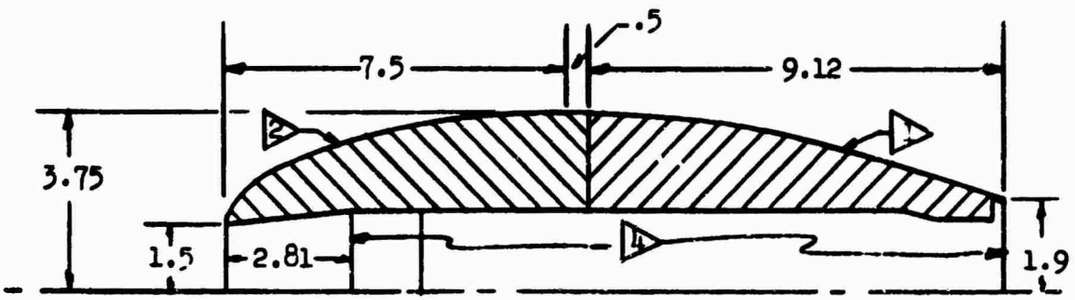

1-40-100 Nacelle

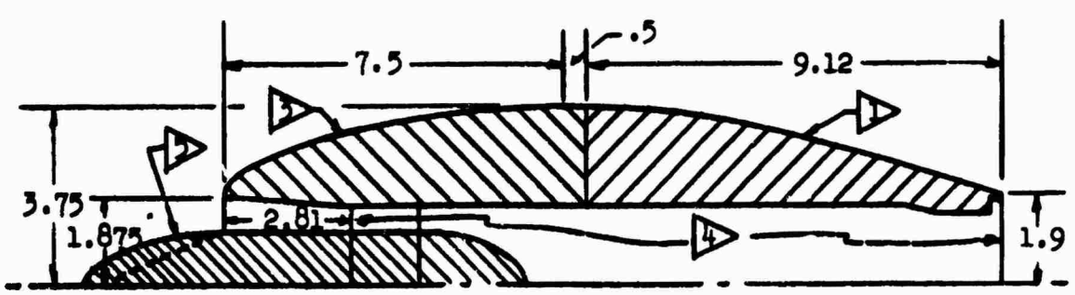

1-50-100 Nacelle

Notes:

Afterbody contour identical all nacelles. See Figure 11.

1-40, 1-50 forebody contour. See Figure 9.

Internal dimensions identical all nacelles. See Figure 6.

Center body profiles detailed on Figure 12.

Figure 19b Single Nacelle Comparisons.

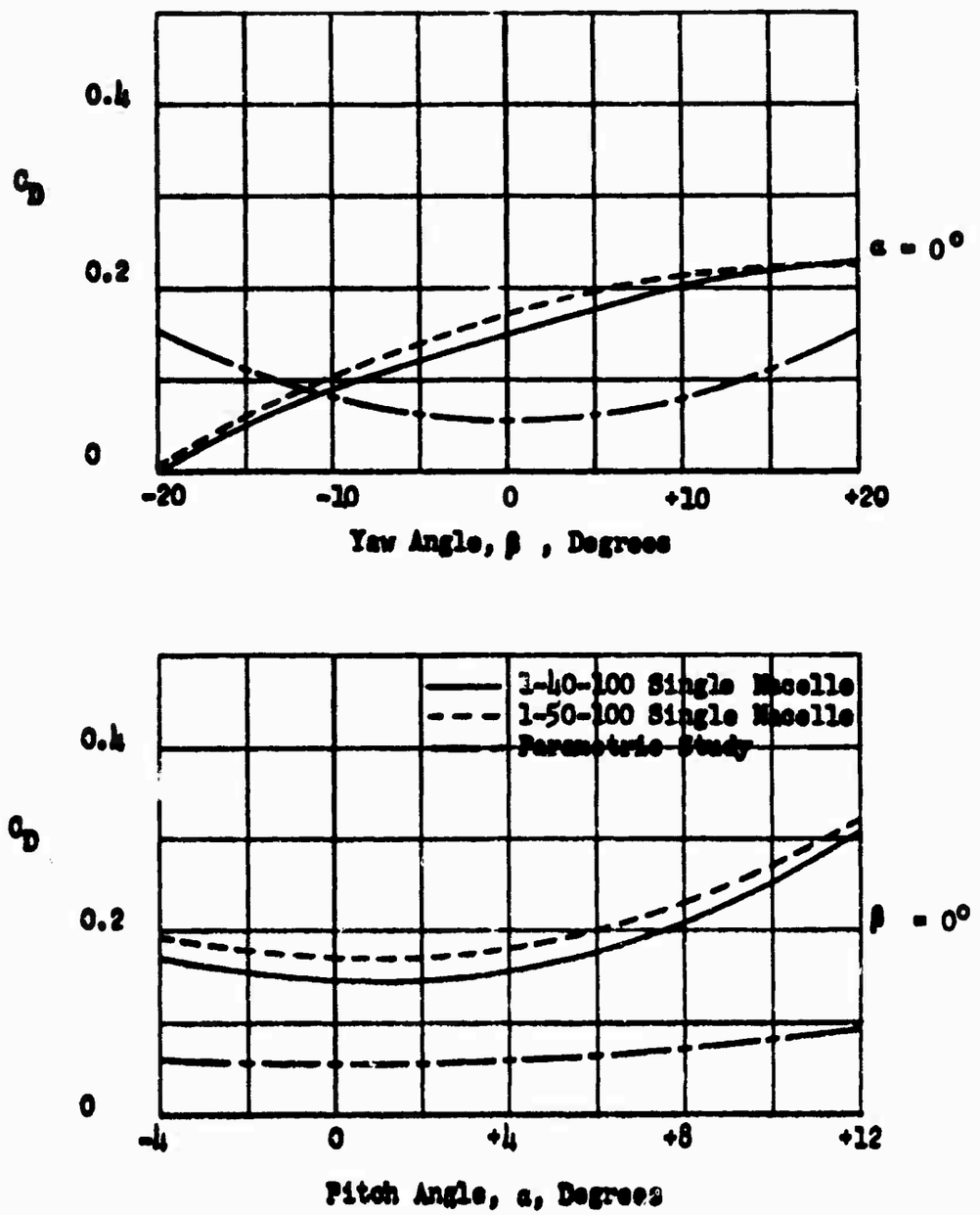

Figure 20. Drag Coefficient Versus Angle of Attack 1-40-100 and 1-50-100 Single Nacelles

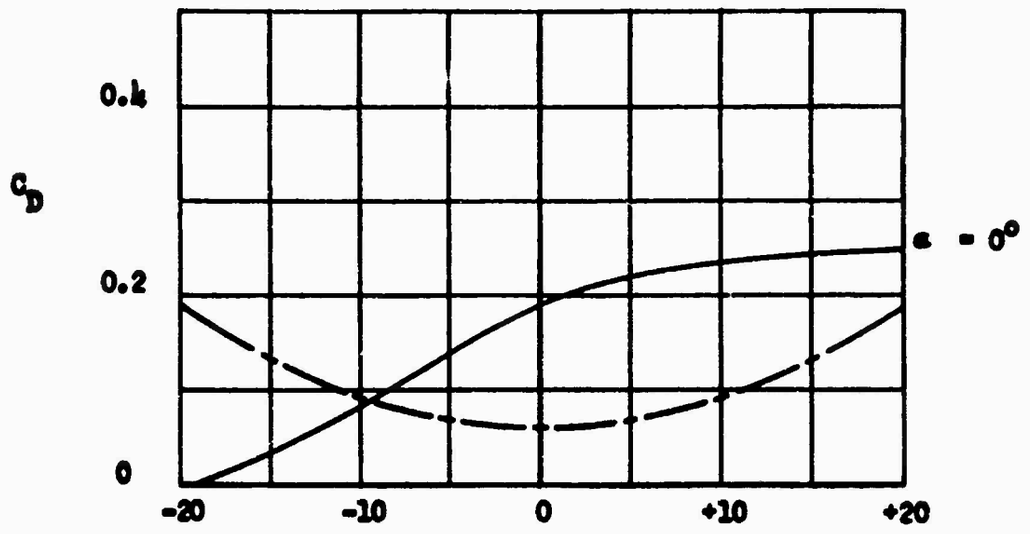

Yaw Angle, β , Degrees

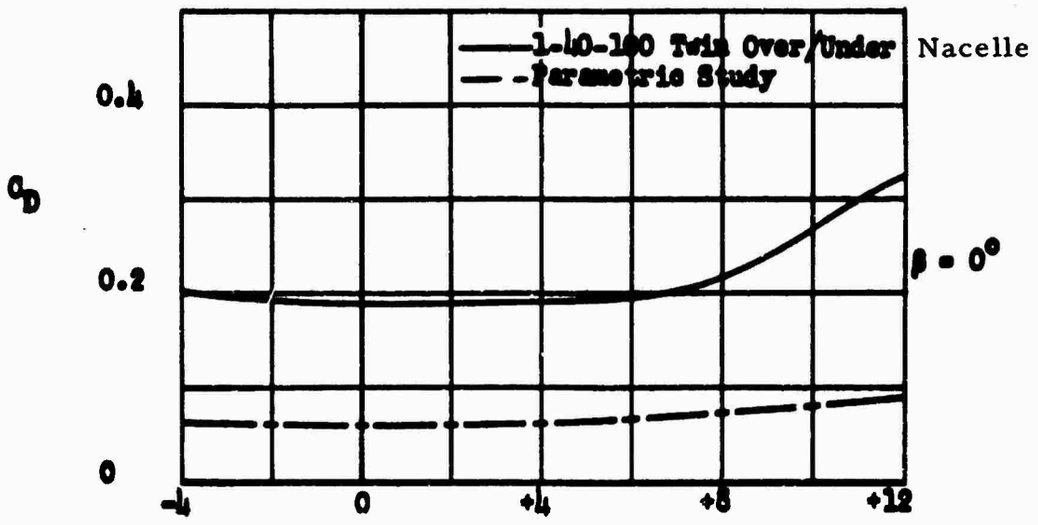

Pitch Angle, α , Degrees

Figure 21. Drag Coefficient Versus Angle of Attack
1-40-100 Twin Over-Under Nacelle

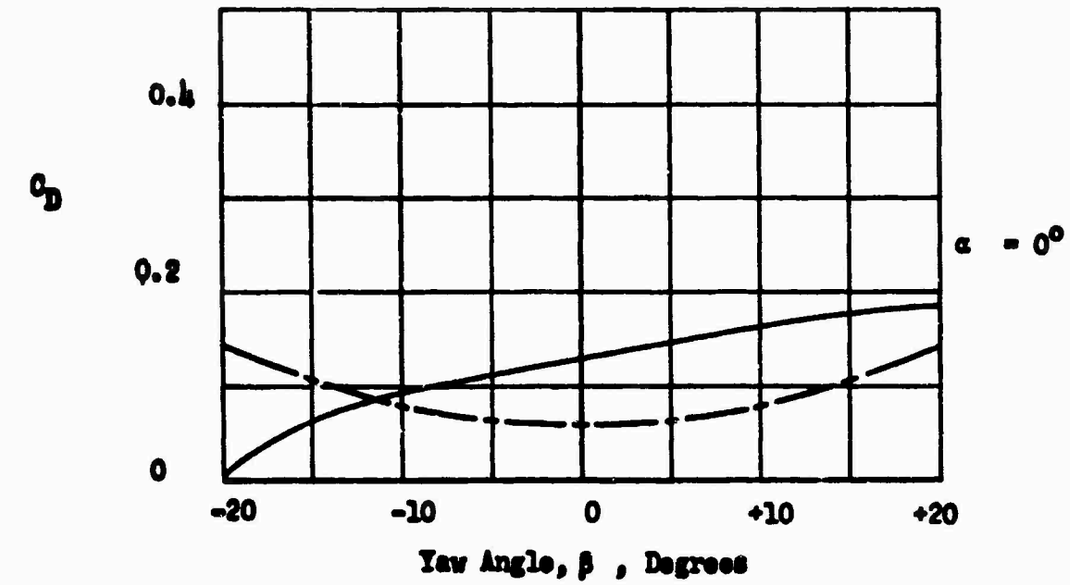

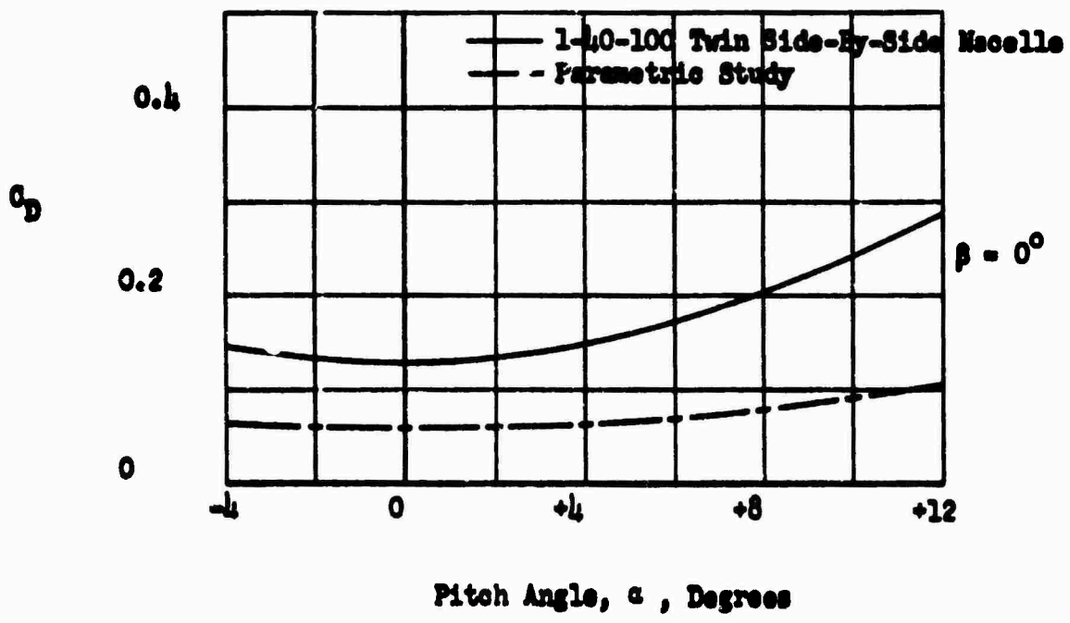

Figure 22. Drag Coefficient Versus Angle of Attack
1-40-100 Twin Side-By-Side Nacelle

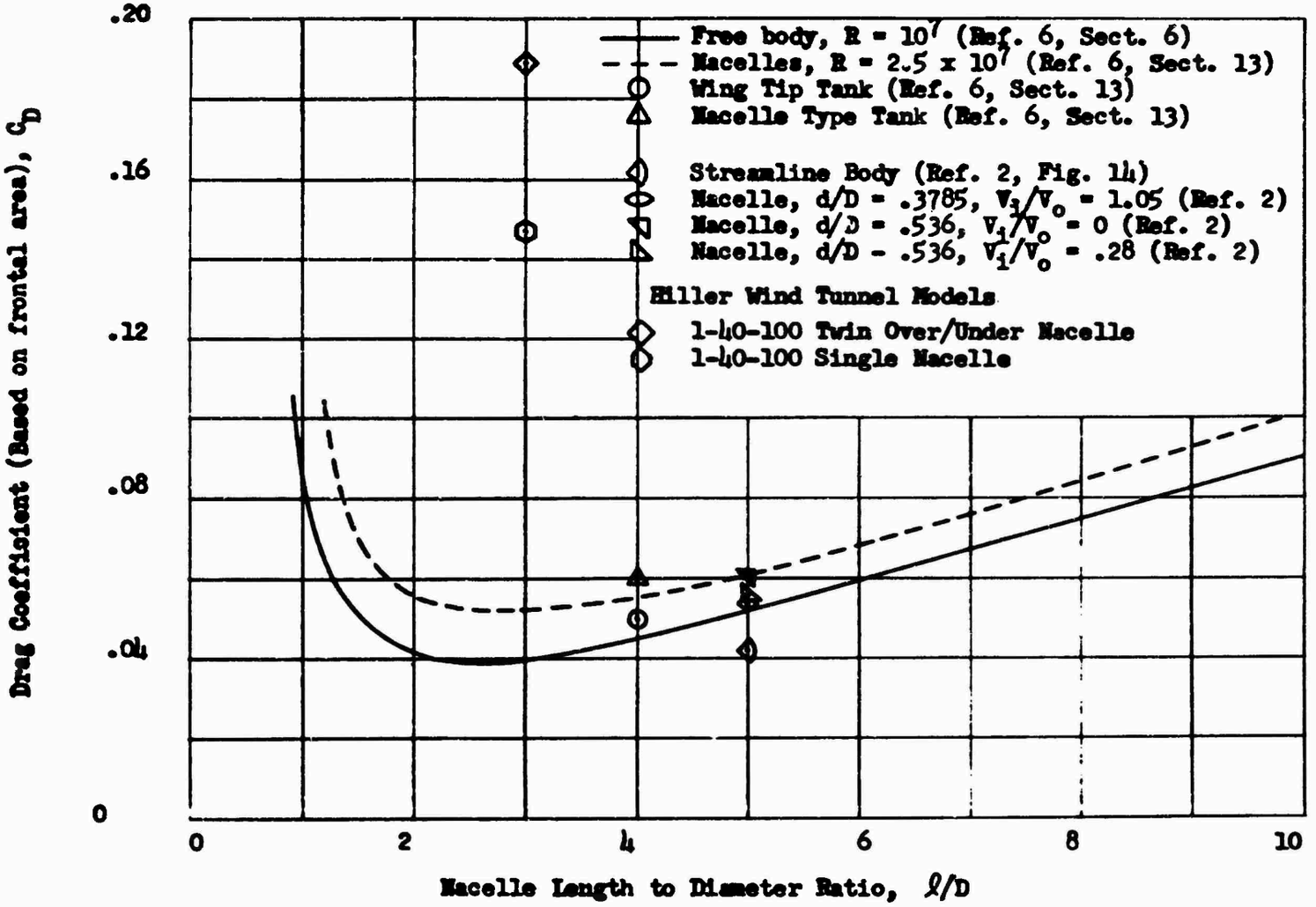

Figure 23. Drag Coefficient Versus Length/Diameter Ratio

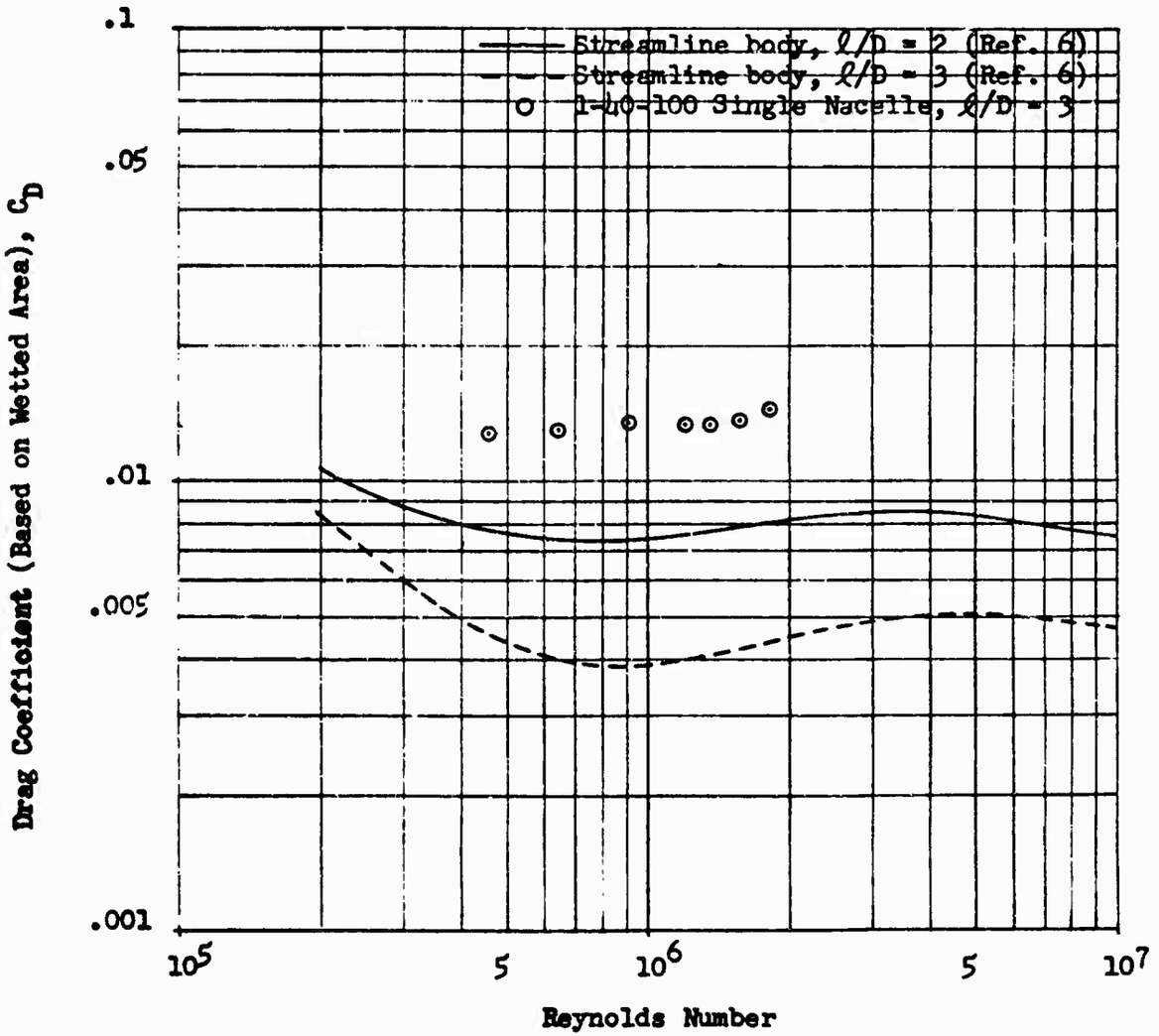

Figure 24. Drag Coefficient versus Reynolds Number

10.0 PERFORMANCE ANALYSIS - MODEL 1108

The performance calculation methods utilized for the Hiller Aircraft Model 1108 tip turbojet-powered helicopter are consistent with standard rotary wing industry performance procedures (Reference 11) with the exception of the determinations of main rotor profile power, power available, and the tail rotor power. These items were necessarily altered to reflect the use of tip turbojet propulsion.

The standard main rotor profile power term was obtained by calculating the hover profile power and then multiplying by K_μ, which increases the hover profile power to account for the differential velocity on the advancing and retreating blades during forward flight. The nacelle profile power term was calculated in a similar manner, except that the $K_{\mu N}$ factor includes not only the increase in profile power due to the differential velocity, but also that due to the integrated side load on the nacelle. The total profile power for the tip turbojet rotor was thus obtained by adding the standard blade profile term to the similar nacelle term.

The power available was calculated by the equation:

$$HP_{A_V} = \frac{F_n V_T n}{550} - \frac{V^2 W_a n}{32.2(1100)}$$

where:

F_n = Engine net thrust at V_{T_V} as supplied by the manufacturer

n = Number of engines operating (eight engines operating for all performance)

V = Freestream helicopter velocity

V_T = Tip speed (for hover or forward flight)

W_a = Engine air flow as supplied by the manufacturer

The second term in the available horsepower equation is the rotor ram drag horsepower. This is obtained by integrating over one revolution the drag component of the radial force caused by turning the engine air flow through the yaw angle of attack.

The tail rotor on a tip-driven helicopter is required basically for maneuvering rather than for torque compensation of the main rotor. The tail rotor power is, therefore, a very small percentage of the total power and for simplification was added as a constant value in the miscellaneous power term.

Main rotor tip stall and compressibility calculations were performed using the standard methods. The nacelles have been designed with a critical Mach number versus angle of attack curve which is less restricting than that of the NACA 0015 airfoil main rotor blades.

The performance summary data listed in Table 8 were calculated using a tip speed of 650 feet per second and an A_π value of 200 square feet except as noted.

TABLE 8
PERFORMANCE SUMMARY

Item	Gross Weight (Lb.)			
	47,680	72,104	90,100	103,000
Max. speed at S.L. - V_T = 592 f.p.s. (knots)	133 (A_x = 200) 146 (A_x = 100)	127	123	-
Cruising speed at S.L. - V_T = 592 f.p.s. (knots)	93	100	105	111
Max. rate of climb at S.L. (ft/min.)	6,040	3,010	1,950	-
Vert. rate of climb at S.L. (ft/min.)	5,900	2,910	1,140	-
Hover ceiling out-of-ground effect - OAT = 95°F. (ft.)	-	6,060	-	-
Hover ceiling out-of-ground effect - standard day (ft.)	26,200	14,100	5,750	750
Service ceiling (ft.)	32,000	22,000	15,800	-

Note: All performance data for MRP.
A_x = 200 ft^2 and standard conditions except as noted. V_T = 650 f.p.s. except as noted.

11.0 STABILITY AND CONTROL STUDIES

The purpose of the analysis reported herein was to evaluate the feasibility of the tip turbo concept from a stability and control standpoint. A crane configuration fuselage was mated to the Model 1108 rotor system as a model for analysis. This helicopter configuration was not intended as an optimum design, but as a realistic configuration suitable for evaluating the flying characteristics. This configuration was evaluated from hover to 108-1/2 knots for both the design gross weight and the return mission gross weight.

The Military Specification for Helicopter Flying Qualities (MIL-H-8501A) was used as a guide for stability and control criteria. Specific items checked against this specification were: control position and body attitude as a function of forward speed; body attitude response at hover; maneuver response at hover and forward speed; response to artificial disturbance at forward speed; and stick-fixed dynamics. All of the requirements were met or exceeded. In many cases the Model 1108 was compared to additional criteria, other than MIL-H-8501A, which were felt to be more applicable to a heavy-lift helicopter. Control power criteria, used as a design objective for this report, far exceeds the requirements of MIL-H-8501A.

All of the analysis is shown for the helicopter configuration alone, with no addition of stability augmentation. While augmentation is not required to satisfy the criteria, it is shown that augmentation will be required to achieve preferred handling qualities.

11.1 Configuration Description

The stability and control analysis was based on the configuration shown on Figure 25. This configuration is not intended to be the optimum helicopter design for the Model 1108 rotor system. It was selected to provide a realistic configuration for stability and control analysis. The dimensions and characteristics are summarized below:

Main Rotor:

Airfoil section (constant)	NACA 0015
Chord (constant), ft.	6.5
Diameter, ft	111.8
Number of blades	4
Solidity	0.148
Tip speed, ft/sec - Hover	650
- Cruise	600
Twist, degrees	10
Type	Teetering

Collective pitch movement, degrees	15
Lateral cyclic movement, degrees	12
Longitudinal cyclic movement, degrees	12
Spring restraint per blade, lb-ft/rad	374,000

Tail Rotors: (characteristics per rotor)

Chord (constant), ft.	0.98
Diameter, ft.	8.0
Moment arm, ft. (main rotor hub to tail rotor ℄)	38.0
Number of blades	5
Number of tail rotors (See Figure 25 for arrangement).	2
Solidity	0.39
Tip speed, ft/sec.	650
Twist, degrees	0
Collective pitch movement, degrees	+11,-9

Stabilizer:

Area, ft^2.	48.0
Aspect ratio	3
Chord (constant), ft.	4.0
Incidence, degrees	0
Moment arm, ft. (main rotor hub to stabilizer quarter chord)	31.2
Span, ft.	12.0

Fuselage:

Equivalent flat plate area, ft^2.	
Including cargo pod	200
Cargo pod removed	100

Tip Turbo Engines:

Inlet area, ft^2 (both engines)	2.08
*Lift curve slope of nacelle, $(\partial C_L/\partial\alpha)_{TT}$ per rad.	4.5
Mounting	Over-Under
Number of engines per blade	2
*Profile drag, $C_{d_{TT}}$	$.282+4.125\alpha^2$

Mass Properties

---

* Based on inlet area.

Blade mass properties, per blade:

(including effect of engines at blade tip)

Mass, slugs	108.7
Distance of c.g. outboard of hub, ft.	29.4
Flapping moment of inertia about hub, slug-ft^2	138,700

Helicopter mass properties:

(See Table 9.)

11.2 Compliance with MIL-H-8501A

Longitudinal Trim Conditions

The Model 1108 has adequate control power to provide trimmed, level flight over the desired speed range. A reasonable body attitude is maintained at all speeds, and sufficient margin of control is available for maneuvering.

Longitudinal cyclic position and fuselage attitude are shown in Figure 26 for level forward flight. The curves are smooth, with no objectionable reversal in slope. The most critical condition for control margin is trimmed level flight at maximum speed, with the aft center of gravity loading. Two degrees of control travel are available beyond trim at this flight condition. This provides a margin of 20 percent of the available control in hovering.

The slope of the cyclic control position is stable over the desired speed range for the normal gross weight. The light gross weight has a stable slope, except for a small region of neutral stability from hover to 20 knots forward. Control force stability with respect to speed follows as a consequence of the control position stability through the use of an irreversible control system.

Pitch Attitude Response at Hover

The response to control input has been designed to provide desirable handling qualities. In order to achieve the desirable characteristics, it was necessary to include a spring system to restrain the flapping motion of the main rotor blades. A spring restraint of 374,000 foot-pounds per radian per blade was found adequate. This amount of spring restraint is equivalent to a flapping hinge offset of 1-1/2 percent of blade radius. The resulting design provides attitude response characteristics which exceed the requirements of MIL-H-8501A (Reference 12). The control power criteria, used as the design objective, is discussed in Section 11.3. Table 10 compares the Model 1108 response with the requirements of Reference 12.

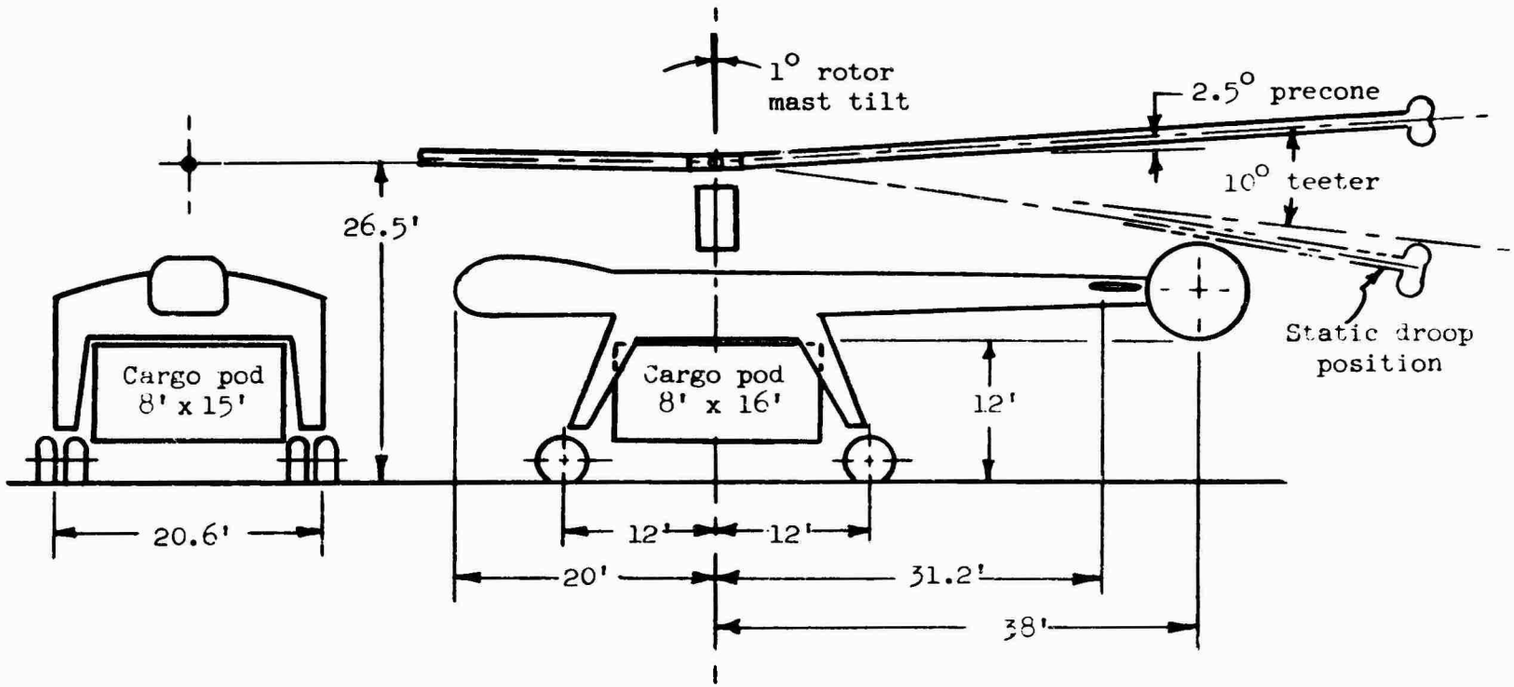

Figure 25. General Arrangement - Stability Analysis Model.

TABLE 9
HELICOPTER MASS PROPERTIES

Condition	Weight Breakdown				c.g.		Moments of Inertia			
	Gross	Empty + Crew	Fuel	Cargo	h	e_f	$I_{\bar{x}\bar{x}}$	$I_{\bar{y}\bar{y}}$	$I_{\bar{z}\bar{z}}$	$I_{\bar{x}\bar{z}}$
	(lb.)				(ft.)		(slug-ft^2)			
Light weight, no cargo	39,200	33,850	5,350	0	5.9	-.10	76,000	131,000	81,400	779.5
Fully loaded, rigid load, mid c.g.	71,700	33,850	13,850	24,000	10.9	-.06	178,000	228,000	117,500	-967.6
Fully loaded, rigid load, aft c.g.	71,700	33,850	13,850	24,000	10.9	-.50	178,000	189,500	78,900	-2770.2
Fully loaded, sling suspended load.	71,700	33,850	13,850	24,000	6.84	-.06	87,000	134,700	87,200	-610.1

e_f = distance of c.g. forward of main rotor hub.

h = distance of main rotor hub above c.g.

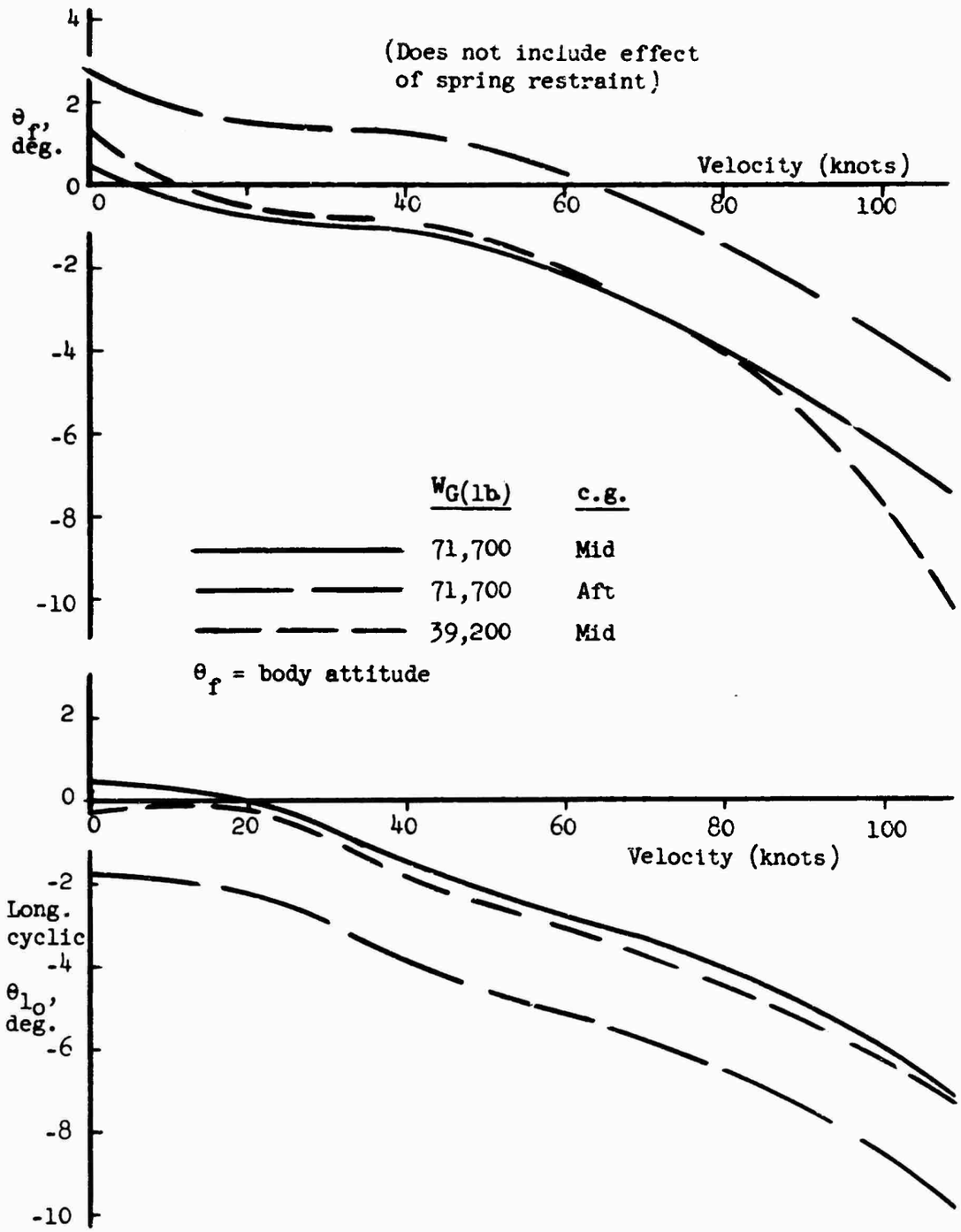

Figure 26. Longitudinal Trim Conditions.

TABLE 10
PITCH ATTITUDE RESPONSE
(HOVER IN STILL AIR, SEA LEVEL, MID c.g.)

Gross Weight (lb.)	Longitudinal Cyclic Stick Input	Angular Displacement in Pitch at the End of One Second	
		Model 1108 $\Delta\alpha_1$, (Deg.)	MIL-H-8501A Requirement $\Delta\alpha_1$, (Deg.)
39,200	One inch	4.6	1.3
71,700	displacement	4.6	1.1
*71,700	from trim.	5.6	1.1
			$\Delta\alpha_1 = \frac{45}{\sqrt[3]{W_G + 1000}}$
39,200	Maximum	26.8	5.2
71,700	displacement	26.7	4.3
*71,700	from trim.	32.1	4.3
			$\Delta\alpha_1 = \frac{180}{\sqrt[3]{W_G + 1000}}$

*Load suspended from c.g. by sling. (All other conditions have rigidly attached load.)

Longitudinal Maneuver Control

The Model 1108 satisfies the maneuver stipulations of MIL-H-8501A for hover and forward speed. These requirements specify the point of inflection in time histories of normal acceleration and angular velocity following step control displacements.

Longitudinal Response to Artificial Disturbance

The response to an artificial input indicates the pilot should have adequate time for corrective action following an attitude disturbance. The MIL-H-8501A requirement specifies the maximum deviation of normal acceleration from the steady trim value, due to an impulse control input.

Longitudinal Stick-Fixed Dynamics

The longitudinal stick-fixed dynamics satisfy the requirements of Reference 12 without the aid of stability augmentation. Some stability augmentation will be required to achieve desirable handling qualities beyond the basic requirements of Reference 12 (MIL-H-8501A).

The dynamic behavior has been determined by examining the roots of the characteristic equation of the longitudinal dynamics. Table 11 presents the roots of the characteristic equation, plus the time and number of

TABLE 11
STICK-FIXED LONGITUDINAL DYNAMICS
(LEVEL FLIGHT AT SEA LEVEL)

Gross Weight	c.g.	Velocity	Roots $\lambda = n \pm i\omega$		Period	$t_{\frac{1}{2}x}$	t_{2x}	$c_{\frac{1}{2}x}$	c_{2x}	MIL-H-8501A, Par. 3.2.11 Requirement
(lb.)		(knots)	(n)	(ω)	(sec.)	(sec.)	(sec.)			
39,200	Mid	0	.007447	.24073	26.1	-	93.2	-	3.57	$t_{2x} > 10$ sec.
			-2.2901	.55050	11.4	.303	-	.0265	-	$t_{2x} > 10$ sec.
			-2.6415	-	-	.262	-	-	-	Not Applicable
		60.0	-.008086	.18576	33.8	85.7	-	2.53	-	$t_{2x} > 10$ sec.
			-2.1908	1.7540	3.58	.316	-	.0883	-	$c_{\frac{1}{2}x} \leqq 2$
			-2.3580	-	-	.294	-	-	-	Not Applicable
		108.5	.009900	.24984	25.1	-	70.0	-	2.78	$t_{2x} > 10$ sec.
			-2.0445	1.7398	3.61	.339	-	.0939	-	$c_{\frac{1}{2}x} \leqq 2$
			-2.8544	-	-	.243	-	-	-	Not Applicable
71,700	Mid	0	.043170	.32118	19.6	-	16.0	-	.821	$t_{2x} > 10$ sec.
			-1.2484	-	-	.555	-	-	-	Not Applicable
			-1.4440	-	-	.480	-	-	-	Not Applicable
			-3.4094	-	-	.203	-	-	-	Not Applicable
		60.0	.006123	.24570	25.6	-	113.2	-	4.43	$t_{2x} > 10$ sec.
			-2.1166	1.3000	4.83	.328	-	.0678	-	$c_{\frac{1}{2}x} \leqq 2$
			-1.3648	-	-	.508	-	-	-	Not Applicable
		108.5	.001235	.24541	25.6	-	561.2	-	21.9	$t_{2x} > 10$ sec.
			-1.5531	1.4158	4.44	.446	-	.1006	-	$c_{\frac{1}{2}x} \leqq 2$
			-2.5022	-	-	.277	-	-	-	Not Applicable
71,700	Aft	108.5	-.00949	.2331	26.9	73.0	-	2.71	-	$t_{2x} > 10$ sec.
			-1.6294	1.7934	3.50	.425	-	.125	-	$c_{\frac{1}{2}x} \leqq 2$
			-2.3631	-	-	.293	-	-	-	Not Applicable

cycles to double or half amplitude. The requirements of Reference 12 are included for comparison. The modes of motion are presented for hover, maximum speed, and an intermediate speed, for both the light and fully loaded gross weights. The data is presented for the nominal center of gravity, with the addition of one aft center of gravity point for comparison. All of the short period and aperiodic roots are well damped. The long period roots are either lightly damped or slowly divergent. Reference 12 allows some divergence for the long period roots, if the time to double amplitude is greater than 10 seconds. The time to double amplitude for the divergent roots far exceeds this requirement.

Roll Response at Hover

The roll angle response in hover is similar to the pitch attitude response in hover. The spring restraint system affects the roll and pitch axes equally, except for the difference in fuselage inertias. Table 12 compares the Model 1108 roll response with the requirements of Reference 12.

TABLE 12
ROLL ANGLE RESPONSE
(HOVER IN STILL AIR, SEA LEVEL, MID C.G.)

Gross Weight (lb.)	Lateral Cyclic Stick Input	Angular Displacement in Roll at the End of 1/2 Second		
		Model 1108 $\Delta\phi$,(Deg.)	MIL-H-8501A Requirement $\Delta\phi$,(Deg.)	
39,200	One-inch	1.8	0.8	$\Delta\phi = \frac{27}{\sqrt[3]{W_G+1000}}$
71,700	displacement	1.4	0.6	
*71,700	from trim.	2.1	0.6	
39,200	Maximum	10.6	2.4	$\Delta\phi = \frac{81}{\sqrt[3]{W_G+1000}}$
71,700	displacement	8.5	1.9	
*71,700	from trim.	12.4	1.9	

*Load suspended from c.g. by sling. (All other conditions have rigidly attached load.)

Directional Response at Hover

The yaw angle developed after one second of step rudder pedal input is given in Table 13 on the following page. The change in yaw angle, required by Reference 12, is also indicated. The required yaw angle is achieved for each condition, although the response for one-inch pedal input is marginal.

TABLE 13
YAW ANGLE RESPONSE
(GROSS WEIGHT = 71,700 LB.)

Rudder Pedal Input	Wind Condition	Angular Displacement in Yaw at the End of 1 Second		
		Model 1108 $\Delta\psi$, (Deg.)	MIL-H-8501A Requirement $\Delta\psi$, (Deg.)	
Full left pedal.	No wind.	-11.8	-7.9	$\Delta\psi = \frac{330}{\sqrt[3]{W_G+1000}}$
" " "	35-knot wind from right.	-4.3	-2.6	$\Delta\psi = \frac{110}{\sqrt[3]{W_G+1000}}$
1 inch left	No wind.	-2.9	-2.6	
Full right pedal.	No wind.	10.3	7.9	$\Delta\psi = \frac{330}{\sqrt[3]{W_G+1000}}$
" " "	35-knot wind from left.	3.2	2.6	$\Delta\psi = \frac{110}{\sqrt[3]{W_G+1000}}$
1 inch right	No wind.	2.4	2.6	

Lateral-Directional Stick-Fixed Dynamics

The lateral-directional behavior has been determined in the same manner as classical fixed-wing airplane stability. Three degrees of freedom have been considered: roll, yaw, and sideslip. The equations of motion combine to form a fourth order characteristic equation of the lateral-directional dynamics. The roots of this equation correspond to the following modes of motion:

Hover:
a. Long period roll oscillation
b. Aperiodic yaw mode
c. Aperiodic roll mode

Forward Speed:
a. Dutch-roll oscillation
b. Aperiodic spiral mode
c. Aperiodic roll mode

The characteristics of these modes are presented in Table 14 for the light and normal gross weight loadings. The speed range is covered by three flight conditions. All of the conditions are for the mid center-of-gravity loading. The aft center-of-gravity loading is also shown at maximum speed for comparison. Table 14 shows all of the modes to be stable, except for the long period hover mode for the fully loaded gross weight. Each mode is more fully discussed in the test following the table.

TABLE 14
STICK-FIXED LATERAL-DIRECTIONAL DYNAMICS
(LEVEL FLIGHT AT SEA LEVEL)

Gross Weight	c.g.	Velocity	Root $\lambda = n \pm i\omega$		Period	$t_{\frac{1}{2}x}$	t_{2x}	$c_{\frac{1}{2}x}$	c_{2x}	Mode
(lb.)		(knots)	(n)	(ω)	(sec.)	(sec.)	(sec.)			
39,200	Mid	0	-.002788	.24303	25.8	248.6	-	9.62	-	*Long period roll oscil.
			-1.3149	-	-	.527	-	-	-	Yaw
			-2.0643	-	-	.336	-	-	-	Roll
		60.0	-.62680	1.6481	3.81	1.11	-	.2901	-	Dutch roll
			-.017015	-	-	40.7	-	-	-	Spiral
			-2.6521	-	-	.261	-	-	-	Roll
		108.5	-.62947	2.2074	2.85	1.10	-	.3869	-	Dutch roll
			-.072840	-	-	9.52	-	-	-	Spiral
			-1.7792	-	-	.390	-	-	-	Roll
71,700	Mid	0	.033484	.32883	19.1	-	20.7	-	1.084	*Long period roll oscil.
			-.80469	-	-	.861	-	-	-	Yaw
			-1.1843	-	-	.585	-	-	-	Roll
		60.0	-.40931	1.4103	4.46	1.69	-	.3801	-	Dutch roll
			-.021868	-	-	31.7	-	-	-	Spiral
			-1.6936	-	-	.409	-	-	-	Roll
		108.5	-.40671	1.8709	3.36	1.70	-	.5075	-	Dutch roll
			-.053909	-	-	12.8	-	-	-	Spiral
			-1.2212	-	-	.568	-	-	-	Roll
71,700	Aft	108.5	-.61601	2.2582	2.78	1.12	-	.4044	-	Dutch roll
			-.055667	-	-	12.4	-	-	-	Spiral
			-1.1713	-	-	.592	-	-	-	Roll

*These two roots obtained from longitudinal equations of motion by substituting roll inertia for pitch inertia. (All other roots obtained from lateral-directional equations of motion.)

Long Period Roll Oscillation in Hover

This mode is the lateral counterpart to the long period oscillation occurring in the longitudinal motion. As in the longitudinal case, it is a function of speed stability and angular velocity damping.

There is no direct military specification requirement for the damping of this mode. The requirement of paragraph 3.2.11 of Reference 12 is the only related reference to dynamic characteristics. This requirement applies to longitudinal behavior in forward flight, but may be considered applicable to the closely related roll mode. It states that for long period oscillations (10- to 20-second periods), the oscillation may be divergent, but double amplitude shall not be achieved in less than 10 seconds.

Table 14 shows this motion to be lightly damped for the light gross weight. The motion is divergent for the fully loaded configuration, but requires 20.7 seconds to achieve double amplitude. The behavior of the long period hover oscillation therefore appears to be satisfactory.

Aperiodic Yaw Mode in Hover

This mode corresponds to the yaw rate damping in hover. Paragraph 3.3.19 of Reference 12 states: "The yaw angular velocity damping should preferably be at least $27(I_z)^{.7}$ foot pounds per radian per second." Table 15 compares the yaw damping for the Model 1108 with this requirement.

TABLE 15
YAW RATE DAMPING IN HOVER

Gross Weight	MIL-H-8501A Requirement		Model 1108
	$27(I_z)^{.7}$	$\frac{27(I_z)^{.7}}{I_z}$	
lb.	$\frac{\text{ft.-lb.}}{\text{rad./sec.}}$	Yaw Damping per Sec.	Yaw Damping per Sec.
39,200	74,100	.91	1.31
71,700	95,500	.81	.80

Aperiodic Roll Mode in Hover and Forward Speed

This mode corresponds to the roll rate damping. Reference 12 has a requirement for the amount of this damping in hover. The requirement for flight at forward speed is not specified. Table 16 shows these minimum requirements to be easily satisfied.

TABLE 16
ROLL RATE DAMPING

Gross Weight	Velocity	MIL-H-8501A Requirement		Model 1108
		$18(I_x)^{.7}$	$\frac{18(I_x)^{.7}}{I_x}$	
lb.	knots	$\frac{\text{ft.-lb.}}{\text{rad./sec.}}$	roll damping per sec.	roll damping per Sec.
39,200	0	47,000	.62	2.06
↓	60.0	N.A.	N.A.	2.65
	108.5	N.A.	N.A.	1.78
71,700	0	85,000	.48	1.18
↓	60.0	N.A.	N.A.	1.69
	108.5	N.A.	N.A.	1.22

Spiral and Dutch Roll Modes at Forward Speed

There is no requirement for the behavior of these modes in Reference 12. Reference 14 provides recommended requirements for lateral-directional handling qualities. These requirements are recommended for inclusion in military specifications for helicopters intended for instrument flight.

The requirements recommended by Reference 14, page 19, for dutch-roll and spiral mode behavior are as follows:

a. "At landing approach speeds and above, the lateral oscillation known as dutch roll shall be well enough damped to lie on the favorable side of the acceptable-marginal boundary of 'Figure 5 herein.' It shall in no case be less than corresponds to half amplitude in two cycles."

b. "A spiral divergence shall in no case be stronger than corresponds to double amplitude in 7 seconds. Although convergence in this mode is desirable, slow divergence is permitted, provided the dutch-roll damping is sufficient."

The Model 1108 dutch-roll and spiral modes, listed in Table 14, are summarized below. The dutch-roll mode shows more damping than the minimum recommended requirement. The dutch-roll oscillation converges to half amplitude in well under two cycles. The spiral mode is stable at both speeds investigated.

The spiral and dutch-roll characteristics fall in the "marginal" region of the applicable "Figure 5" of item a. This demonstrates that although the basic configuration is flyable without augmentation, stability augmentation will be required to provide acceptable handling qualities.

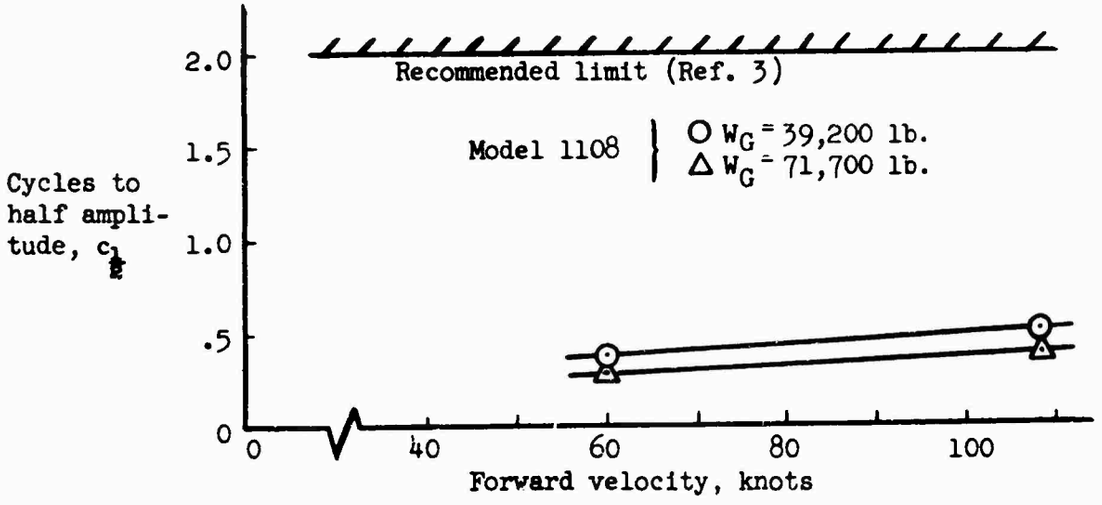

Figure 27. Dutch-Roll Mode.

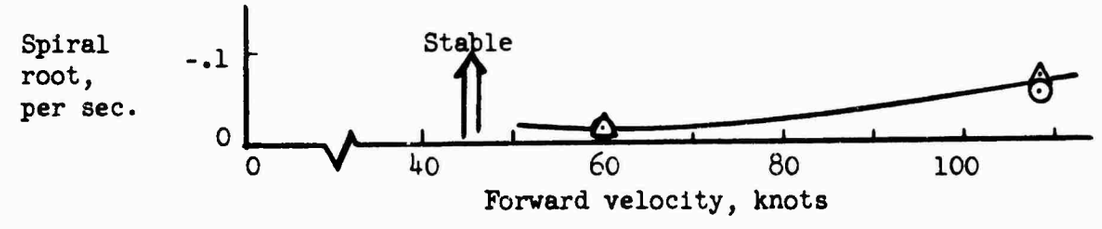

Figure 28. Spiral Mode

11.3 Increased Control Requirements for Heavy-Lift Helicopters

The control power requirements of Reference 12, are felt to be unrealistic for heavy-weight helicopters. This military specification states control power requirements in terms of a minimum allowable displacement of helicopter attitude resulting from a step control application. The required attitude displacement is given by:

$$\left.\begin{matrix}\Delta\alpha_1 \\ \Delta\phi\end{matrix}\right\} = \frac{K}{\sqrt[3]{W + 1000}} \quad \text{degrees}$$

or

where K depends on the magnitude of control input and the axis of interest. This formula has provided an adequate criteria as a function of gross weight for nominal weight helicopters, but is not adequate for very heavy gross weights.

The angular acceleration due to a given control input is considered to be a more basic criteria. Since the angular acceleration is determined by dividing the control moment by the helicopter inertia, weight effects are inherently accounted for. Preferred levels of angular acceleration and damping have been determined from helicopter flight test, and are presented in Reference 14. This information has been used as a design objective for the Model 1108. The Reference 14 boundaries will next be substantiated by comparison with additional NASA references. The Model 1108 characteristics will then be compared with the Reference 14 boundaries and the requirements of MIL-H-8501A.

Comparison of Pilot Opinion Boundaries

Pilot opinion boundaries for roll and pitch handling qualities are shown in Figures 29 and 30. These boundaries were taken from three separate NASA studies, described below.

Reference 14, NASA TN D-58: A flight test research program conducted with the S-51 helicopter. The boundaries are related to characteristics for visual and instrument flight operations.

Reference 15, NASA TN D-792: A piloted simulator investigation to establish attitude control requirements for hovering flight. Boundaries are given in terms of the "Cooper Pilot Opinion Rating System."

Reference 16, NASA TN D-1328: A flight test program conducted with the X-14A VTOL research vehicle to establish handling qualities requirements during hovering under visual flight conditions. Boundaries are given in terms of the "Cooper Pilot Opinion Rating System."

A direct comparison of these pilot opinion boundaries is not possible

because of the differences in test vehicles and rating systems. The latter two references relate to handling qualities, generally, whereas the first reference differentiates between instrument and visual flight operations. Regardless of the cited differences existing in the three references, the latter two references do substantiate the preferred level of control power established by the first. One exception to this is the low level of control power indicated by Reference 16 for the pitch axis. No apparent reason is available for this discrepancy.

It seems reasonable to interpret the "desirable" (good handling qualities for instrument flight operations) boundary of Reference 14 as indicative of preferred characteristics for precision visual flying. This should be an optimum criteria for design, and was used as a design objective for the Model 1108.

Model 1108 Control Power

Model 1108 control power and damping, for several loading conditions, are shown on Figures 31 through 34. Also shown on these figures are pilot opinion boundaries of NASA TN D-58, and curves corresponding to the requirements of MIL-H-8501A, are derived as follows:

For a single degree of freedom system with rate damping and a step input forcing function, we have,

$$\delta = \frac{F}{D^2}\left[e^{(D)t} - (D)t - 1\right]$$

where, δ = angular displacement at time, t., radians.

F = magnitude of step input forcing function, rad/sec^2.

D = rate damping, $\frac{rad/sec^2}{rad/sec} = \frac{1}{sec.}$

t = time from initiation of step input, seconds.

for $\delta = \frac{K}{\sqrt[3]{W + 1000}}$, deg., from MIL-H-8501A, we have

$$\frac{1}{57.3}\left(\frac{K}{\sqrt[3]{W + 1000}}\right) = \frac{F}{D^2}\left[e^{(D)t} - (D)t - 1\right]$$

This equation provides a relationship of damping versus control power, at constant gross weight, corresponding to the requirements of MIL-H-8501A.

Figures 32 and 34 show that the military specification requirement brackets the "desirable" boundary for gross weights of 2,000 to 10,000 pounds, but specifies too little control power for the heavier gross weights. The Model 1108 has been designed to provide control power approaching the

"desirable" boundary, as an optimum, rather than the minimum military specification requirement.

Figures 31 through 34 show the Model 1108 to meet the control power objective, with the spring restraint system included in the design. The spring restraint also has a significant effect on the damping. Even without the spring restraint, the control power would meet the MIL-H-8501A requirement. Pitch and roll damping, while not within the desirable boundary, exceeds the MIL-H-8501A requirements. Some stability augmentation should be added to achieve preferable damping.

Boundary	Descriptive Pilot Opinion	Reference
(A)	"Desirable" - "good handling qualities for instrument flight operations"	NASA TN D-58 (Ref.8) (S-51 flight test)
(B)	"Acceptable" - "acceptable for instrument flight operations"	
(C)	"Marginal" - "acceptable for visual flight operations only"	
(1)	"Satisfactory for normal operation" (Cooper Rating = 3-1/2)	NASA TN D-792 (Ref.9) (simulator test)
(2)	---Same as above---	NASA TN D-1328 (Ref.10) (X-14A flight test)

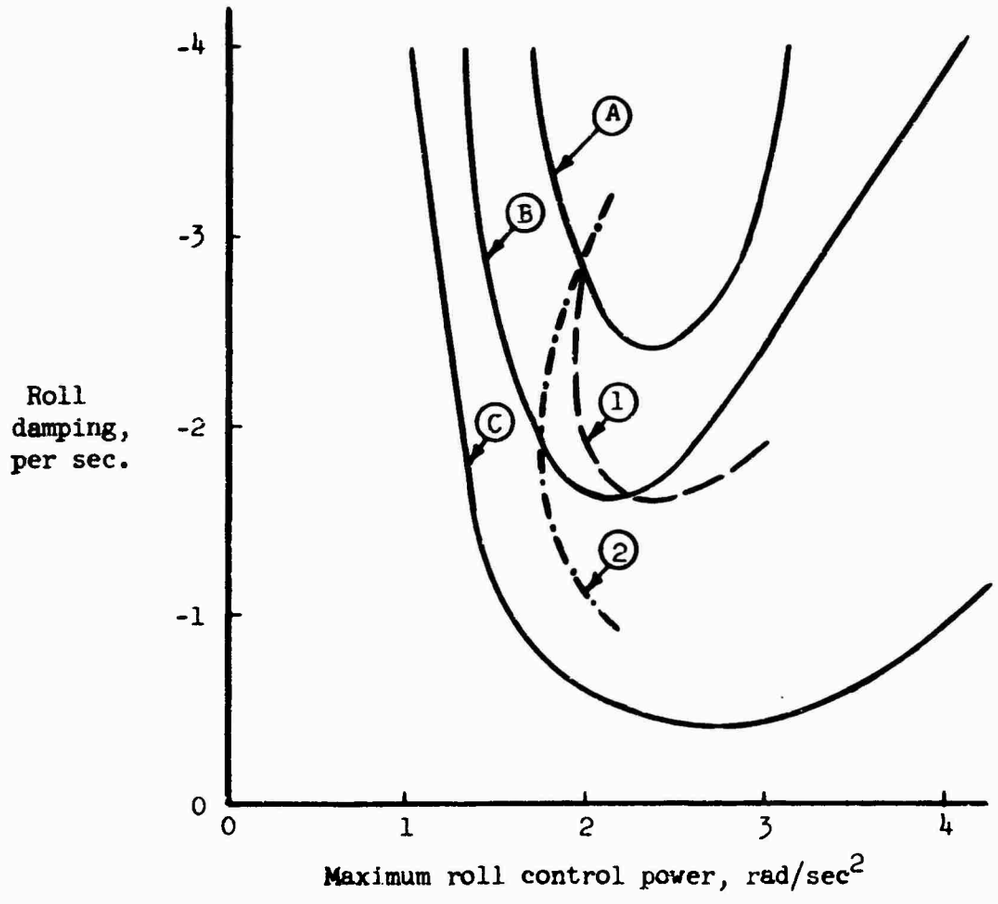

Figure 29. Pilot Opinion Comparison, Roll Axis.

Boundary	Descriptive Pilot Opinion	Reference
(A)	"Desirable" - "good handling qualities for instrument flight operations"	NASA TN D-58, (Reference 8) (S-51 flight test)
(B)	"Acceptable" - "acceptable for instrument flight operations"	
(C)	"Marginal" - "acceptable for visual flight operations only"	
(1)	"Satisfactory for normal operation" (Cooper Rating = 3-1/2)	NASA TN D-792, (Reference 9) (simulator test)
(2)	---Same as above---	NASA TN D-1328 (Reference 10) (X-14A flight test)

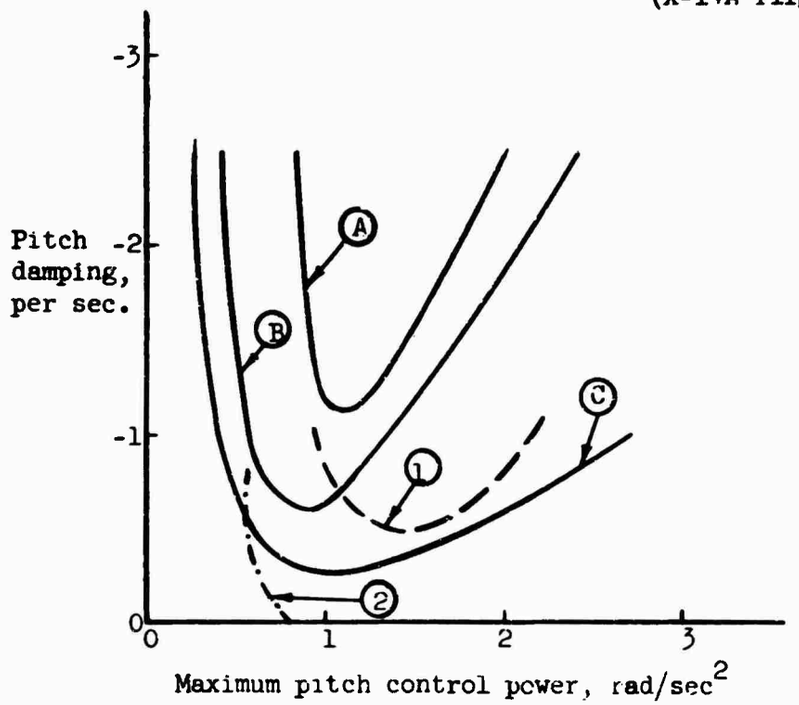

Figure 30. Pilot Opinion Comparison, Pitch Axis.

Boundary	Descriptive Pilot Opinion	Reference
(A)	"Desirable" - "good handling qualities for instrument flight operations"	NASA TN D-58 (Reference 8) (S-51 flight test)
(B)	"Acceptable" - "acceptable for instrument flight operations"	
(C)	"Marginal" - "acceptable for visual flight operations only"	

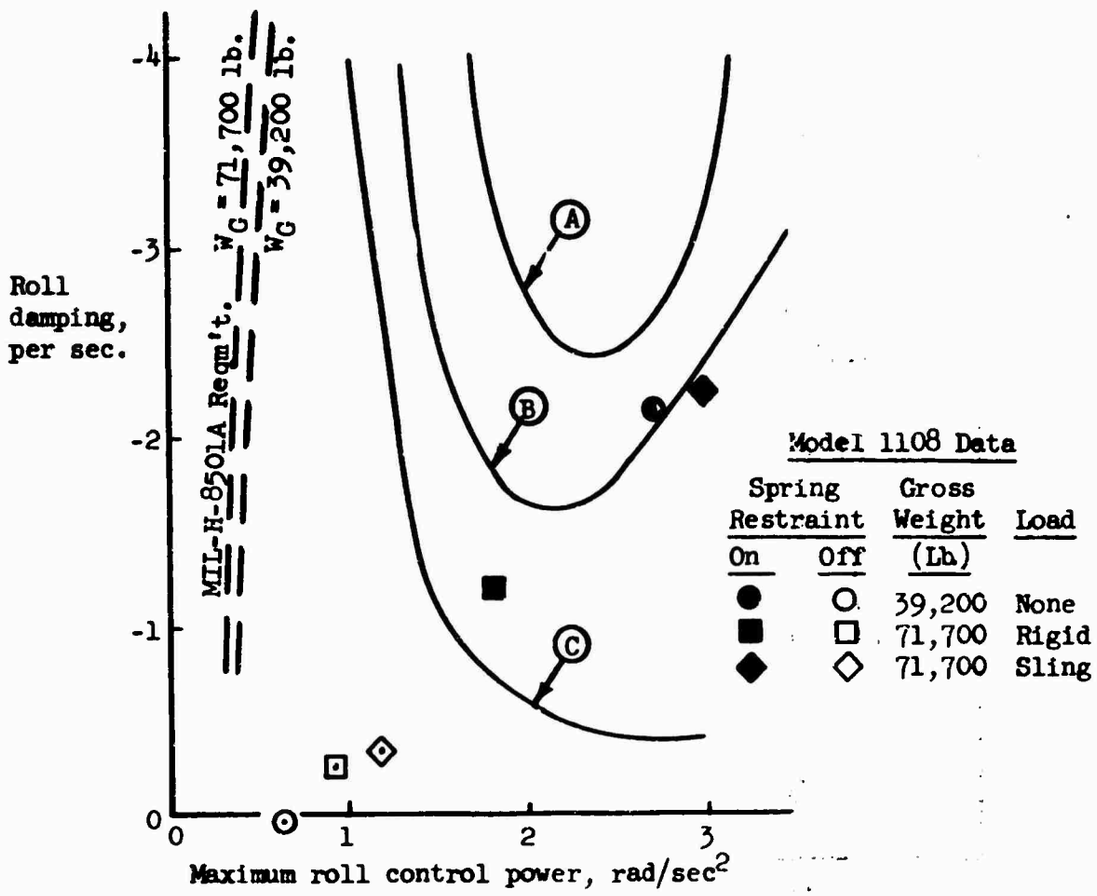

Figure 31. Maximum Control Power, Roll Axis.

Boundary	Descriptive Pilot Opinion	Reference
Ⓐ	"Desirable" - "good handling qualities for instrument flight operations"	NASA TN D-58, Ref. 8 (S-51 flight test)
Ⓑ	"Acceptable" - "acceptable for instrument flight operations"	
Ⓒ	"Marginal" - "acceptable for visual flight operations only"	

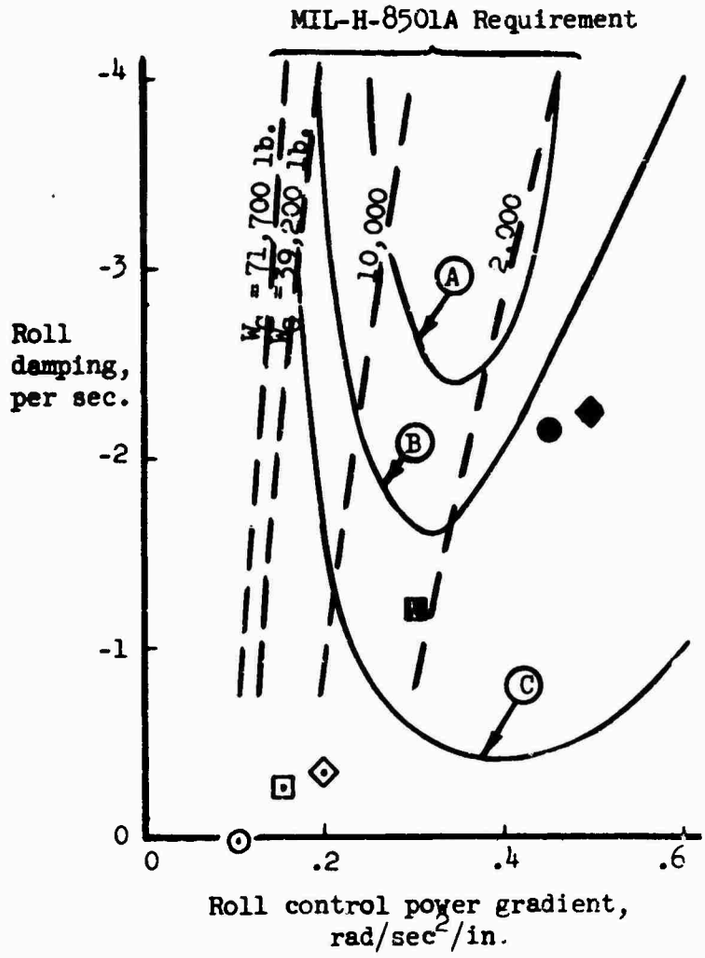

Model 1108 Data

Spring Restraint On	Spring Restraint Off	Gross Weight (lb.)	Load
●	○	39,200	None
■	□	71,700	Rigid
◆	◇	71,700	Sling

Figure 32. Control Power Gradient, Roll Axis.

Boundary	Descriptive Pilot Opinion	Reference
Ⓐ	"Desirable" - "good handling qualities for instrument flight operations"	NASA TN D-58 (Reference 8) (S-51 flight test)
Ⓑ	"Acceptable" - "acceptable for instrument flight operations"	
Ⓒ	"Marginal" - "acceptable for visual flight operations only"	

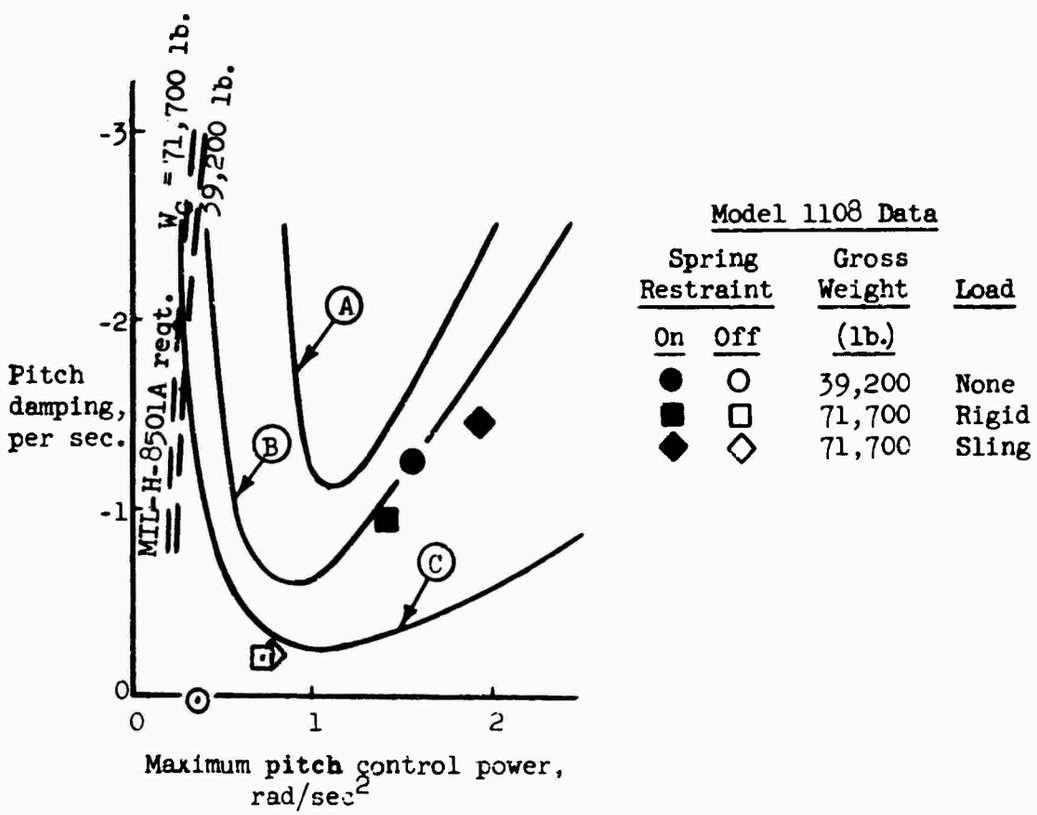

Figure 33. Maximum Control Power, Pitch Axis.

Boundary	Descriptive Pilot Opinion	Reference
Ⓐ	"Desirable" - "good handling qualities for instrument flight operations"	NASA TN D-58 (Reference 8) (S-51 flight test)
Ⓑ	"Acceptable" - "acceptable for instrument flight operations"	
Ⓒ	"Marginal" - "acceptable for visual flight operations only"	

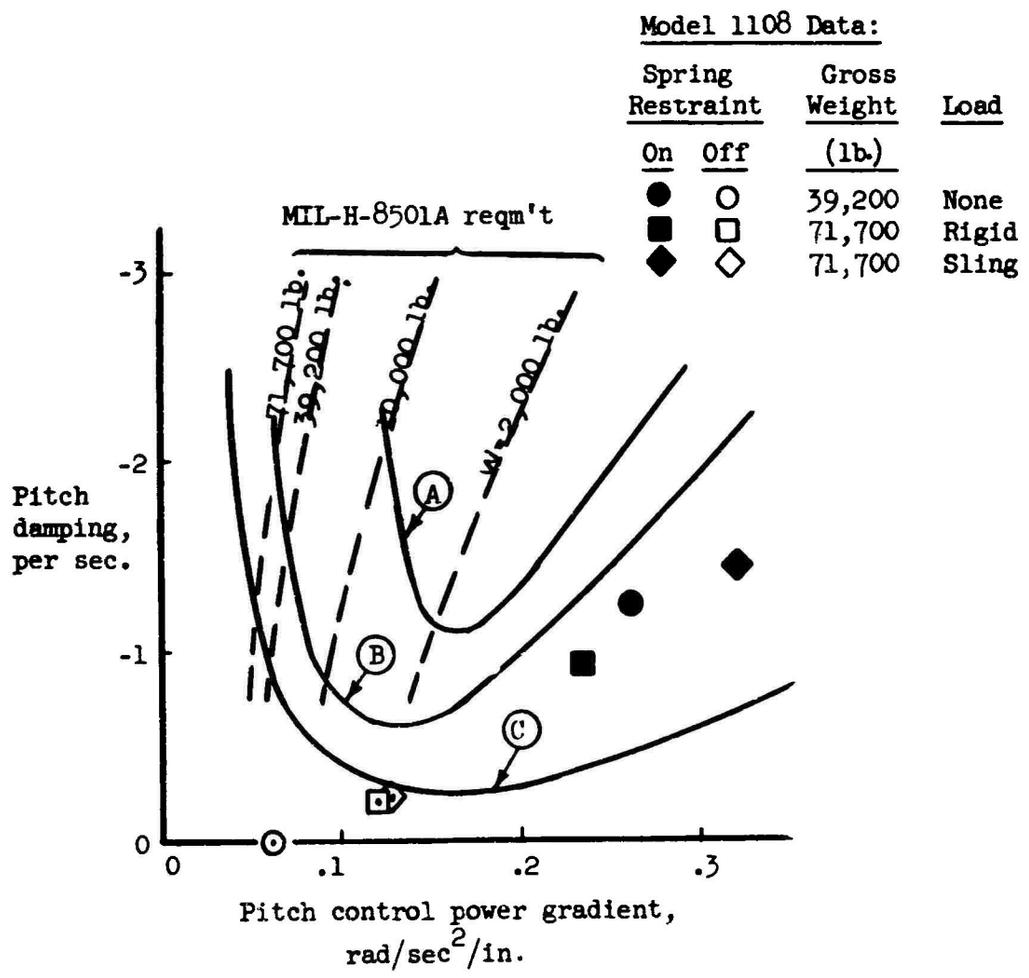

Figure 34. Control Power Gradient, Pitch Axis.

REFERENCES

1. "Parametric Design Study," Heavy-Lift Tip Turbojet Rotor System, Volume II, Hiller Engineering Report No. 64-42, U. S. Army Transportation Research Command,* Fort Eustis, Virginia, Oct 1965.

2. "Design Layout Studies," Heavy-Lift Tip Turbojet Rotor System, Volume III, Hiller Engineering Report No. 64-43, U. S. Army Transportation Research Command,* Fort Eustis, Virginia, Oct 1965.

3. "Static and Dynamic Loads," Heavy-Lift Tip Turbojet Rotor System, Volume IV, Hiller Engineering Report No. 44, U. S. Army Transportation Research Command,* Fort Eustis, Virginia, Oct 1965.

4. "Structural Analysis," Heavy-Lift Tip Turbojet Rotor System, Volume V, Hiller Engineering Report No. 64-45, U.S. Army Transportation Research Command,* Fort Eustis, Virginia, Oct 1965.

5. "Dynamic and Aeroelastic Studies," Heavy-Lift Tip Turbojet Rotor System, Volume VI, Hiller Engineering Report No. 64-46, U. S. Army Transportation Research Command,* Fort Eustis, Virginia, Oct 1965.

6. "Weight and Balance Studies," Heavy-Lift Tip Turbojet Rotor System, Volume VII, Hiller Engineering Report No. 64-47, U. S. Army Transportation Research Command,* Fort Eustis, Virginia, Oct 1965.

7. "Wind-Tunnel Studies," Heavy-Lift Tip Turbojet Rotor System, Volume VIII, Hiller Engineering Report No. 64-48, U. S. Army Transportation Research Command,* Fort Eustis, Virginia, Oct 1965.

8. "Performance Analysis," Heavy-Lift Tip Turbojet Rotor System, Volume IX, Hiller Engineering Report No. 64-49, U. S. Army Transportation Research Command,* Fort Eustis, Virginia, Oct 1965.

9. "Stability and Control," Heavy-Lift Tip Turbojet Rotor System, Volume X, Hiller Engineering Report No. 64-50, U. S. Army Transportation Research Command,* Fort Eustis, Virginia, Oct 1965.

10. "Performance Data Report," Proposal for the Light Observation Helicopter (Army), Hiller Engineering Report No. 60-92, Hiller Aircraft Company, Inc., Palo Alto, California, December 1960.

11. Schlichting, Hermann, "Boundary Layer Theory", Pergamon Press, New York, N. Y., 1955.

12. "Helicopter Flying and Ground Handling Qualities; General Requirements for," Military Specification MIL-H-8501A, September 7, 1961.

*Changed to U. S. Army Aviation Materiel Laboratories in March 1965.

REFERENCES (CONTINUED)

13. Required Lateral Handling Qualities for Helicopters in Low-Speed Instrument Flight, TREC Report 60-66, Department of Aeronautical Engineering, Princeton University, Report No. 496, U. S. Army Transportation Research Command,* Fort Eustis, Virginia, February 1960.

14. Salmirs, Seymour and Tapscott, Robert J., "The Effects of Various Combinations of Damping and Control Power on Helicopter Handling Qualities During Both Instrument and Visual Flight," NASA TN D-58, October 1959.

15. Faye, Alan E., Jr., "Additional Control Requirements for Hovering Determined Through the Use of a Piloted Flight Simulator," NASA TN D-792, April 1961.

16. Rolls, L. Stewart, and Drinkwater, Fred J., III. "A Flight Determination of the Attitude Control Power and Damping Requirements for a Visual Hovering Task in the Variable Stability and Control X-14A Research Vehicle," NASA TN D-1328, May 1962.

17. "Continental Model 357-1 Tip Turbojet Engine - Engine Design," Heavy-Lift Tip Turbojet Rotor System, Volume XI, CAE Report No. 942, U. S. Army Transportation Research Command,* Fort Eustis, Virginia, October 1965.

18. "Continental Model 357-1 Tip Turbojet Engine - Fuel Pump and Control System Design," Heavy-Lift Tip Turbojet Rotor System, Volume XII, CAE Report No. 943, U. S. Army Transportation Research Command,* Fort Eustis, Virginia, October 1965.

19. "Continental Model 357-1 Tip Turbojet Engine - Preliminary Model Specification," Heavy-Lift Tip Turbojet Rotor System, Volume XIII, CAE Model Specification No. 2253, U. S. Army Transportation Research Command,* Fort Eustis, Virginia, October 1965.

*Changed to U. S. Army Aviation Materiel Laboratories in March 1965.

Unclassified

Security Classification

DOCUMENT CONTROL DATA - R&D

(Security classification of title, body of abstract and indexing annotation must be entered when the overall report is classified)

1. ORIGINATING ACTIVITY (Corporate author) Hiller Aircraft Company, Inc. Palo Alto, California	2a. REPORT SECURITY CLASSIFICATION Unclassified 2b GROUP

3. REPORT TITLE

Heavy-Lift Tip Turbojet Rotor System, (Summary Report), Volume I

4. DESCRIPTIVE NOTES (Type of report and inclusive dates)

5. AUTHOR(S) (Last name, first name, initial)

6. REPORT DATE	7a. TOTAL NO. OF PAGES	7b. NO. OF REFS
October 1965	105	19

8a. CONTRACT OR GRANT NO. DA 44-177-AMC-25(T) b. PROJECT NO. c. Task 1M121401D14412 d.	9a. ORIGINATOR'S REPORT NUMBER(S) USAAVLABS Technical Report 64-68A 9b. OTHER REPORT NO(S) (Any other numbers that may be assigned this report) Hiller Engineering Report No. 64-41

10. AVAILABILITY/LIMITATION NOTICES

Qualified requesters may obtain copies of this report from DDC.
This report has been furnished to the Department of Commerce for sale to the public.

11. SUPPLEMENTARY NOTES	12. SPONSORING MILITARY ACTIVITY
	US Army Aviation Materiel Laboratories Fort Eustis, Virginia

13. ABSTRACT

The study of a tip-turbojet-powered rotor system for a heavy-lift helicopter, which is presented in thirteen volumes, is summarized in this report. Included under this general subject are studies on parametric design, performance, structures and dynamics, wind tunnel, preliminary design, weight and balance, stability, and power plant.

DD FORM 1 JAN 64 1473

Unclassified

Security Classification

Unclassified

Security Classification

14. KEY WORDS	LINK A		LINK B		LINK C	
	ROLE	WT	ROLE	WT	ROLE	WT
Tip Turbojet Rotor System						

INSTRUCTIONS

1. ORIGINATING ACTIVITY: Enter the name and address of the contractor, subcontractor, grantee, Department of Defense activity or other organization *(corporate author)* issuing the report.

2a. REPORT SECURITY CLASSIFICATION: Enter the overall security classification of the report. Indicate whether "Restricted Data" is included. Marking is to be in accordance with appropriate security regulations.

2b. GROUP: Automatic downgrading is specified in DoD Directive 5200.10 and Armed Forces Industrial Manual. Enter the group number. Also, when applicable, show that optional markings have been used for Group 3 and Group 4 as authorized.

3. REPORT TITLE: Enter the complete report title in all capital letters. Titles in all cases should be unclassified. If a meaningful title cannot be selected without classification, show title classification in all capitals in parenthesis immediately following the title.

4. DESCRIPTIVE NOTES: If appropriate, enter the type of report, e.g., interim, progress, summary, annual, or final. Give the inclusive dates when a specific reporting period is covered.

5. AUTHOR(S). Enter the name(s) of author(s) as shown on or in the report. Enter last name, first name, middle initial. If military, show rank and branch of service. The name of the principal author is an absolute minimum requirement.

6. REPORT DATE: Enter the date of the report as day, month, year, or month, year. If more than one date appears on the report, use date of publication.

7a. TOTAL NUMBER OF PAGES: The total page count should follow normal pagination procedures, i.e., enter the number of pages containing information.

7b. NUMBER OF REFERENCES: Enter the total number of references cited in the report.

8a. CONTRACT OR GRANT NUMBER: If appropriate, enter the applicable number of the contract or grant under which the report was written.

8b, 8c, & 8d. PROJECT NUMBER: Enter the appropriate military department identification, such as project number, subproject number, system numbers, task number, etc.

9a. ORIGINATOR'S REPORT NUMBER(S): Enter the official report number by which the document will be identified and controlled by the originating activity. This number must be unique to this report.

9b. OTHER REPORT NUMBER(S): If the report has been assigned any other report numbers *(either by the originator or by the sponsor)*, also enter this number(s).

10. AVAILABILITY/LIMITATION NOTICES: Enter any limitations on further dissemination of the report, other than those imposed by security classification, using standard statements such as:

(1) "Qualified requesters may obtain copies of this report from DDC."

(2) "Foreign announcement and dissemination of this report by DDC is not authorized."

(3) "U. S. Government agencies may obtain copies of this report directly from DDC. Other qualified DDC users shall request through _____."

(4) "U. S. military agencies may obtain copies of this report directly from DDC. Other qualified users shall request through _____."

(5) "All distribution of this report is controlled. Qualified DDC users shall request through _____."

If the report has been furnished to the Office of Technical Services, Department of Commerce, for sale to the public, indicate this fact and enter the price, if known.

11. SUPPLEMENTARY NOTES: Use for additional explanatory notes.

12. SPONSORING MILITARY ACTIVITY: Enter the name of the departmental project office or laboratory sponsoring *(paying for)* the research and development. Include address.

13. ABSTRACT: Enter an abstract giving a brief and factual summary of the document indicative of the report, even though it may also appear elsewhere in the body of the technical report. If additional space is required, a continuation sheet shall be attached.

It is highly desirable that the abstract of classified reports be unclassified. Each paragraph of the abstract shall end with an indication of the military security classification of the information in the paragraph, represented as *(TS)*, *(S)*, *(C)*, or *(U)*.

There is no limitation on the length of the abstract. However, the suggested length is from 150 to 225 words.

14. KEY WORDS: Key words are technically meaningful terms or short phrases that characterize a report and may be used as index entries for cataloging the report. Key words must be selected so that no security classification is required. Identifiers, such as equipment model designation, trade name, military project code name, geographic location, may be used as key words but will be followed by an indication of technical context. The assignment of links, rules, and weights is optional.

Unclassified

Security Classification

6494-65